

AD A 130458

(12)

RADC-TR-83-32
Final Technical Report
Februray 1983



MODELING OF PARASITIC EFFECTS IN DISCRETE PASSIVE COMPONENTS

Georgia Institute of Technology

J. A. Woody

APPROVED FOR PUBLIC RELEASE; DISTRIBUTION UNLIMITED

DTIC
ELECTE
JUL 19 1983
A

DTIC FILE COPY

ROME AIR DEVELOPMENT CENTER
Air Force Systems Command
Griffiss Air Force Base, NY 13441

83 07 19 062

This report has been reviewed by the RADC Public Affairs Office (PA) and is releasable to the National Technical Information Service (NTIS). At NTIS it will be releasable to the general public, including foreign nations.

RADC-TR-83-32 has been reviewed and is approved for publication.

APPROVED:

Carmen A. Paludi, Jr.

CARMEN A. PALUDI, JR.
Project Engineer

APPROVED:

Robert W. McGregor

ROBERT W. MCGREGOR
Acting Chief, Reliability & Compatibility Division

FOR THE COMMANDER:

John P. Huss

JOHN P. HUSS
Acting Chief, Plans Office

If your address has changed or if you wish to be removed from the RADC mailing list, or if the addressee is no longer employed by your organization, please notify RADC (RBCT) Griffiss AFB NY 13441. This will assist us in maintaining a current mailing list.

Do not return copies of this report unless contractual obligations or notices on a specific document requires that it be returned.

UNCLASSIFIED

SECURITY CLASSIFICATION OF THIS PAGE(When Data Entered)

develop appropriate modeling techniques for these frequencies. In addition, measurement techniques were identified for obtaining the necessary data and modeling techniques were developed for frequencies up to 1 GHz. Examples of the modeling techniques are presented and the resulting recommended modeling techniques for use with various types of components and data are summarized. It is concluded that at frequencies up to 1 GHz passive components can be accurately modeled with simple 3-element models.

UNCLASSIFIED

SECURITY CLASSIFICATION OF THIS PAGE(When Data Entered)

PREFACE

The work described in this report was performed by personnel of the Electronics Technology Laboratory (ETL) of the Georgia Tech Engineering Experiment Station. This program was sponsored by the United States Air Force (AFSC), Rome Air Development Center (RADC) as Contract No. F30602-78-C-0230. The program was monitored by Mr. C. A. Paludi, Jr., of RADC. The described work was directed by Mr. J. A. Woody, Project Director, under the technical supervision of Mr. H. W. Denny, Head of the Electromagnetic Compatibility Branch. General supervision was provided by Mr. D. W. Robertson, Director of ETL. This report summarizes the objectives, activities, and results of an investigation to develop modeling techniques for passive components, including their parasitics, for frequencies up to 1 GHz. The report was authored by Mr. Woody.

The author wishes to express his appreciation to all the component manufacturers that furnished data and information on the components and measurement techniques and that granted permission to reprint data and/or curves from their current sales literature.



TABLE OF CONTENTS

	<u>Page</u>
1. INTRODUCTION	1
1.1 Background	1
1.2 Program Scope and Objective.	2
1.3 Program Approach	2
1.4 Report Organization.	3
2. MODELING TECHNIQUES	4
2.1 Introduction	4
2.2 Direct Calculation Approach.	4
2.3 Engineering Approximation Approach	7
2.4 Analytical Approximation	9
3.0 MODELING AND ANALYSIS USING AVAILABLE DATA (TASK 1)	12
3.1 Introduction	12
3.2 Modeling and Analysis of Component A1.	13
3.2.1 Application of Technique #1A.	13
3.2.1.1 Modeling Procedure	13
3.2.1.2 Analysis of Technique #1A.	16
3.2.2 Application of Technique #2A.	18
3.2.2.1 Modeling Procedure	18
3.2.2.2 Analysis of Technique #2A.	22
3.2.3 Application of Technique #2B.	22
3.2.3.1 Modeling Procedure	24
3.2.3.2 Analysis of Technique #2B.	25
3.2.4 Application of Technique #2C.	27
3.2.4.1 Modeling Procedure	27
3.2.4.2 Analysis of Technique #2C.	27
3.3 Modeling and Analysis of Remaining Capacitors.	29
3.4 Modeling and Analysis of Inductors	31
3.5 Modeling and Analysis for Resistors.	37
3.6 Observations Relative to the Modeling of Components Using Available Data	43
4.0 MODELING AND ANALYSIS OF MEASURED DATA (TASK 2)	46
5.0 RECOMMENDED MODELING TECHNIQUES	63
5.1 Capacitors	63
5.2 Inductors.	64
5.3 Resistors.	66
6.0 CONCLUSIONS AND RECOMMENDATIONS	68
7.0 REFERENCES.	70
APPENDIX A	A-1
APPENDIX B	B-1
APPENDIX C	C-1
APPENDIX D	D-1
APPENDIX E	E-1
APPENDIX F	F-1

LIST OF FIGURES

		<u>Page</u>
Figure 1.	Assumed Model Circuit Configurations Used in Direct Calculation Modeling Approach	5
Figure 2.	Data Sheet for Component A1 (0.1 μ F)	14
Figure 3.	Calculated $ Z $ of Model Resulting from Technique #1A for Component A1 Plotted on the Manufacturer's Curve . .	17
Figure 4.	Low Frequency Asymptote ("A") and Straight Line Approximation of the Resistance ("R") for Component A1	19
Figure 5.	Calculated $ Z $ of Model Resulting from Technique #2A for Component A1 Plotted on Manufacturer's Curve	24
Figure 6.	Extrapolated Manufacturer's Curve for Component A1 with Asymptotes	25
Figure 7.	Calculated $ Z $ of Model Resulting from Technique #2B for Component A1 Plotted on the Manufacturer's Curve . .	26
Figure 8.	Calculated $ Z $ of Model Resulting from Technique #2C for Component A1 Plotted on the Manufacturer's Curve . .	28
Figure 9.	Data Sheet for Component S1 (Part Number TA-1, 0.1 H inductor)	32
Figure 10.	Calculated Q (line "A") for Model of Inductor S1 Obtained by Assuming R_s to Be a Parabola	35
Figure 11.	Calculated Q (line "B") for Model of Inductor S1 Obtained by Assuming the Existence of Two Constant-Value Resistors (R_w and R_c) in the Model	38
Figure 12.	Modeling and Analysis Data for U-type Resistors	39
Figure 13.	Modeling and Analysis Data for V-type Resistors	41
Figure 14.	Modeling and Analysis Data for Y-type Resistors	42
Figure 15.	Generic Curve of the Magnitude of Impedance of the Measured Capacitors and Configuration of the Resulting Model	48
Figure 16.	Generic Curve of the Magnitude of Impedance of the Measured Inductors and Configuration of the Resulting Model	48
Figure 17.	Generic Curve of the Magnitude of Impedance of the Measured Resistors and Configurations of the Resulting Models	49

LIST OF TABLES

	<u>Page</u>
Table 1. Magnitude of Impedance of Model Resulting from Technique #1A for Component A1	17
Table 2. Magnitude of Impedance of Model Resulting from Technique #2A for Component A1	23
Table 3. Magnitude of Impedance of Model Resulting from Technique #2B for Component A1	26
Table 4. Magnitude of Impedance of Model Resulting from Technique #2C for Component A1	28
Table 5. Model Configuration Selection Criteria	50
Table 6. Resulting Model Elements and Data Parameters for Measured Capacitors	53
Table 7. Resulting Model Elements and Data Parameters for Measured Inductors.	56
Table 8. Resulting Model Elements and Data Parameters for Measured Resistors.	58

LIST OF FIGURES IN APPENDICES

	<u>Page</u>
Figure A-1. Examples of Manufacturers' ΔC vs f and DF vs f Curves . .	A-4
Figure A-2. Examples of Manufacturers' $ Z $ vs f and ESR vs f Curves .	A-5
Figure A-3. Examples of Various Forms of Manufacturer Impedance vs Frequency Data	A-6
Figure A-4. Examples of Quality Factor Curves	A-7
Figure C-1. Vector Impedance Meters -- HP 4800A on the Top and HP 4815A on the Bottom	C-4
Figure C-2. Vector Impedance Meters and Network Analyzer System -- GR 1710 Network Analyzer System on the Right	C-4
Figure C-3. Component Mount/Probe for HP 4815A Vector Impedance Meter	C-5
Figure C-4. GR 1710 Network Analyzer System	C-5
Figure C-5. Component Mount for GR 1710 Network Analyzer System . . .	C-6
Figure C-6. Insertion Loss Measurement System in Component Mounts . .	C-7
Figure C-7. Reflectometer Measurement System	C-8
Figure D-1. Data for the Capacitor Representing Group #1 in Table D-7	D-3
Figure D-2(a). Data for the Capacitor Representing Group #2 in Table D-7	D-4
Figure D-2(b). Difference Between Calculated and Measured $ Z $ in (a) . .	D-4
Figure D-3(a). Data for the Capacitor Representing Group #3 in Table D-7	D-5
Figure D-3(b). Difference Between Calculated and Measured $ Z $ in (a) . .	D-5
Figure D-4(a). Data for the Capacitor Representing Group #4 in Table D-7	D-6
Figure D-4(b). Difference Between Calculated and Measured $ Z $ in (a) . .	D-6
Figure D-5. Data for the Capacitor Representing Group #5 in Table D-7	D-7
Figure D-6(a). Data for the Capacitor Representing Group #6 in Table D-7	D-8
Figure D-6(b). Difference Between Calculated and Measured $ Z $ in (a) . .	D-8
Figure D-7(a). Data for the Capacitor Representing Group #7 in Table D-7	D-9
Figure D-7(b). Difference Between Calculated and Measured $ Z $ in (a) . .	D-9

LIST OF FIGURES IN APPENDICES (continued)

	<u>Page</u>
Figure D-8(a). Data for the Inductor Representing Group #1 in Table D-8	D-10
Figure D-8(b). Difference Between Calculated and Measured $ Z $ in (a) .	D-10
Figure D-9(a). Data for the Inductor Representing Group #2 in Table D-8	D-11
Figure D-9(b). Difference Between Calculated and Measured $ Z $ in (a) .	D-11
Figure D-10(a). Data for the Inductor Representing Group #3 in Table D-8	D-12
Figure D-10(b). Difference Between Calculated and Measured $ Z $ in (a) .	D-12
Figure D-11(a). Data for the Inductor Representing Group #4 in Table D-8	D-13
Figure D-11(b). Difference Between Calculated and Measured $ Z $ in (a) .	D-13
Figure D-12. Data for the Resistor Representing Group #1 in Table D-9	D-14
Figure D-13. Data for the Resistor Representing Group #2 in Table D-9	D-15
Figure D-14(a). Data for the Resistor Representing Group #3 in Table D-9	D-16
Figure D-14(b). Difference Between Calculated and Measured $ Z $ in (a) .	D-16
Figure D-15(a). Data for the Resistor Representing Group #4 in Table D-9	D-17
Figure D-15(b). Difference Between Calculated and Measured $ Z $ in (a) .	D-17
Figure D-16(a). Data for the Resistor Representing Group #5 in Table D-9	D-18
Figure D-16(b). Difference Between Calculated and Measured $ Z $ in (a) .	D-18
Figure D-17(a). Data for the Resistor Representing Group #6 in Table D-9	D-19
Figure D-17(b). Difference Between Calculated and Measured $ Z $ in (a) .	D-19
Figure E-1. Measured Impedance of Various Cardinal Values of 1/4-watt Carbon Composition Allen-Bradley Resistors . .	E-4
Figure E-2. Circuit Showing Possible Instrumentation Parasitics Relative to the Measured Z and the Component-under- Test.	E-5
Figure F-1. Data for the Capacitor Representing Group #1 in Table D-7	F-4
Figure F-2. Data for the Capacitor Representing Group #3 in Table D-7	F-5

LIST OF FIGURES IN APPENDICES (concluded)

	<u>Page</u>
Figure F-3. Difference in Model and Measured Impedance in F-2 . . .	F-5
Figure F-4. Data for the Inductor Representing Group #4 in Table D-8	F-6

LIST OF TABLES IN APPENDICES

	<u>Page</u>
Table A-1. Capacitor Manufacturers From Which Data Was Obtained	A-8
Table A-2. Inductor Manufacturers From Which Data Was Obtained	A-9
Table A-3. Resistor Manufacturers From Which Data Was Obtained	A-9
Table A-4. Available Data on Capacitors.	A-10
Table A-5. Available Data on Inductors	A-17
Table A-6. Available Data on Resistors	A-20
Table B-1. Specific Components Selected for Modeling in Task 1	B-3
Table C-1. Task 2 Measurement Equipment and Systems.	C-9
Table D-1. Capacitors Selected for Measurement	D-20
Table D-2. Inductors Selected for Measurement.	D-23
Table D-3. Resistors Selected for Measurement.	D-24
Table D-4. Characteristics of Each Group of Measured Capacitor Data. .	D-27
Table D-5. Characteristics of Each Group of Measured Inductor Data . .	D-27
Table D-6. Characteristics of Each Group of Measured Resistor Data . .	D-28
Table D-7. Measured Capacitors--Listed According to the Groups Defined in Table D-4.	D-29
Table D-8. Measured Inductors--Listed According to the Groups Defined in Table D-5.	D-33
Table D-9. Measured Resistors--Listed According to the Groups Defined in Table D-6.	D-34
Table E-1. Magnitude of the Impedance Measured for Selected Components at 100 MHz using Different Measurement Techniques	E-6
Table E-2. Measured Complex Impedance for Various Cardinal Values of 1/4-watt, Carbon Composition Resistors.	E-6
Table E-3. Unknown Component Impedance Calculated from Measured Impedance Assuming Instrumentation Parasitics Given in Figure E-2.	E-7
Table E-4. Synthesized Circuit Models for Corrected Impedance Data Given in Table C-4.	E-8

1.0 INTRODUCTION

1.1 Background

Passive components such as capacitors, inductors, and resistors are combined with active devices in electronic circuits to perform specific operations on the signals passing through the circuits. The nature of the effect that each component has on a time-varying waveform is well defined at low frequencies[1]. Furthermore, analytical techniques are generally available at all frequencies for calculating the circuit's output waveform (or spectrum), given the input waveform and an accurate mathematical model (i.e., equivalent circuit) of the constituent elements of the circuit.

Where more than a few components are involved, the mathematical analysis becomes complex and tedious when performed by hand. As a result, several computer-aided network analysis or simulation techniques have been developed. Typical of the resulting computer programs are CIRCUS, SCEPTRE, ECAP, SPICE and NCAP. These programs have made circuit analysis faster and simpler. As an example, NCAP, the acronym for Nonlinear Circuit Analysis Program, provides the EMC community with a usable procedure for analyzing electronic circuits operating in a multi-signal RFI environment [2], [3]. It uses a circuit-oriented procedure based upon frequency domain analysis for computing the nonlinear transfer functions and for predicting many nonlinear effects in electronic circuits.

The validity of the results obtained with any of these computer analysis programs is strongly dependent upon the accuracy with which the various circuit elements are modeled. If all the circuit elements are assumed to be ideal components, large errors can result [4]. All components and their leads exhibit parasitic, or stray, capacitances, inductances, and resistances. Such parasitics arise because conductors exhibit a certain amount of intrinsic inductance and resistance, and wherever conductors are separated by a dielectric a capacitor is formed. These unintentional, but unavoidable, properties associated with every type of component are ignored when the components are modeled as ideal components and, hence, errors result. For example, if a resistor has sufficient parasitic capacitance and inductance to make its impedance properties strongly frequency-dependent, calculations of circuit

behavior at frequencies where the reactive effects are significant will be in error unless these parasitic parameters are included in the model.

Including the parasitic effects of passive components in models is particularly important in a program like NCAP that has a major function of computing the out-of-band performance properties (i.e., EMI characteristics) of circuits. Therefore, in order to enhance the capabilities of NCAP and other similar computer-aided analysis programs, more accurate models including the parasitics of passive components must be available.

1.2 Program Scope and Objective

The scope of this program was the improvement of the capabilities for modeling of passive components for use in computer-aided analysis of electronic circuits.

The objective of this effort was to develop modeling techniques which will generate models that predict the parasitic behavior of discrete passive components (capacitors, inductors, and resistors) over the frequency range of 1 Hz to 1 GHz. The modeling techniques are to generate models which include parasitic effects for use in computer-aided analysis of the out-of-band frequency responses of electronic circuits constructed on printed circuit boards used in Air Force electronic equipments.

1.3 Program Approach

To accomplish the above objective, a 12-month analysis and measurement program was conducted. This technical program consisted of two basic tasks. To facilitate program management, these two contractually defined tasks were divided into the following subtasks:

Task 1: Development of modeling techniques using manufacturers' available data over the frequency range for which data exist.

- Subtask 1A: Prepare a suggested component list
- Subtask 1B: Survey and classify the available data
- Subtask 1C: Perform initial modeling and analysis
- Subtask 1D: Prepare Test Plan 1
- Subtask 1E: Perform analysis based on available data
- Subtask 1F: Give oral presentation of results

Task 2: Extension of modeling techniques to 1 GHz using data obtained from measurement techniques to be developed.

- Subtask 2A: Define additional data requirements
- Subtask 2B: Develop measurement techniques
- Subtask 2C: Measure data
- Subtask 2D: Perform initial modeling
- Subtask 2E: Perform initial analysis
- Subtask 2F: Prepare Test Plan 2
- Subtask 2G: Perform final modeling and analysis based on available and measured data
- Subtask 2H: Give oral presentation of results

Thus, Task 1 emphasizes the collection and classification of the data available from manufacturers and the use of this data in developing models that include the parasitic effects of passive components. Since manufacturers' available data is limited primarily to the lower frequencies (typically <100 MHz and in many cases <10 MHz) data was needed for the higher frequencies (up to 1 GHz). Therefore, Task 2 was directed toward gathering this data through laboratory measurements of representative components and then using this measured data in developing models.

1.4 Report Organization

The material which follows in this report is divided into five major sections. Section 2 presents the identified modeling approaches. Section 3 describes the modeling and analysis performed on Task 1 using manufacturers' available data. Section 4 presents the measurement techniques employed on Task 2 and describes the modeling and analysis performed based on the measured data. The recommended modeling procedures defined as a result of the efforts on Task 1 and 2 are summarized in Section 5. The conclusions drawn from the program are given in Section 6.

Six appendices are included in the report. Appendix A discusses the collection and classification of the data available from manufacturers and summarizes this data. The components selected for use on Task 1 and the applicability of the selected modeling approaches to the available data are given in Appendix B. Appendix C describes the measurement techniques used on Task 2 and representative samples of the measured data are given in Appendix D. Appendix E describes and gives an initial analysis of some of the measurement problems encountered. The modeling and analysis of the exceptions to the generic curves for the measured data are summarized in Appendix F.

2.0 MODELING TECHNIQUES

2.1 Introduction

Three candidate modeling approaches were identified during this program. They are:

1. Direct Calculation
2. Engineering Approximation
3. Analytical Approximation

Each of these three basic approaches may be used for developing models of the parasitic behavior of passive components.

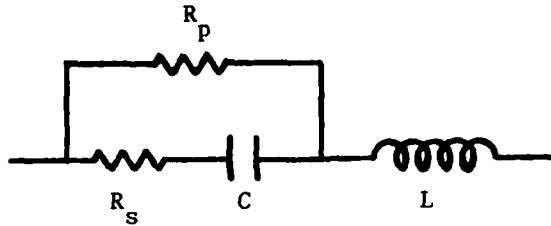
A number of specific modeling techniques can be obtained as variations of the methods of each basic approach. For example, once a modeling technique based on one of the above approaches has been developed, it may be possible to develop a second, more appropriate, technique by making assumptions on the resulting model to make it more accurate or less complex. Generally, as the accuracy requirement for the model increases, the complexity of the resulting model configuration increases. Thus the selection of the most appropriate modeling technique for a given set of data involves a trade-off between accuracy and model complexity.

2.2 Direct Calculation Approach

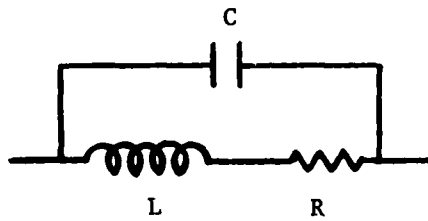
The direct calculation modeling approach is the simplest approach for generating a model of a passive component. It requires a minimum amount of parametric data and yields the most straightforward model.

This approach must initially assume an appropriate equivalent circuit for the component to be modeled. This equivalent circuit reflects the known (or surmised) physical and electrical attributes of the component. For example, the equivalent circuit commonly suggested as representing a capacitor is shown in Figure 1(a). In addition to the cardinal value*

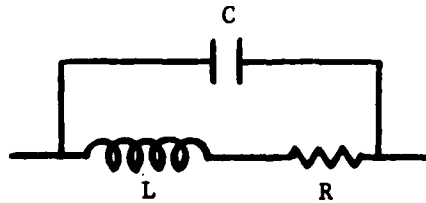
* "Cardinal value" is defined in this report to be that value of the component assigned by the manufacturer in his catalog and in most cases printed on the component.



(a) Simple model circuit configuration for capacitors.



(b) Simple model circuit configuration for inductors.



(c) Simple model circuit configuration for resistors.

Figure 1. Assumed Model Circuit Configurations Used in Direct Calculation Modeling Approach.

of capacitance (C), the model includes a series inductance (L) which represents the lead inductance and other intrinsic inductance between the device terminals and the effective capacitance element. Also, included in this model are two resistors. The parallel resistor (R_p) provides a dc leakage path around the capacitor element while the series resistor (R_s) represents the dielectric losses and determines the dissipation factor (DF) of the capacitor.

The commonly accepted model, or equivalent circuit, of an inductor is shown in Figure 1(b). It includes a resistor (R) in series with the cardinal value of the inductance (L) and a capacitor (C) in parallel with the RL series circuit. The resistor represents the losses in the winding and core of the inductor which determine the dc resistance as well as the quality factor (QF) of the inductor. The C in the model represents the stray or distributed capacitance between the windings and leads of the inductor and determines the parallel resonance frequencies.

The assumed model of a resistor is identical to that of the inductor in arrangement of the elements (see Figure 1(c)). The differences are in the values of the ideal elements in the model and in their physical bases. The R is the cardinal resistance; the L represents the lead and intrinsic inductance of the resistance element; and the C is again the stray capacitance between the various parts of the resistance element.

The application of the direct calculation approach involves the following four basic steps:

1. Assume one of the circuit configurations given in Figure 1 based on the type of component being modeled;
2. Assume that the cardinal value of the component is one element of the model;
3. Calculate the values of the other elements in the model from known component parameters (such as quality factor, dissipation factor, dc resistance, resonance frequency, etc.); and then
4. Eliminate all elements from the model for which there is insufficient available data to determine their values.

The advantages of the direct calculation approach are that:

- o It is simple to apply.

- o It yields simple models.
- o It requires only limited data.
- o It is the only applicable approach when only limited component data is available.

The disadvantages of this approach include:

- o The configuration of the model circuit must be assumed.
- o The accuracy of the resulting model is in general poor at frequencies other than those for which data was used in determining the values of the elements.
- o The model is generally inaccurate at higher frequencies since data is usually not available.

This approach was used primarily on Task 1 with data available from manufacturers, i.e., when insufficient data was available to permit the use of the engineering approximation approach.

2.3 Engineering Approximation Approach

The engineering approximation approach is of moderate complexity. It is based on the application of good engineering judgement in deciding the type of ideal components and their interconnections that can produce the given behavior of a component characteristic as a function of frequency such as the magnitude of the impedance ($|Z|$). This approach requires that a characteristic curve for a component, e.g., $|Z|$ vs f , be given. The complexity of the model resulting from the engineering approximation approach can vary from a simple three-element model to a complex multi-element model, depending on the complexity of the given curve and the detail with which it is analyzed.

The application of this approach involves the following four basic steps:

1. Assume that the behavior of a portion of the given curve (that part below the first resonant frequency) is produced by an ideal component of the same type as the component being modeled. For example, on a log-log plot of $|Z|$ versus frequency, ideal components have the following characteristics:
 - o A resistor has a constant non-zero value of $|Z|$;
 - o The value of $|Z|$ for an inductor increases at 6 dB/octave;
 - o The value of $|Z|$ for a capacitor decreases at 6 dB/octave.
2. Determine the dc resistance of the component from given data.

3. Use engineering approximations and best judgement to determine the types of ideal components, and the configuration in which they should be interconnected, to produce the behavior of the given curve at the higher frequencies. This analysis of the higher frequency behavior of the given curve is based on engineering rules-of-thumb, guidelines, and rigorous analytical procedures such as the following:
 - o The value of $|Z|$ for an inductor (capacitor) increases (decreases) at 6 dB/octave.
 - o Relative maximums and minimums, i.e., changes in the sign of the slope, of the curve indicate parallel and series resonances, respectively.
 - o The location of a maximum or minimum determines a resonance frequency (f_R).
 - o With one reactive element known at a resonance frequency, $f_R = 1/2\pi\sqrt{LC}$ can be used to calculate the other reactive element.
 - o The value of the $|Z|$ curve at a series resonance (i.e., a minimum) can be used as the ideal series resistor associated with the reactive elements producing the resonance.
 - o The 3 dB bandwidth of a peak or null determines the quality factor (Q) at that resonance and, hence, the associated resistance.
 - o The shape of the curve, i.e., its slope and breakpoint frequencies, indicate the pole-zero locations and, thus, the interconnection of specific ideal components.
4. Define the overall circuit configuration and all the elements in the component model based on the analysis of the given curve and any other given data.

The advantages of engineering approximation are:

- o Generally, it is simpler to apply than the analytical approximation approach.
- o With experience, specific elements or groups of elements can be quickly related to the various shapes of the given curve.
- o The resulting model is more accurate over a wider range of frequencies than a model obtained using the direct calculation approach.
- o In many situations, the resulting model is expected to be as accurate as the model obtained using analytical approximation.
- o In other situations, the resulting model may be adequate depending on the accuracy required and the location of the component in the overall circuit.
- o The complexity of the resulting model depends on the detail to which the given curve is analyzed; therefore, within the limits of the given data, the resulting model can be made as complex or accurate as desired.

The disadvantages of this approach include:

- o It requires that a curve of some component function, such as $|Z|$, be given versus frequency.

- o It requires knowledge based on experience of how the various shapes of the given curve can be produced by different types of ideal passive components and their interconnections.
- o Generally, this approach requires more time to apply than direct calculations.
- o The accuracy of the resulting model depends on the engineering approximations and judgement used in analyzing the given curve as well as on the complexity of the resulting model, i.e., the accuracy is a function of the detail with which the given curve is analyzed.

This approach was used with both available (Task 1) and measured (Task 2) data. In general, the data available from manufacturers is inappropriate for using this technique whereas the type data measured on Task 2 was specifically chosen for use with this approach.

2.4 Analytical Approximation

The analytical approximation approach is a complex approach. It is similar to engineering approximation except that it is more analytically rigorous. This approach is based on the application of well defined analytical procedures and principles [5]. This approach also requires that a curve of some component function, such as $|F|$ where $F = A + jB$, be given as a function of frequency. In a manner similar to that for the previous approach, the complexity of the model resulting from analytical approximation can also vary from a simple three-element model to a complex multi-element model depending on the complexities of the given curve. However, unlike the previous approach, the degree to which the given curve is analyzed and, thus, the complexity of the resulting model is predetermined by the specific analytical procedures used.

The application of this approach involves the following three basic steps:

1. Determine an algebraic expression for the given curve of $|F|$, $\text{Arg } F$, A , or B , where $F = A + jB$ represents a complex function describing the component, such as impedance ($Z = R + jX$). This algebraic expression is determined by using a classical approximation method such as the following:
 - o Cut-and-try
 - o Breakpoint/Bode/Straight Line

- o Butterworth
 - o Chebyshev
 - o Fourier
 - o Semi-infinite slope
 - o Equiripple
2. Determine the complete algebraic expression for the total complex function $F = A + jB$ by using one of the following:
- o One of the above classical methods on a given curve of another part of the function such as $\text{Arg } F$.
 - o One of the methods for determining F if $|F|$, $\text{Arg } F$, A , or B is given. These methods yield the unknown part of the function within an arbitrary limit.
3. Apply a realization method to the resulting algebraic expression to determine the model circuit elements. Possible realization methods include:
- o Foster
 - o Canonic
 - o Cauer
 - o Partial Fraction Expansion
 - o Continued Fraction Expansion
 - o Brune
 - o Bott and Duffin
 - o Darlington

The advantages of the analytical approximation approach include the following:

- o It is more analytically rigorous and, therefore, is expected to give more accurate results than either of the other two approaches.
- o The circuit configuration for the resulting model does not have to be assumed or be based on engineering judgement.
- o The complexity and accuracy of the resulting model depends on the degree of detail used in approximating the given curve.
- o This approach does not require before-hand knowledge of how different types of model elements and their interconnections will affect the behavior of a component function, such as $|Z|$ versus frequency.

The disadvantages of this approach include the following:

- o It requires that a curve of some component function such as $|Z|$ be given versus frequency.
- o This approach is the most complicated of the three modeling approaches.
- o It is difficult and tedious to apply.
- o It requires a thorough understanding of each classical approximation method and each realization method.

- o It also requires a working knowledge of the conditions under which each approximation and realization method is, and is not, applicable.

This modeling approach was not needed for use on this program. Because of its complexity and time-consuming nature, the analytical modeling approach was not considered cost-effective; however, in the future the applicability and appropriateness of this approach should be reviewed.

Thus, three basic approaches for modeling the parasitic behavior of passive components are available. In the following Sections, the first two of these approaches are used to illustrate specific modeling techniques with both manufacturers' and measured data.

3.0 MODELING AND ANALYSIS USING AVAILABLE DATA (TASK 1)

3.1 Introduction

Task 1 involved the use of manufacturers' data to develop modeling techniques which would generate models of passive components including their parasitics. Therefore, the first steps on this task were the collection and categorization (or classification) of the available data as discussed in Appendix A. This appendix also presents by category, or type of component, a tabulated summary of the types of data available. In general, appropriate data as a function of frequency is provided over a limited frequency range for only a few types of capacitors and resistors. On the other hand, practically none is available for inductors as a function of frequency. Furthermore, when data is available the majority of it is labeled as "typical" for a specific type component. Therefore, the major drawbacks of the manufacturers' available data on most passive components are the lack of data as a function of frequency and the limited frequency range when such data is available.

The specific components selected for use on Task 1 are identified in Appendix B (see also Reference 6). The initial modeling effort on this task was for the purpose of determining whether the data available from manufacturers was sufficient to support the direct calculation and engineering approximation approaches. This effort showed (see Appendix B) that the direct calculation approach can be applied, at least partially, to roughly 90 percent of the components examined. Because of the nature of much of the available data, however, the engineering approximation approach could be used for only some 40 percent of these components.

The final effort on Task 1 was the detailed modeling of selected examples of the components listed in Table B-1. The modeling techniques were analyzed by comparing the impedance versus frequency behavior of the resulting models with the data provided by the manufacturers. (The degree to which the model behavior matches the published data is defined as the accuracy of the model.) Illustrations of the steps involved in the use of selected variations of the direct calculation and engineering approximation approaches and examples of the means for analyzing the results obtained are presented in the following paragraphs.

3.2 Modeling and Analysis of Component A1^{*}

Component A1 is a 0.1 μF (35V) Corning MD solid tantalum capacitor (the manufacturer's catalog number is MD2-035-104-20). The data given by the manufacturer includes a curve of the magnitude of impedance as a function of frequency ($|Z|$ vs f), the maximum dissipation factor at 120 Hz (DF_{max} @ 120 Hz), and the maximum dc leakage current (DCL_{max}) as follows:

$|Z|$ vs f (100 Hz to 100 MHz)

$DF_{\text{max}} = 8\%$ @ 120 Hz

$DCL_{\text{max}} = 1 \mu\text{A}$

This data is shown in Figure 2. (The impedance curve is identified as MD2-104 and the other data is tabulated with the catalog, or part, number.)

3.2.1 Application of Technique #1A^{*}

The first modeling technique to be illustrated is an application of the direct calculation approach. It is usable where the resonance frequency (f_R) can be determined from the $|Z|$ vs f curve.

3.2.1.1 Modeling Procedure

Step 1 - Assume the model of a capacitor is as shown in Figure 1(a).

Step 2 - Assume C is the cardinal value of the capacitor, i.e.,

$$C = 0.1 \mu\text{F}$$

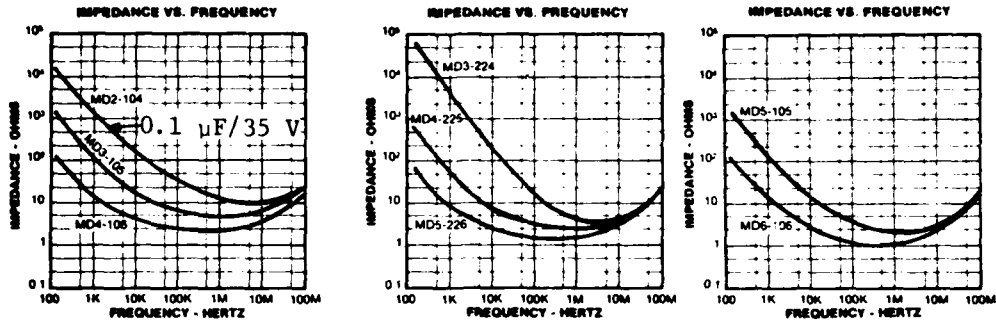
Step 3 - Calculate the minimum value of R_p (i.e., the dc resistance):

$$\begin{aligned} R_{p \text{ min}} &= \frac{V_{\text{test}}}{DCL_{\text{max}}} & (1) \\ &= \frac{35 \text{ V}}{1 \mu\text{A}} \\ &= 35 \text{ M}\Omega \end{aligned}$$

^{*}The component under consideration is identified by its "ID #" as given in Table B-1. Also, the modeling technique is identified by a number and a letter. The number, either 1 or 2, identifies the modeling approach to be direct calculation or engineering approximation, respectively. The letter identifies the specific variation of the approach that is being used, i.e., the specific modeling technique.

Solid Tantalum Capacitors

3-02507-

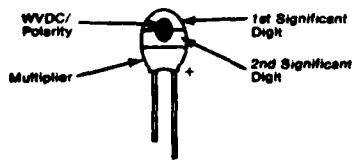


PART NUMBERS AND ORDERING INFORMATION

Value (Mfd)	Part Number	Case Size	Max D.F. (%)	Max DCL (μs)	Value (Mfd)	Part Number	Case Size	Max D.F. (%)	Max DCL (μs)	Value (Mfd)	Part Number	Case Size	Max D.F. (%)	Max DCL (μs)
2 Volts					6 Volts					20 Volts				
2.2	MD2-002-225-20	MD2	10	1.0	.68	MD2-006-684-20	MD2	8	1.0	.15	MD2-020-154-20	MD2	8	1.0
4.7	MD3-002-475-20	MD3	10	1.0	1.5	MD3-006-155-20	MD3	8	1.0	.22	MD2-020-224-20	MD2	8	1.0
10.0	MD4-002-106-20	MD4	10	1.0	3.3	MD4-006-335-20	MD4	8	1.0	.33	MD3-020-334-20	MD3	8	1.0
22.0	MD5-002-226-20	MD5	10	1.0	8.8	MD5-006-885-20	MD5	8	1.0	.47	MD3-020-474-20	MD3	8	1.0
68.0	MD6-002-686-20	MD6	15	1.5	22.0	MD6-006-226-20	MD6	8	1.5	.68	MD4-020-684-20	MD4	8	1.0
3 Volts					10 Volts					35 Volts				
1.5	MD2-003-155-20	MD2	10	1.0	.47	MD2-010-474-20	MD2	8	1.0	.10	MD2-035-104-20	MD2	8	1.0
3.3	MD3-003-335-20	MD3	10	1.0	1.0	MD3-010-106-20	MD3	8	1.0	.15	MD3-035-154-20	MD3	8	1.0
6.8	MD4-003-685-20	MD4	10	1.0	2.2	MD4-010-225-20	MD4	8	1.0	.22	MD3-035-224-20	MD3	8	1.0
15.0	MD5-003-156-20	MD5	10	1.0	4.7	MD5-010-475-20	MD5	8	1.0	.33	MD4-035-334-20	MD4	8	1.0
47.0	MD6-003-476-20	MD6	10	1.5	15.0	MD6-010-156-20	MD6	8	1.5	.47	MD4-035-474-20	MD4	8	1.0
4 Volts					15 Volts									
1.0	MD2-004-106-20	MD2	8	1.0	.33	MD2-015-334-20	MD2	8	1.0	.68	MD5-035-684-20	MD5	8	1.0
2.2	MD3-004-225-20	MD3	8	1.0	.68	MD3-015-684-20	MD3	8	1.0	1.0	MD5-035-105-20	MD5	8	1.0
4.7	MD4-004-475-20	MD4	8	1.0	1.5	MD4-015-155-20	MD4	8	1.0	1.5	MD5-035-155-20	MD5	8	1.0
10.0	MD5-004-106-20	MD5	10	1.0	3.3	MD5-015-335-20	MD5	8	1.0	2.2	MD6-035-225-20	MD6	8	1.0
33.0	MD6-004-336-20	MD6	10	1.5	10.0	MD6-015-106-20	MD6	8	1.5	3.3	MD6-035-335-20	MD6	8	1.0
										4.7	MD6-035-475-20	MD6	8	1.5

MARKING — Capacitance value in pF is shown by means of standard EIA color code rings. Polarity and rated voltage is indicated by a colored dot.

PART MARKING



Note: With part oriented as shown, positive lead is on the right.

Capacitance Code

Color	Significant Figures	Multiplier	Color	WVDC
Black	0		Brown	2v
Brown	1		White	3v
Red	2		Purple	4v
Orange	3	1,000	Yellow	8v
Yellow	4	10,000	Black	10v
Green	5	100,000	Green	15v
Blue	6	1,000,000	Blue	20v
Violet	7		Pink	35v
Grey	8			
White	9			

PART NUMBER EXPLANATION

MD	2	035	104	20
Minidip Series Designator	Case Size	Rated Voltage	Capacitance in pF. First two digits are significant figures. Third digit is the number of zeros following.	Tolerance ±20% ±10%

Reprinted Courtesy of Corning Glass Works

Figure 2. Data Sheet for Component A1 (0.1 μF).

Step 4 - Calculate the maximum value of R_s (at 120 Hz):

$$DF = \omega R_s C \quad (2)$$

or

$$\begin{aligned} R_{s \text{ max}} &= \frac{DF_{\text{max}}}{\omega C} = \frac{DF_{\text{max}}}{2\pi f C} \quad (3) \\ &= \frac{0.08}{2\pi(120)(0.1 \times 10^{-6})} \\ &= 1.06 \text{ k}\Omega @ 120 \text{ Hz} \end{aligned}$$

Step 5 - Calculate L from the resonant frequency (f_R):

Assume f_R is the frequency at which the $|Z|$ vs f curve (see the MD2-104 curve in Figure 2) is a minimum. Then from Figure 2,

$$f_R = 5 \text{ MHz}$$

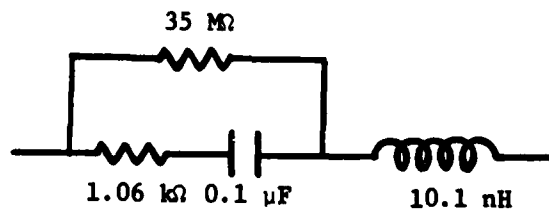
but

$$f_R = \frac{1}{2\pi\sqrt{LC}} \quad (4)$$

Therefore,

$$\begin{aligned} L &= \frac{1}{(2\pi f_R)^2 C} \\ &= \frac{1}{[2\pi(5 \times 10^6)]^2 (0.1 \times 10^{-6})} = 10.1 \times 10^{-9} \\ &= 10.1 \text{ nH} \end{aligned}$$

Step 6 - Draw circuit of final model:



3.2.1.2 Analysis of Technique #1A

The impedance of the model in Step 6 above is given by

$$\begin{aligned} Z_1 &= \frac{R_p (R_s - jX_C)}{R_p + R_s - jX_C} + jX_L \\ &= \frac{R_s - jX_C}{1 + \frac{R_p}{R_s - jX_C}} + jX_L \end{aligned}$$

If $R_p \gg R_s$ and $R_p \gg X_C$, then R_p can be neglected or

$$\begin{aligned} Z_1 &\approx Z_2 = R_s - jX_C + jX_L \\ &= R_s + j(X_L - X_C) \end{aligned} \quad (5)$$

The values of both $|Z_1|$ and $|Z_2|$ were calculated as a function of frequency. These two calculated impedances are compared in Table 1 and Figure 3 with the manufacturer's curve, i.e., $|Z_{\text{manuf}}|$, given in Figure 2. At all frequencies, the differences in impedance arising from neglecting R_p is negligible; therefore, the model can be made less complex by omitting R_p .

Table 1 and Figure 3 indicate that the model for Component A1 resulting from Modeling Technique #1A is unfortunately not very accurate. This disagreement between the calculated $|Z|$ and $|Z_{\text{manuf}}|$ results from assuming that

$$R_s = \text{a constant} = R_{s \text{ max}} @ 120 \text{ Hz}$$

This value of R_s is 1.06 k Ω which means that $|Z|$ of the series resonance model (see the circuit in Step 6 above) can never be less than 1.06 k Ω ; however, $|Z_{\text{manuf}}|_{\text{min}}$ is 10 Ω . Therefore, using DF_{max} @ 120 Hz with the direct calculation approach gives an inaccurate model. This same inaccuracy can be expected to occur when using this approach to model other capacitors unless the R_s calculated from DF_{max} @ 120 Hz is less than $|Z_{\text{manuf}}|_{\text{min}}$. (It should be noted that it can not be determined if this condition has been met unless a $|Z|$ vs f curve is available.)

TABLE 1
MAGNITUDE OF IMPEDANCE OF MODEL RESULTING
FROM TECHNIQUE #1A FOR COMPONENT A1

Frequency (Hz)	$ Z_{\text{manuf}} $ (Ω)	$ Z_1 $ (Ω)	$ Z_2 $ (Ω)
1×10^2	$\approx 17 \text{ k}$	16 k	16 k
1×10^3	1.4 k	1.91 k	1.91 k
1×10^4	170	1.07 k	1.07 k
1×10^5	34	1.06 k	1.06 k
1×10^6	13	1.06 k	1.06 k
1×10^7	10	1.06 k	1.06 k
1×10^8	25	1.06 k	1.06 k

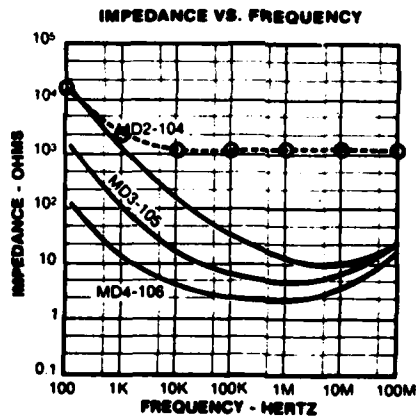


Figure 3. Calculated $|Z|$ of Model Resulting from Technique #1A for Component A1 Plotted on the Manufacturer's Curve.

3.2.2 Application of Technique #2A

Based on the analysis of the use of the direct calculation approach for modeling Component A1 and on the fact that a $|Z|$ vs f curve (MD2-104 in Figure 1) is available from the manufacturer, it was decided that the engineering approximation approach would probably be more appropriate for this capacitor. The first variation of the engineering approximation approach used is #2A.

3.2.2.1 Modeling Procedure

Step 1 - Since the component is a capacitor, assume that one of the elements in the model is an ideal capacitor equal to the cardinal value, i.e., $C = 0.1 \mu\text{F}$. Then at the lower frequencies (100 Hz to 10 kHz), the MD2-104 curve in Figure 4 (reproduced from Figure 2) can be assumed to be produced by this ideal capacitor that has an impedance at 10 kHz of

$$\begin{aligned} Z &= X_C = \frac{1}{\omega C} = \frac{1}{2\pi f C} & (6) \\ &= \frac{1}{2\pi(10 \times 10^3)(0.1 \times 10^{-6})} \\ &= 159\Omega \end{aligned}$$

Thus, the $X_C = 1/\omega C$ asymptote to the curve can be obtained by drawing a straight line through the point $Z(10 \text{ kHz}) = 159 \Omega$ with a slope of -6 dB/octave (-20 dB/decade). This is line "A" in Figure 4.

Step 2 - Calculate the minimum dc resistance:

$$\begin{aligned} R_{dc \text{ min}} &= \frac{V_{\text{rated}}}{DCL_{\text{max}}} & (7) \\ &= \frac{35 \text{ V}}{1 \times 10^{-6} \text{ A}} \\ &= 35 \text{ M}\Omega \end{aligned}$$

This dc resistance must form a parallel path around the ideal capacitor for current flow at low frequencies. Therefore, it is labeled as $R_p \text{ min}$ and is in parallel with C:

$$R_p \text{ min} = R_{dc \text{ min}} = 35 \text{ M}\Omega$$

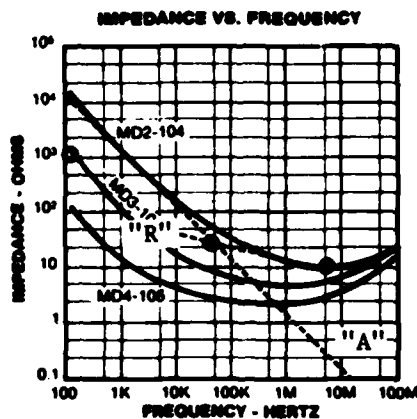


Figure 4. Low Frequency Asymptote ("A") and Straight Line Approximation of the Resistance ("R") for Component A1.

Step 3 - The MD2-104 curve in Figure 4 has the general shape of a series resonance circuit (see Sec. 4.0). Therefore, the parallel combination of C and $R_{p \text{ min}}$ must have an inductor (L) in series with it. The value of L can be determined as follows:

- o Assume that the resonance frequency (f_R) is the frequency at which the $|Z|$ vs f curve is a minimum. Then,

$$f_R = 5 \text{ MHz}$$

- o Calculate L from

$$f_R = \frac{1}{2\pi\sqrt{LC}}$$

or

$$L = \frac{1}{[2\pi(5 \times 10^6)]^2(0.1 \times 10^{-6})} = 1.01 \times 10^{-8} \\ = 10.1 \text{ nH}$$

Step 4 - Since the impedance curve does not go to zero at f_R , there must be a resistor in series with the series resonance circuit. This series resistance (R_s) can be calculated at three specific frequencies as follows:

- o At $f = f_R = 5 \text{ MHz}$,

$$R_s = |Z_{\text{manuf}}|_{\text{min}} = 10 \Omega$$

- o At $f = 120 \text{ Hz}$, $DF_{\text{max}} = 8\%$ and

$$\begin{aligned} R_{s \text{ max}} &= \frac{DF_{\text{max}}}{\omega C} \\ &= \frac{0.08}{2\pi(120)(0.1 \times 10^{-6})} \\ &= 1.06 \text{ k}\Omega \end{aligned}$$

- o At $f = f_{3 \text{ dB}}$, the $|Z|$ vs f curve and the $X_C = 1/\omega C$ asymptote (line "A" in Figure 4) differ by 3 dB, i.e., $X_C = 0.707|Z|$.
At this frequency,

$$R_s = X_C$$

From Figure 4, this point occurs at

$$f_{3 \text{ dB}} = 48 \text{ kHz}$$

Therefore,

$$\begin{aligned} R_s = X_C &= \frac{1}{\omega C} = \frac{1}{2\pi f C} \\ &= \frac{1}{2\pi(48 \times 10^3)(0.1 \times 10^{-6})} \\ &= 33.2 \Omega \end{aligned}$$

These three points, $R_s(5 \text{ MHz}) = 10 \Omega$, $R_s(48 \text{ kHz}) = 33.2 \Omega$, and $R_{s \text{ max}}(120 \text{ Hz}) = 1.06 \text{ k}\Omega$ are plotted in Figure 4. Note that the three do not fall in a straight line on this log-log graph. However, to compute the value of the series resistance of the capacitor, initially assume that the curve for R_s is a straight line through the two lower resistance values (see dotted line "R"). (Projection of this line to the left of the graph indicates a resistance at 120 Hz less than that corresponding to the dissipation factor (DF) stated by the manufacturer. Since the published DF is specified as the highest value to be exhibited by this class of capacitors, the actual value of a particular one should be expected to be less.) The equation for this straight line on log-log paper is

$$\log R_s = m \log f + k \quad (8)$$

where $\log = \log_{10}$, m is the slope of the line, and k is a constant.

The values of m and k can be determined from the two points as follows:

$$\begin{aligned} m &= \frac{\log R_{s1} - \log R_{s2}}{\log f_1 - \log f_2} \\ &= \frac{\log(10) - \log(33.2)}{\log(5 \times 10^6) - \log(48 \times 10^3)} \\ &= -0.258 \end{aligned}$$

Since,

$$\log R_1 = m \log f_1 + k$$

then, at $f_1 = 5 \text{ MHz}$,

$$\begin{aligned} k &= \log R_1 - m \log f_1 \\ &= \log(10) - (-0.258) \log(5 \times 10^6) \\ &= 2.73 \end{aligned}$$

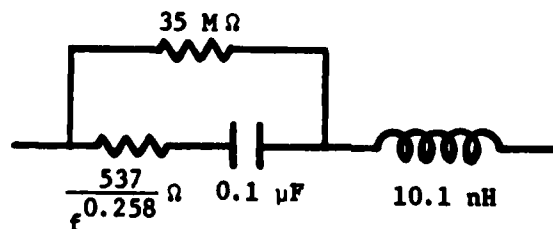
Thus,

$$\begin{aligned} \log R_s &= m \log f + k \\ &= \log f^m + k \end{aligned}$$

or

$$\begin{aligned} R_s &= f^m (10^k) \\ &= f^{-0.258} (10^{2.73}) \\ &= \frac{537}{f^{0.258}} \Omega \end{aligned} \quad (9)$$

Step 5 - Draw the circuit for the resulting model:



3.2.2.2 Analysis of Technique #2A

First, it should be noted that for Capacitor A1 the model resulting from Technique #2A has the same configuration as the model resulting from the use of the direct calculation approach (Technique #1A). In fact, with the exception of the series resistance all the elements in the two models have the same values. It was shown earlier that R_p is large enough to be neglected; however, for confirmation, it was included in the calculations of $|Z_1|$ and $|Z_2|$. These two calculated impedances are compared with manufacturer's data in Table 2 and Figure 5. As expected, the difference between $|Z_1|$ and $|Z_2|$ was again negligible; therefore, the model can be made less complex by omitting R_p .

At frequencies less than f_R , the model is fairly accurate, i.e., the difference between $|Z_2|$ (the impedance calculated from the model) and $|Z_{\text{manuf}}|$ is <25%. In fact, at frequencies below 100 kHz the differences in are <20%. However, at frequencies above f_R , the calculated curves appear to diverge and large differences result. Since this part of the manufacturer's curve has a positive slope, i.e., is inductive, $|Z_2|$ was calculated at two additional frequencies as shown in Table 2. These two frequencies are higher than the manufacturer's curve extends but they show that the calculated $|Z_2|$ curve does begin to increase at higher frequencies. In other words, the minimum on the calculated $|Z|$ vs f curve is at a higher frequency than on the manufacturer's $|Z|$ vs f curve. It is, therefore, concluded that using this specific variation of the engineering approximation approach (Modeling Technique #2A) yields a model whose resonance frequency is too high.

3.2.3 Application of Technique #2B

To more accurately describe the resonance frequency behavior of Component A1, a further refinement was made using a second variation of the engineering approximation approach. It is the same as Technique #2A except that f_R is determined by drawing an asymptote to the published $|Z|$ vs f curve on each side of the minimum and then selecting the intersection of these two asymptotes as f_R .

TABLE 2

MAGNITUDE OF IMPEDANCE OF MODEL RESULTING
FROM TECHNIQUE #2A FOR COMPONENT A1

Frequency (Hz)	$ Z_{\text{manuf}} $ (Ω)	$ Z_2 = Z_1 $ (Ω)	ϵ^* (%)
1×10^2	$\approx 17 \text{ k}$	15.9 k	-6.5
5×10^2	3 k	3.18 k	+6.0
1×10^3	1.4 k	1.59 k	+13.6
5×10^3	310	324	+4.5
1×10^4	170	167	-1.8
5×10^4	55	45.8	-16.7
1×10^5	34	31.8	-6.5
5×10^5	15	18.5	+23.3
1×10^6	13	15.3	+17.7
5×10^6	10	10	0
1×10^7	10	8.41	-15.9
5×10^7	17	6.37	-62.5
1×10^8	25	7.85	-68.6
5×10^8	--	31.9	--
1×10^9	--	63.5	--

$$*\epsilon = \frac{|Z_2| - |Z_{\text{manuf}}|}{|Z_{\text{manuf}}|} \times 100\%$$

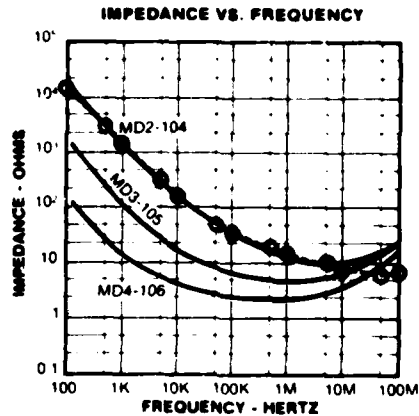


Figure 5. Calculated $|Z|$ of Model Resulting from Technique #2A for Component A1 Plotted on Manufacturer's Curve.

3.2.3.1 Modeling Procedure

Steps 1 and 2 - Same as Steps 1 and 2 of Technique #2A.

Step 3 - Since the impedance curve is increasing with increasing frequency above approximately 5 MHz, it is assumed that the component is inductive at these frequencies. Thus, the asymptote to the curve at these frequencies will represent $X_L = \omega L$ and will have a slope of +6 dB/octave (+20 dB/decade)*. In order to determine the location of this asymptote, it is necessary to extrapolate the MD2-104 curve to frequencies above 100 MHz as shown in Figure 6. The high frequency asymptote is then drawn, as line "B" in Figure 6, tangent to the extrapolated curve and with a slope of +20 dB/decade. The resonance frequency is then assumed to be the frequency at which the low frequency ("A") and the high frequency ("B") asymptotes cross. Thus, from Figure 6,

$$f_R = 2.6 \text{ MHz}$$

Then calculate L from

$$\begin{aligned} L &= \frac{1}{(2\pi f)^2 C} \\ &= \frac{1}{[2\pi(2.6 \times 10^6)]^2 (0.1 \times 10^{-6})} \\ &= 37.5 \text{ nH} \end{aligned}$$

* For a detailed discussion of the construction and interpretation of these asymptotes, see Section 4.0.

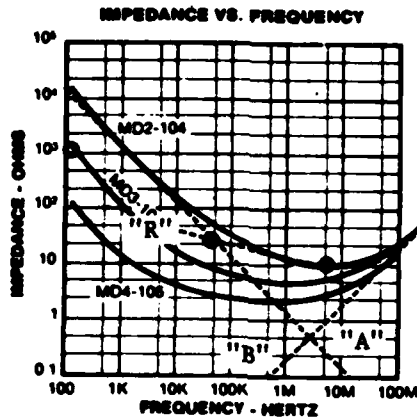
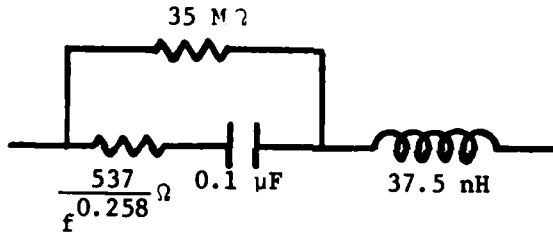


Figure 6. Extrapolated Manufacturer's Curve for Component A1 with Asymptotes.

Step 4 - Same as Step 4 of Technique #2A.

Step 5 - Draw the circuit for the resulting model:



3.2.3.2 Analysis of Technique #2B

As expected the only difference between the model produced by Technique #2B and the model produced by Technique #2A is the value of L. As shown before, R_p is large enough that it can be neglected. The magnitude of the impedance ($|Z|$) of the above model is given in Table 3 and Figure 7. With this modeling technique, the accuracy of the resulting model is greatly improved; the difference between the magnitudes of the calculated impedance ($|Z|$) and of the impedance from the manufacturer's curve ($|Z_{manuf}|$) is less than 25% at all analysis frequencies. Also, visual examination of the curves for the two sets of data in Figure 7 indicates that they are within the width of a line of being the same. Therefore, this modeling technique (#2B) provides the most accurate model for capacitor A1 and it (omitting R_p) is:

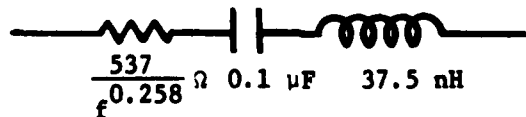


TABLE 3

MAGNITUDE OF IMPEDANCE OF MODEL RESULTING FROM TECHNIQUE #2B FOR COMPONENT A1

Frequency (Hz)	$ Z_{\text{manuf}} $ (Ω)	$ Z ^*$ (Ω)	ϵ (%)
1×10^2	$\approx 17 \text{ k}$	15.9 k	-6.5
5×10^2	3 k	3.18 k	+6
1×10^3	1.4 k	1.59 k	+13.6
5×10^3	310	324	+4.5
1×10^4	170	167	+1.8
5×10^4	55	45.8	-16.7
1×10^5	34	31.8	-6.5
5×10^5	15	18.4	+23
1×10^6	13	15.3	+18
5×10^6	10	10.1	+1
1×10^7	10	8.68	-13
5×10^7	17	13	-24
1×10^8	25	24	-4

* $|Z|$ is the magnitude of the impedance calculated from the model

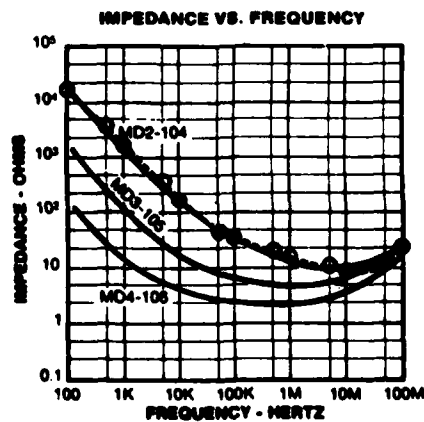


Figure 7. Calculated $|Z|$ of Model Resulting from Technique #2B for Component A1 Plotted on the Manufacturers' Curve.

It is noted that the series resistor resulting from this modeling technique is frequency dependent. One possible way of simplifying the resulting model is to assume that this resistance is constant with frequency; this simplification is the basis for Technique #2C.

3.2.4 Application of Technique #2C

One final variation of the engineering approximation approach for Component A1 was investigated. This modeling technique assumes that the series resistance in the model resulting from Technique #2B is a constant.

3.2.4.1 Modeling Procedure

Steps 1 through 3 - Same as Steps 1 through 3 for Technique #2B.

Step 4 - Since R_s must be $\leq 10 \Omega$ @ 5 MHz ($|Z_{\text{manuf}}|_{\text{min}}$), assume that

$$\begin{aligned} R_s &= \text{a constant} \\ &= |Z_{\text{manuf}}|_{\text{min}} \\ &= 10 \Omega \end{aligned}$$

Step 5 - Draw the circuit for the resulting modeling neglecting R_p for the reasons given previously (i.e., it is large compared to the impedance of the elements it is in parallel with):



3.2.4.2 Analysis of Technique #2C

This simplification does not reduce element count in the resulting model; however, it does change the resistance from a frequency dependent element to a constant (which may make it more usable in computer-aided circuit analyses). Therefore, its impedance was calculated and compared with $|Z_{\text{manuf}}|$ to determine the effect of the simplification on the accuracy of the resulting model. The calculated impedance ($|Z|$) is compared with $|Z_{\text{manuf}}|$ in Table 4 and Figure 8. This comparison indicates that the difference in impedance

TABLE 4

MAGNITUDE OF IMPEDANCE OF MODEL RESULTING FROM TECHNIQUE #2C FOR COMPONENT A1

Frequency (Hz)	$ Z_{\text{manuf}} $ (Ω)	$ Z $ (Ω)	ϵ (%)
1×10^2	$\approx 17 \text{ k}$	15.9 k	-6.5
5×10^2	3 k	3.18 k	+6
1×10^3	1.4 k	1.59 k	+13.6
5×10^3	310	318	+2.6
1×10^4	170	115	-32.4
5×10^4	55	33.4	-39.3
1×10^5	34	18.8	-44.7
5×10^5	15	10.5	-30.0
1×10^6	13	10.1	-22.3
5×10^6	10	10	0
1×10^7	10	10.2	+2.0
5×10^7	17	15.4	-9.4
1×10^8	25	25.6	+2.4

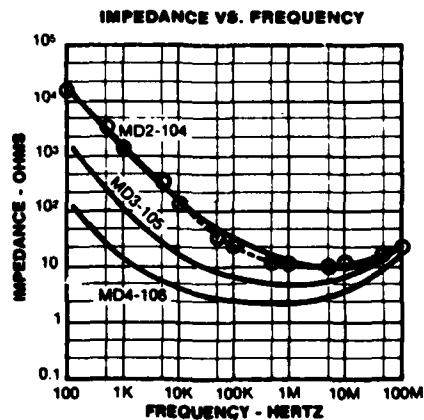


Figure 8. Calculated $|Z|$ of Model Resulting from Technique #2C for Component A1. Plotted on the Manufacturers' Curve.

increases from $\approx 20\%$ (Table 3) to $\approx 40\%$ (Table 4) at one to two frequency decades below f_R but decreases from $\approx 20\%$ to $\approx 10\%$ at frequencies greater than f_R . Thus, simplifying the resulting model for the capacitor by using a modeling technique that assumes the series resistance to be constant instead of a function of frequency considerably improves the accuracy of the model at frequencies above resonance and significantly compromises the accuracy at frequencies immediately below resonance. Even though the accuracy is decreased at some frequencies, the difference between the calculated $|Z|$ and $|Z_{\text{manuf}}|$ is less than 45% at all the analysis frequencies.

3.3 Modeling and Analysis of Remaining Capacitors

The detailed modeling and analysis described in the preceding paragraphs have shown that the use of the direct calculation approach for modeling capacitors does not result in an accurate model at higher frequencies; however, variations of the engineering approximation approach can produce relatively accurate models. To confirm this conclusion, several of the remaining selected capacitors were modeled using both approaches and the resulting models were analyzed. The results of these analyses are comparable to the results discussed in the preceding paragraphs.

Applying the engineering approximation approach to other capacitors required some additional variations in the specific steps. The major reason for these variations is that the different manufacturers do not provide the same type data nor data over the same frequency range (see Appendix A). For example, the $|Z|$ vs f curve for capacitors B1, B2, and B3 only goes to 1 MHz and the minimum of this curve is not shown. Therefore, the minimum value of $|Z|$ and the resonance frequency can not be determined. However, for these components a curve of effective series resistance (ESR) is also given. Hence, R_s can be determined from a straight line approximation to the ESR curve. The most detailed model that can be obtained via these techniques is thus



For the three "B" capacitors, the values of R_s and C were calculated to be

Capacitor	C (μF)	R_s (Ω)
B1 - 0.1 μF (50V)	0.1	$182 f^{-0.191}$
B2 - 3.3 μF (50V)	3.3	$1.61 f^{-0.103}$
B3 - 56 μF (6V)	56	$0.356 f^{-0.077}$

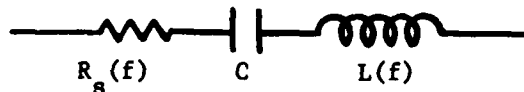
For some of the other capacitors, a $|Z|$ vs f curve is not available from the manufacturers. However, some manufacturers do provide a curve of the change in C as a function of frequency (ΔC vs f). Another variation of the engineering approximation approach can be used with this data to determine the series inductance for the model as follows:

- o Assume the ΔC vs f curve is a plot of the change in the equivalent capacitance (C_{eq}) as a function of frequency.
- o Assume the model is an CLR series circuit as has been shown to be the case with other capacitors.
- o Then, the reactance of the C_{eq} should be the same as the reactance of the model, or

$$-\frac{1}{\omega C_{eq}} = -\frac{1}{\omega C} + \omega L$$

$$L = \frac{1}{\omega^2} \left(\frac{C_{eq} - C}{C_{eq} C} \right)$$

This technique was used for capacitors such as B3 and C1. It gives the following model configuration:



where the methods for calculating R_s and C have been described previously for the three "B" capacitors. For capacitors B3 and C1, the following element values were calculated:

Capacitor	$\frac{C}{(\mu F)}$	$\frac{L}{(H)}$	$\frac{R_s}{(\Omega)}$
B3 - 56 μF (6V)	56	0.111 $f^{-1.3}$	0.356 $f^{-0.077}$
C1 - 4.7 μF (20V)	4.7	0.652 $f^{-1.4}$	1.05*

3.4 Modeling and Analysis of Inductors

The majority of the manufacturers of inductors do not furnish impedance data (or curves) as a function of frequency. In fact, of all the manufacturers' data surveyed in Appendix A, none of the inductor manufacturers have $|Z|$ vs f curves available. The only data given as a function of frequency is the quality factor (Q); Q vs f is available for approximately 20% of the surveyed components. Furthermore, when Q vs f is given, it typically covers only a small frequency range around resonance. Since data describing the overall characteristics of the inductor as a function of frequency is not available, the engineering approximation approach can not be used for modeling inductors. Even though the direct calculation approach can be used with manufacturers' data to model inductors, it is not possible to assess the merits of the various modeling techniques nor determine the accuracy of the resulting model since the $|Z|$ vs f type data is not available with which to compare.

For these reasons, only limited modeling of inductors was performed to basically illustrate how the direct calculation approach would be applied. To illustrate the application of this approach, the modeling of one inductor is presented. Component S1 is a 0.1 μH Torotel TA subminiature RF coil. The data given by the manufacturer is

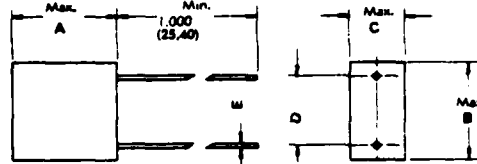
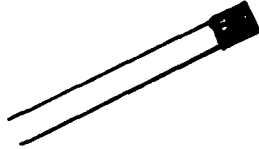
$$\begin{array}{ll}
 L = 0.1 \mu H \quad 10\%; & Q_{\text{typical}} \text{ vs } f \text{ (8 MHz to 50 MHz);} \\
 f_{R \text{ min}} = 450 \text{ MHz;} & Q_{\text{min}} @ 25 \text{ MHz} = 60; \\
 R_{dc \text{ max}} = 0.04 \Omega; & \text{Core} = \text{powered iron}
 \end{array}$$

This data is shown in Figure 9. The direct calculation approach for modeling inductors consists of the following steps:

* Since the $|Z|$ vs f curve does not extend below f_R by more than one-half of one frequency decade, the $f_{3 \text{ dB}}$ point can not be determined and a line for R_s can not be determined. Therefore, R_s was assumed to be a constant equal to $|Z_{\text{manuf}}|_{\text{min}}$.



MINI-L ENCAPSULATED INDUCTORS

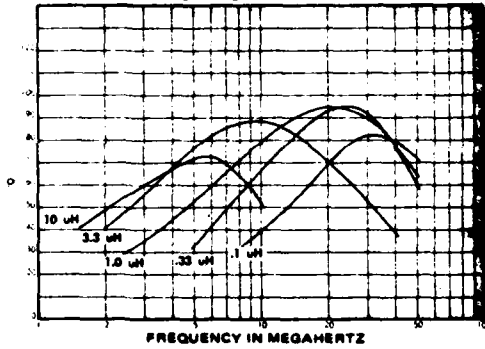


TYPE	A	B	C	D	E
TA-TF	225 (8.72)	210 (8.33)	110 (2.79)	100 (2.54)	020 (.51)
TB	300 (7.62)	280 (7.11)	160 (4.08)	200 (5.08)	025 (.64)
TD	350 (8.91)	350 (8.91)	197 (5.00)	200 (5.08)	025 (.64)

TA SERIES

- FREQUENCY RANGE: 1 TO 50 MHz.
- INDUCTANCE TOLERANCES: LESS THAN 1.0 μH , $\pm 10\%$. GREATER THAN OR EQUAL TO 1.0 μH , $\pm 5\%$. CLOSER TOLERANCES AVAILABLE BY SPECIAL REQUEST.
- INDUCTANCE TC: $+30$ PPM/ $^{\circ}\text{C}$ MAXIMUM.
- MAXIMUM POWER DISSIPATION: 0.2 WATT.
- LEADS: 1 INCH MINIMUM AWG 24 TINNED COPPER WIRE. ADD SUFFIX "D" TO PART NUMBER FOR WELDABLE GOLD PLATED DUMET LEADS.
- METHOD OF MEASUREMENT: APPARENT INDUCTANCE MEASURED ON BOONTON 260-A "Q" METER WITH LEADS CONNECTED $\frac{1}{4}$ INCH FROM INDUCTOR BODY DIRECTLY TO "Q" METER TERMINALS. RESIDUAL "Q" METER INDUCTANCE OF 0.01 μH SHOULD BE SUBTRACTED FROM READING.
- MIL-C-15305, GRADE 1, CLASS B

TYPICAL "Q" VS FREQUENCY

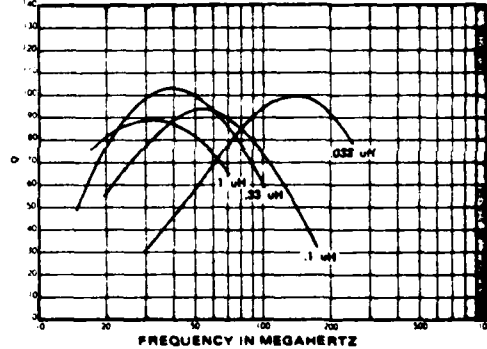


PART NUMBER	APPARENT INDUCTANCE (μH)	MINIMUM "Q"	TEST FREQUENCY (MHz)	MINIMUM SWR	MAXIMUM QCR (ohms)	DC CURRENT (mA)
*TA 1	0.10	60	25	430	0.04	2230
*TA 2	0.12	60	25	410	0.05	2000
*TA 3	0.15	65	25	330	0.06	1825
*TA 4	0.18	65	25	325	0.07	1675
*TA 5	0.22	65	25	300	0.08	1550
*TA 6	0.27	65	25	280	0.08	1475
*TA 7	0.33	65	25	260	0.10	1400
*TA 8	0.39	70	25	240	0.11	1325
*TA 9	0.47	70	25	220	0.15	1125
*TA 10	0.56	70	25	200	0.20	1000
*TA 11	0.68	70	25	180	0.25	900
*TA 12	0.82	70	25	165	0.30	810
*TA 13	1.0	70	25	150	0.35	750
*TA 14	1.2	65	7.9	130	0.25	675
*TA 15	1.5	65	7.9	120	0.30	600
*TA 16	1.8	65	7.9	110	0.30	600
*TA 17	2.2	65	7.9	100	0.75	500
*TA 18	2.7	65	7.9	90	0.90	450
*TA 19	3.3	65	7.9	70	1.0	425
*TA 20	3.9	65	7.9	60	1.2	400
*TA 21	4.7	60	7.9	50	1.5	350
*TA 22	5.6	60	7.9	45	1.7	325
*TA 23	6.8	60	7.9	40	2.0	300
*TA 24	8.2	60	7.9	37	2.4	290
*TA 25	10.0	60	7.9	35	2.6	280

TF SERIES

- FREQUENCY RANGE: 25 TO 300 MHz.
- INDUCTANCE TOLERANCES: LESS THAN 0.1 μH , $\pm 20\%$. GREATER THAN OR EQUAL TO 0.1 μH , $\pm 10\%$. CLOSER TOLERANCES AVAILABLE BY SPECIAL REQUEST.
- INDUCTANCE TC: $+200$ PPM/ $^{\circ}\text{C}$ MAXIMUM.
- MAXIMUM POWER DISSIPATION: 0.2 WATT.
- LEADS: 1 INCH MINIMUM AWG 24 TINNED COPPER WIRE. ADD SUFFIX "D" TO PART NUMBER FOR WELDABLE GOLD PLATED DUMET LEADS.
- METHOD OF MEASUREMENT: APPARENT INDUCTANCE MEASURED ON BOONTON 190-A "Q" METER WITH LEADS CONNECTED $\frac{1}{4}$ INCH FROM INDUCTOR BODY DIRECTLY TO "Q" METER TERMINALS. RESIDUAL "Q" METER INDUCTANCE OF 0.0026 μH SHOULD BE SUBTRACTED FROM VALUE CALCULATED FROM C AND F READINGS.
- MIL-C-15305, GRADE 1, CLASS B

TYPICAL "Q" VS FREQUENCY



PART NUMBER	APPARENT INDUCTANCE (μH)	MINIMUM "Q"	TEST FREQUENCY (MHz)	MINIMUM SWR	MAXIMUM QCR (ohms)	DC CURRENT (mA)
*TF 1	0.01	60	150	1000	0.02	3100
*TF 2	0.012	60	150	900	0.02	3100
*TF 3	0.015	60	150	800	0.02	3100
*TF 4	0.018	60	150	1000	0.02	3100
*TF 5	0.022	60	150	900	0.02	3100
*TF 6	0.027	60	150	800	0.02	3100
*TF 7	0.033	60	150	750	0.02	3100
*TF 8	0.039	60	150	700	0.02	3100
*TF 9	0.047	60	150	650	0.02	3100
*TF 10	0.056	60	150	600	0.02	3100
*TF 11	0.068	60	150	550	0.03	2900
*TF 12	0.082	60	150	500	0.03	2500
*TF 13	0.10	60	150	450	0.04	2200
*TF 14	0.12	60	150	400	0.05	2000
*TF 15	0.15	60	150	350	0.06	1800
*TF 16	0.18	60	150	320	0.07	1650
*TF 17	0.22	60	150	300	0.08	1500
*TF 18	0.27	60	150	280	0.10	1400
*TF 19	0.33	60	150	260	0.12	1300
*TF 20	0.39	60	150	240	0.15	1150
*TF 21	0.47	60	150	220	0.20	1000
*TF 22	0.56	70	150	200	0.25	900
*TF 23	0.68	70	150	180	0.30	800
*TF 24	0.82	70	150	160	0.35	750
*TF 25	1.0	70	150	150	0.40	700

*DISTRIBUTOR ITEM

Reprinted courtesy of Torotel, Inc.

Figure 9. Data Sheet for Component S1 (Part Number TA-1, 0.1 μH inductor).

Step 1 - Assume the configuration of the model is as given in Figure 1(b).

Step 2 - Assume L is the cardinal value of the inductor; then

$$L = 0.1 \mu\text{H}$$

Step 3 - Calculate C from the resonance frequency (f_R) (since the given f_R is a minimum, the calculated value for C will be a maximum):

$$f_R = \frac{1}{2\pi\sqrt{LC}} \quad (10)$$

Therefore,

$$\begin{aligned} C_{\text{max}} &= \frac{1}{(2\pi f_{R \text{ min}})^2 L} \\ &= \frac{1}{[2\pi(450 \times 10^6)]^2 (0.1 \times 10^{-6})} \\ &= 1.25 \times 10^{-12} \\ &= 1.25 \text{ pF} \end{aligned}$$

Step 4 - Calculate R from Q_{min} @ 25 MHz (since the given value of Q is the minimum at 25 MHz, the calculated value of R will be the maximum value at 25 MHz):

$$Q = \frac{\omega L}{R} \quad (11)$$

Thus,

$$\begin{aligned} R_m(25 \text{ MHz}) &= \frac{\omega L}{Q_{\text{min}}(25 \text{ MHz})} \\ &= \frac{2\pi(25 \times 10^6)(0.1 \times 10^{-6})}{60} \\ &= 0.262 \Omega \\ &= 262 \text{ m}\Omega \end{aligned}$$

If Q_{min} at one frequency was the only data given for the quality factor (as is the case for approximately 80% of the inductors surveyed in Appendix A), there are two possible ways of proceeding beyond Step 4. The first possibility is to assume that R is a constant and equal to R_{max} (at 25 MHz). The second possibility is to approximate R by a straight line through $R_{\text{dc max}}$ and R_{max} (25 MHz) as follows:

$$\begin{aligned}
R &= \frac{R_{\max}(25 \text{ MHz}) - R_{\text{dc}}}{25 \text{ MHz} - 0} f + R_{\text{dc}} & (12) \\
&= \frac{0.262 - 0.04}{25 \times 10^6} f + 0.04 \\
&= 8.88 \times 10^{-9} f + 4 \times 10^{-2}
\end{aligned}$$

The available data is insufficient to analyze the accuracy of the models resulting from these two alternatives. However, based upon the analyses of capacitor modeling techniques presented previously, it is likely that the first way will result in an inaccurate model. Also, it is concluded that the second possibility, even though it is probably more accurate than the first, is unlikely to result in an accurate model since both values of R used in determining the equation for R are maximums.

If a curve of Q vs f is given, as is the case for S1, then R can be calculated as a function of frequency in Step 4. The resulting curve of R vs f can then be approximated by a straight line or by a parabola. A second-order equation describing the resistance of an inductor as a parabola has been set forth [7] as follows:

$$R = L(k_1 + k_2 f^2) \quad (13)$$

where L = cardinal value of inductance,
 k_1 = a dc resistance factor, and
 k_2 = an eddy current factor

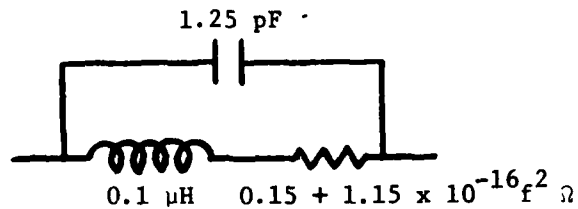
This equation as applied to the illustrative example becomes

$$R = 0.15 + 1.15 \times 10^{-16} f^2 \quad (14)$$

where k_1 and k_2 were evaluated using

$$\begin{aligned}
R(8 \text{ MHz}) &= 157 \text{ m}\Omega, \text{ and} \\
R(50 \text{ MHz}) &= 436 \text{ m}\Omega
\end{aligned}$$

(These two values of R were calculated from the values of Q at these frequencies as determined from the Q vs f curve.) The model resulting from this technique is



The Q calculated from this model is shown as dotted line "A" in Figure 10.

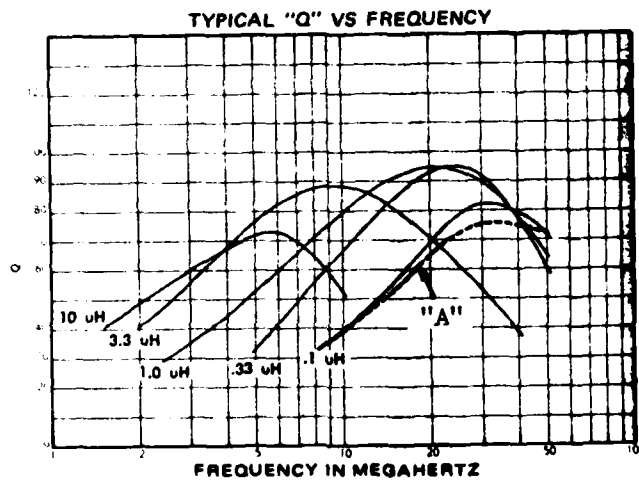
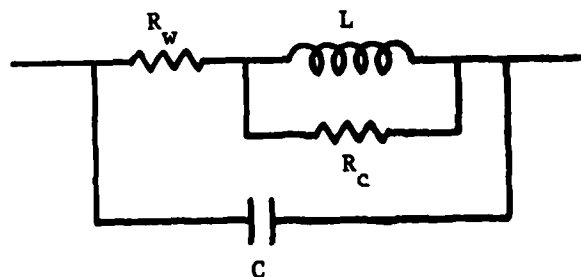


Figure 10. Calculated Q (line "A") for Model of Inductor S1 Obtained by Assuming R_s to be a parabola.

One final technique for modeling inductors when a curve of Q vs f is given has been documented by Bourns, Inc. [8]. Using this technique, the circuit configuration for the model is



where R_w = the winding loss

$$= \frac{\omega_{\max} L}{2Q_{\max}} \quad (15)$$

R_c = the core loss

$$= 4Q_{\max}^2 R_w, \text{ and} \quad (16)$$

L and C are determined as in Steps 2 and 3 on page 33. That is, L is the cardinal value of the inductance and C is calculated from L and the resonance frequency (f_R). In Equation 15, ω_{\max} is the frequency at which Q is a maximum and, hence, does not necessarily correspond to f_R .

For inductor S1 in the preceding example

$$R_w = \frac{2\pi(32 \times 10^6)(0.1 \times 10^{-6})}{2(82)}$$

$$= 122.6 \text{ m}\Omega$$

and

$$R_c = 4(82)^2(122.6 \times 10^{-3})$$

$$= 3.3 \text{ k}\Omega$$

Thus, the resulting model is shown above with the following values for the elements:

$$L = 0.1 \text{ }\mu\text{H}$$

$$C = 1.25 \text{ pF}$$

$$R_w = 122.6 \text{ m}\Omega$$

$$R_c = 3.3 \text{ k}\Omega$$

The total Q of this circuit is [8]

$$Q = \frac{1}{\frac{1}{Q_w} + \frac{1}{Q_c}} = \frac{Q_w Q_c}{Q_w + Q_c} \quad (17)$$

where $Q_w = \omega L/R_w$ is the low frequency part of the Q vs f curve and $Q_c = R_c/\omega L$ is the high frequency part of the Q vs f curve. This total Q was calculated and is plotted as dotted line "B" in Figure 11.

Figures 10 and 11 indicate that both the modeling technique using a parabolic representation of R and the above technique provide relatively accurate approximations to the Q vs f curve. However, it should be noted that both of the techniques increase the complexity of the resulting model. The former requires that R be a second-order function of f while the latter increases the element count in the model.

In summary, the direct calculation approach can be used to model essentially all the inductors surveyed in Appendix A. However, there is insufficient manufacturers' data to analyze the accuracy of the resulting models. For approximately 20% of the surveyed inductors, a Q vs f curve is available. Various approximation techniques can be used to determine the resistance of the model from this curve and some of them provide a relatively accurate value for Q as a function of frequency. However, their impact on the overall model is unknown since insufficient data describing the overall characteristics of the inductors is available for comparison.

3.5 Modeling and Analysis for Resistors

Approximately two-thirds of the resistor manufacturers surveyed (see Appendix A) provide data that yields the magnitude of impedance as a function of frequency. The various forms of data are identified in Table A-3 and examples of these forms are given in Figure A-3 of Appendix A. This data is generally labeled as "typical" for all the cardinal values of a given type of resistor and, in some instances, this data is only given for a limited number (sometimes one) of resistor types. Review of the data below 200 MHz indicates that except for large cardinal values of resistance the information on the impedance curves is not enough to model the resistor as more than an ideal resistor. Above 200 MHz, the data provided by manufacturers is typically in the form of $|Z|$ vs $(f \times R)$ curves; it was available for less than 15% of the resistors examined. The impedance curves that are given in the form of $|Z|$ vs $(f \times R)$ can be used to obtain the $|Z|$ vs f curve up to frequencies higher than one gigahertz, depending on the cardinal value of the resistor. (For smaller cardinal values, the upper frequency for which the curve applies

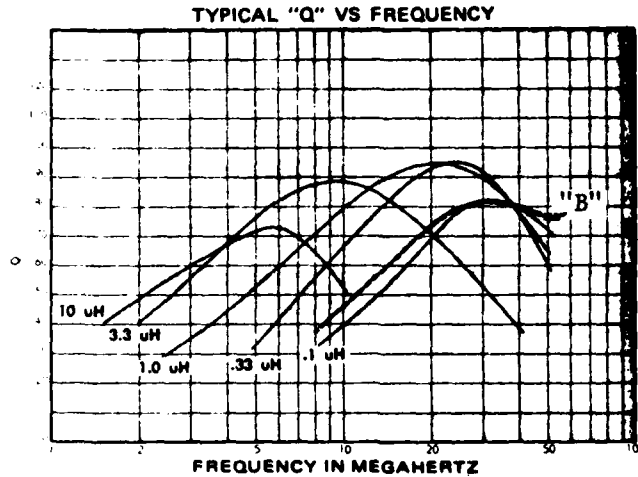


Figure 11. Calculated Q (line "B") for Model of Inductor S1 Obtained by Assuming the Existence of Two Constant-Value Resistors (R_w and R_c) in the Model.

is higher.) Again, it is noted that this data must be "typical" since only one curve is given generally for all cardinal values and all power ratings of a type of resistors.

Resistors U(1 and 2), V(1 and 2), and Y(1 and 2) (see Appendix B) were selected as resistors with manufacturers data that is representative of the three forms of impedance data illustrated in Figure A-3. Resistors U1 and U2 are 100Ω and $100\text{ k}\Omega$, respectively, 1/4-watt Allen-Bradley Type CB hot molded (carbon) composition resistors. Their available impedance data is in the form of curves of the ratio of $|Z|$ to R_{dc} versus the nominal R_{dc} for various frequencies (i.e., ($|Z|$ vs R_{dc}) @ f 's in Table A-3). This data, plus the data for the $1\text{ k}\Omega$, $10\text{ k}\Omega$, and $1\text{ M}\Omega$ resistors of the same type, are replotted in the more convenient (for modeling) form of $|Z|$ vs f in Figure 12. Impedance curves with this general shape (i.e., a constant $|Z|$ at the lower frequencies and a decreasing $|Z|$ with increasing f at the higher frequencies) imply a canonic model in the form of an ideal resistor in parallel with an ideal capacitor for a model. The ideal resistor produces the low frequency part of the curve where $|Z|$ is constant while the capacitor determines the high frequency part where $|Z|$ is decreasing with frequency. The engineering approximation steps for determining the values of the ideal resistor and capacitor are as follows:

- Step 1. Draw a horizontal asymptote to the curve at low frequencies. This asymptote represents the behavior of the ideal resistor.

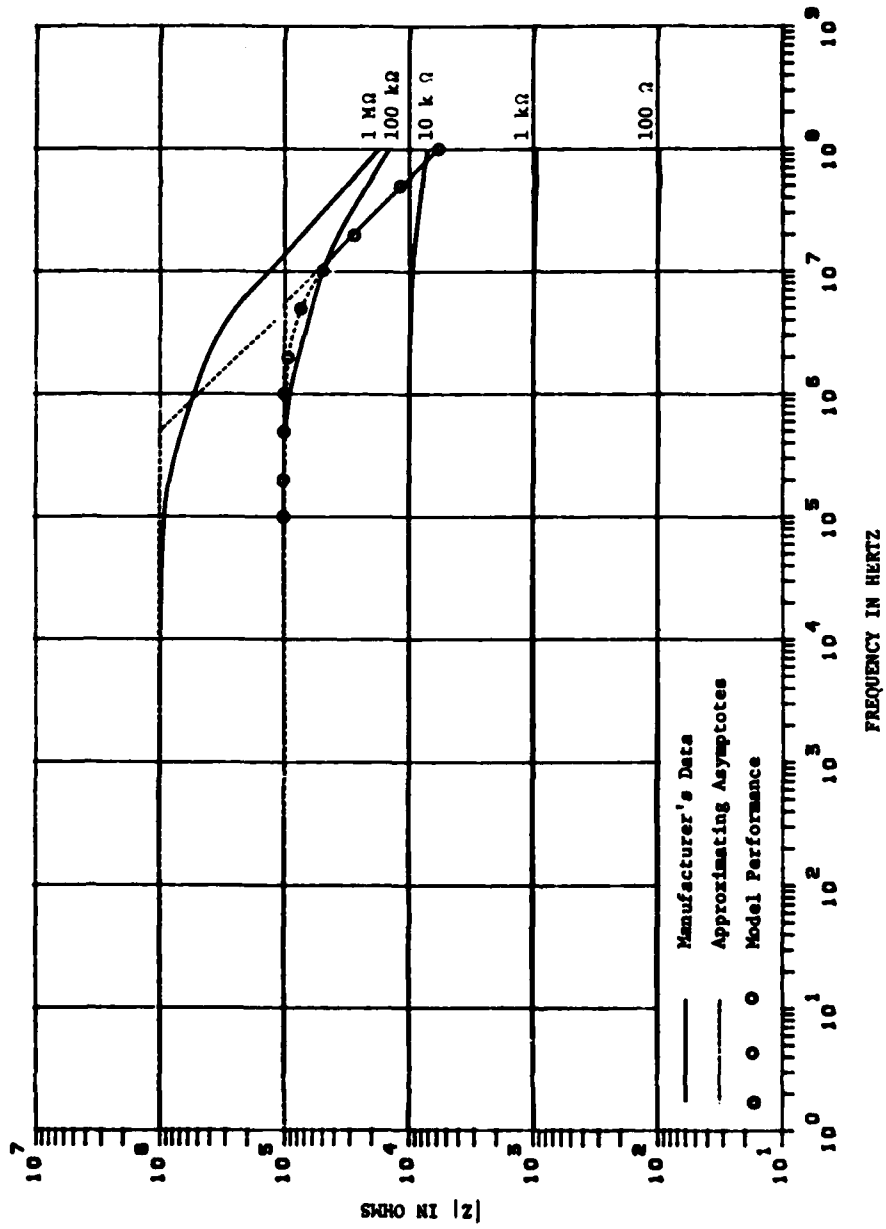


Figure 12. Modeling and Analysis Data for U-type Resistors.

Step 2. Locate $f_{3 \text{ dB}}$ which is the frequency at which the low frequency asymptote and the $|Z|$ curve differ by 3 dB. (In Figure 12, the $|Z|$ curve for the 100 k Ω resistor is 3 dB below (i.e., 0.707 of) the horizontal asymptote at 5.7 MHz. Thus, $f_{3 \text{ dB}} = 5.7 \text{ MHz}$.)

Step 3. Draw a straight line with a slope of -6 dB/octave (-20 dB/decade) that intersects the horizontal low frequency asymptote at $f_{3 \text{ dB}}$. (This line should be asymptotic to the high frequency part of the impedance curve.) This line represents the reactance of the ideal capacitor ($X_c = 1/\omega C$) in the model and, thus, the value of C can be calculated as $C = 1/\omega X_c$.

Insufficient data is available in Figure 12 to model the parasitics of resistor U1 (100 Ω) beyond an ideal resistor of 100 Ω . Therefore, the three steps above were applied to resistor U2 (100 k Ω) and the 1 M Ω resistor. (The resulting "asymptotes" are shown as dotted straight lines in Figure 12.) The straight line above $f_{3 \text{ dB}}$ that decreases at 6 dB/octave is not asymptotic to the high frequency part of the $|Z|$ curve. Even so, the technique was carried on through to define a "model" for resistor U2. For example, the straight lines drawn for resistor U2 were used to calculate the value of R and C as 100 k Ω and 0.27 pF, respectively. Next, the impedance of this "model" was calculated as a function of frequency and plotted in Figure 12 as a dotted curve with circles on it. As expected, this calculated $|Z|$ curve is tangent to the straight line approximations but is not an accurate representation of the manufacturer's $|Z|$ curve at frequencies above approximately 10 MHz. Consequently, it was concluded that this type of data is not adequate for modeling purposes.

The available impedance data for resistors V1 and V2 and resistors Y1 and Y2 are replotted as solid curves in the form of $|Z|$ vs f in Figures 13 and 14, respectively. Data for other cardinal values are also included on each graph. The three steps described above were applied to these curves. The resulting approximations are shown as dotted lines on the curves. Unfortunately, the -6 dB/octave lines are not asymptotic to any of the curves. Therefore, it appears that the manufacturers' curves for resistors do not support the generation of simple models.*

* Task 2 measurements - see Sec. 4.0 - showed that most resistors can indeed be represented by simple, three-element models.

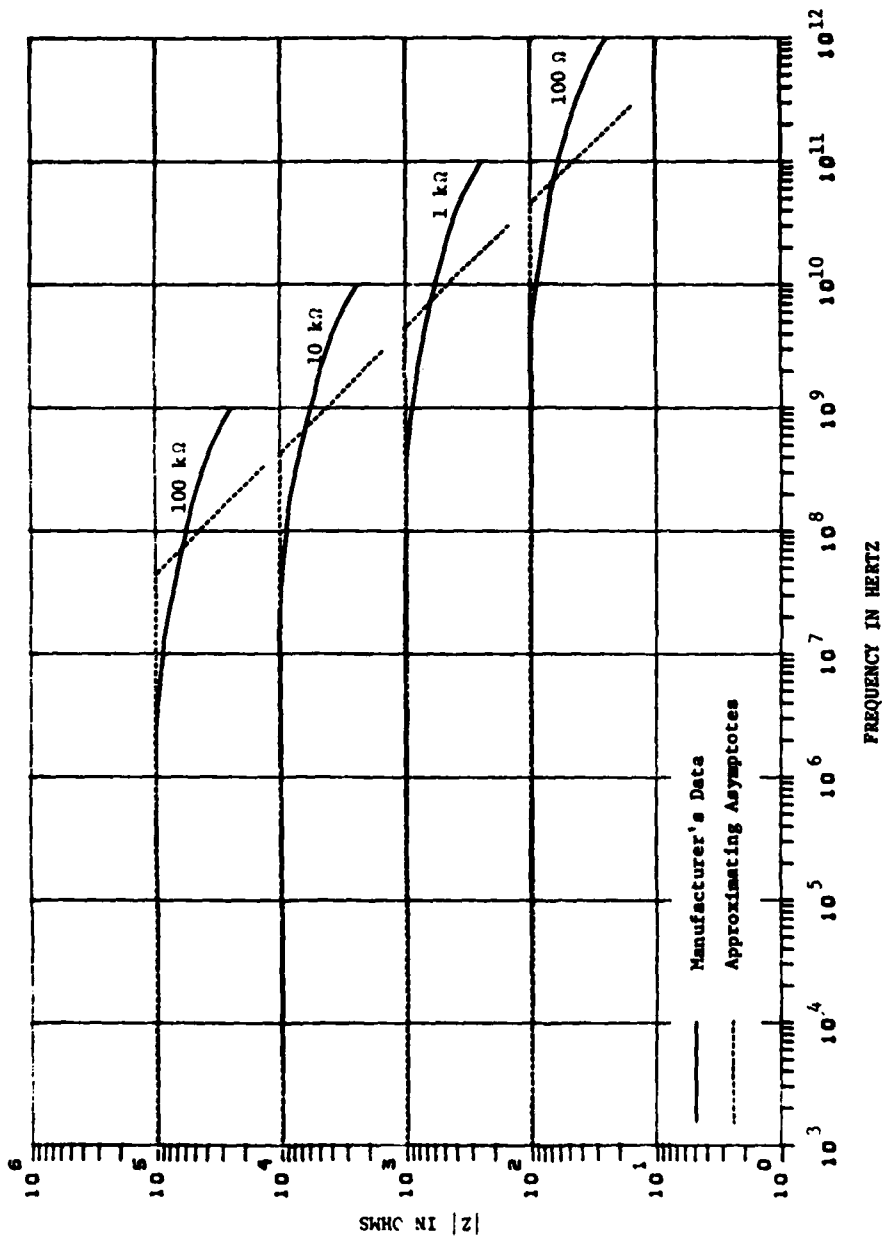


Figure 13. Modeling and Analysis Data for V-type Resistors.

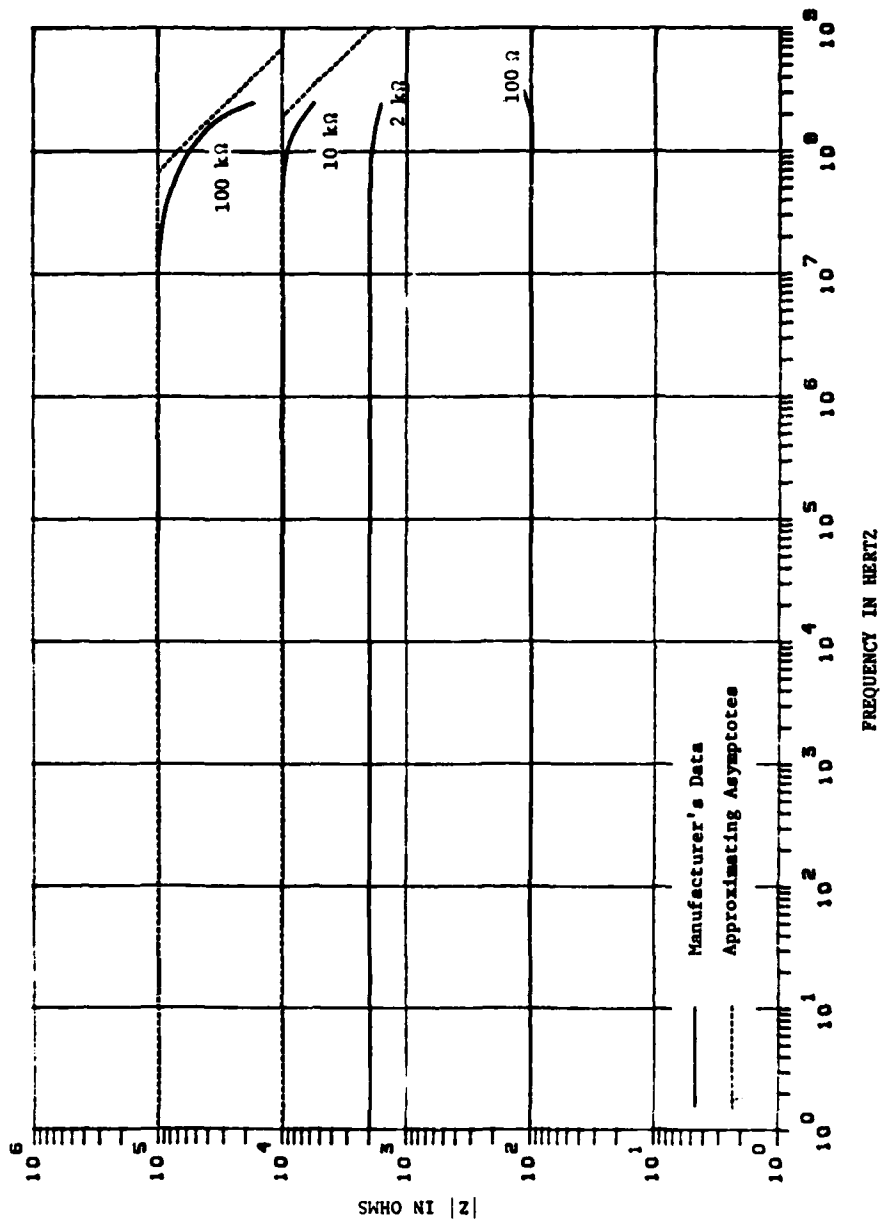


Figure 14. Modeling and Analysis Data for Y-type Resistors.

For all of the resistors examined, the difference between the straight line approximations with a -6 dB/octave slope and the $|Z|$ curves may be due to a combination of the following:

- o In general, the small size and lack of resolution of the manufacturers' curves prevent reading data accurately from these curves.
- o The manufacturers curves are, in general, labeled as "typical" and are intended to show the general shape of the impedance characteristics for a large class of resistors and, thus, are not intended to accurately depict any single component.
- o The ordinate axis of the manufacturers' curves are normally given in percent of R_{dc} . Hence, the top half of the ordinate axis represents only 6 dB on a log scale, the top 90% represents only 10 dB, while the bottom 10% represents several tens of dB. Therefore, the $|Z|$ curve in percent of R_{dc} is distorted relative to the $|Z|$ curve in dB which is most appropriate for modeling. Replotting this type of curve can introduce errors.

In summary, the resistor data available from manufacturers in general only covers a limited frequency range. Even the data that is available does not lend itself to the generation of simple models.

3.6 Observations Relative to the Modeling of Components Using Available Data

During the Task 1 modeling and analysis effort using data available from the manufacturers, several observations were made. These observations are summarized as follows:

- o Of the 53 components suggested for consideration on Task 1, the available data for only 51% could be completely modeled with the direct engineering approach. This approach could be used to partially model 38% of the selected components, but could not be used with the available data for 11% of the components.
- o The available data for only 15% of the suggested components could be completely modeled with the engineering approximation approach. This approach could be used to partially model 25% of the components and could not be used with the available data for 60% of the components.
- o When either approach is used to model capacitors, the resulting parallel resistance (R_p) can generally be eliminated from the model since normally R_p is much greater than the series resistance and the capacitive reactance that is in parallel with R_p .

- o Use of the direct calculation modeling approach for capacitors typically produces an inaccurate model at higher frequencies since the series resistance (R) is calculated from the dissipation factor (DF) at 120 Hz. This R is assumed to be a constant and its value is generally much greater than the minimum value of Z . Thus, large errors occur at the higher frequencies where the $|Z|$ curve goes through a minimum.
- o The accuracy of the models resulting from the use of the direct calculation approach with available inductor and resistor data is not expected to be significantly improved over that obtained for capacitors. Unfortunately, the information provided by the manufacturers is not sufficient to check this hypothesis; however, the reasons for these inaccuracies in the capacitor models should also apply to the inductor and resistor model. The major difference is expected to be the frequencies at which the inaccuracies occur.
- o A curve of impedance versus frequency ($|Z|$ vs f) appears to be the most appropriate type of data for modeling passive components.
- o In general, only a few manufacturers have $|Z|$ vs f data available and, when it is available, it is typically only for a limited frequency range.
- o In general, $|Z|$ vs f type data is available only for electrolytic capacitors and for resistors.
- o For electrolytic capacitors, the $|Z|$ vs f data is available only for a small percentage of the cardinal values of a given type capacitor and is generally labeled as "typical."
- o For the resistors, the $|Z|$ vs f data is generally "typical" for all cardinal values of a given type component.
- o Many of the $|Z|$ vs f curves available from manufacturers are relatively small physically. Thus, it is difficult to read them accurately. For example, an error of 0.5 mm in reading the curve for Component A1 results in an error of approximately 15% in the value of the impedance. Similarly, an error of 1 mm is equivalent to a 30% error. Thus, some of the inaccuracy in the resulting model can be due to errors in reading the manufacturers curves.
- o When a component can be modeled using manufacturers' data, the resulting model necessary to obtain relatively accurate results is a fairly simple model. In general, it has at most three ideal elements.
- o Capacitors that have a $|Z|$ vs f curve for a high enough frequency range can be accurately modeled as an RLC series circuit where:
 - C is the cardinal value

- L is determined from the resonance frequency which is determined as the intersection of the low (-6 dB/octave) and high (+6 dB/octave) frequency asymptote to the given curve
- R is a function of frequency of the form $k_1 f^{-k_2}$.
- o The capacitor model can be simplified by assuming the series resistor to be a constant that is equal to the minimum value of the $|Z|$ vs f curve; however, this assumption reduces the model accuracy.
- o In general, inductors and resistors either can not be accurately modeled using available data or the available data is insufficient to determine the accuracy of the resulting model.

4.0 MODELING AND ANALYSIS OF MEASURED DATA (TASK 2)

The survey and classification of manufacturers' data on Task 1 showed that the type of data appropriate for modeling passive components, including their parasitics, is only available over a limited frequency range for a small number of components. For this reason, Task 2 was directed toward extending the modeling techniques to 1 GHz using measured data. Thus, the specific steps on this task included defining the appropriate data requirements, developing measurement techniques for obtaining this data, selecting and measuring specific components, and developing and analyzing modeling techniques for use with the measured data.

Based on the results of Task 1, it was decided that the most appropriate data for modeling passive components is a curve of impedance as a function of frequency. This type of data completely describes the characteristics of the component; it is appropriate for use with the engineering approximation modeling approach* (see Sec. 2); and it is straightforward to obtain. In fact, potential measurement techniques appropriate for determining $|Z|$ from 5 Hz** to 1 GHz were identified and analyzed on this task. (Appropriate measurement techniques are described in Appendix C.)

A total of 68 capacitors, inductors, and resistors were selected for measurement on Task 2 (see Appendix D). Using the measurement techniques discussed in Appendix C, the magnitude and phase of the complex impedance ($|Z|$ and θ_z) were measured for each of the selected components. The measured data from the various instruments were combined into single graphs from 5 Hz to 1 GHz for $|Z|$ and θ_z . The resulting $|Z|$ vs f curves were then grouped according to their frequency characteristics. Finally, in order to reduce the amount of data handling, a representative component was selected from each group. (The definition of the various groups and the selected components

* In task 1, it was shown that this modeling approach provided more accurate models than the direct calculation modeling approach. Therefore, the engineering approximation approach was used exclusively on Task 2.

** The lower frequency of 5 Hz was used because of limitations of the measurement instrument; however, if required, the $|Z|$ vs f curve can be extrapolated down to 1 Hz.

identified in Appendix D. The associated $|Z|$ vs f curves are presented (see Figures 9-1 through 9-17.)*

For each of the three types of components, the $|Z|$ vs f curves in Appendix D can be generalized to produce generic curves.** These generic curves were used to illustrate the application of engineering approximation to the measured data. The generic $|Z|$ curves for the measured capacitors, inductors, and resistors are given in Figures 15, 16, and 17, respectively. (Note that no generic curves are required to represent the resistor data.) Variations

The curves resulting from the measured data have discontinuities at the common frequencies where the various measurement systems overlap, particularly the network analyzer system (e.g., see the representative curves given in Appendix D). It appears that the discrepancies in the measured data are due to the different parasitics associated with the various instrumentation systems, their cabling, and the component mounts. These instrumentation parasitics will exist at all frequencies even though their effects are observed only at the common measurement frequencies. The presence of these parasitics is considered to be responsible for the resonance behavior exhibited by some of the measured impedance curves obtained with the reflectometer system. This conclusion is supported by the existence of parallel resonance peaks (between the parasitic inductance of the reflectometer system and component stray capacitance) in data obtained (below 500 MHz) with the reflectometer but not in data obtained with the network analyzer. A preliminary analysis of these parasitics and potential methods of removing their effects are described in Appendix E. It appears that the measured data used to develop the modeling techniques in this section includes these instrumentation parasitics. However, the techniques developed for modeling the data are valid independent of the source of the data. Whether the parasitics indicated by the data and, thus, in the resulting model are due to the component-under-test or the instrumentation is irrelevant as far as developing the modeling techniques on this program is concerned. The initial analysis in Appendix E indicates that it is feasible to account for the instrumentation parasitics and analytically reduce their effects on the measured data; however, these instrumentation parasitics need to be measured in greater detail and a more thorough investigation of these analytical procedures is necessary prior to using any of the potentially feasible data correction techniques. For this reason, modeling techniques were developed on this task using the measured data as in. At points of discontinuity, the discrepancy was either ignored by averaging the various curves or one of the curves was selected for use in the modeling and analysis. In general, when other data was in disagreement with the reflectometer data, the other data was used.

** There are three exceptions in Appendix D to the generic curves. The techniques for refining the models for these exceptions are described in Appendix

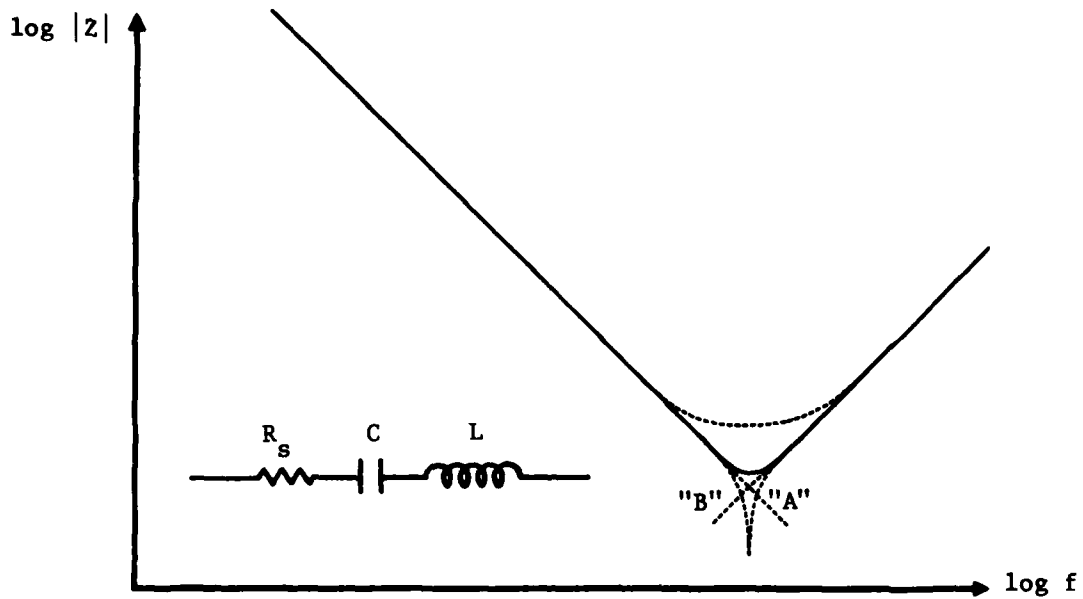


Figure 15. Generic Curve of the Magnitude of Impedance of the Measured Capacitors and Configuration of the Resulting Model.

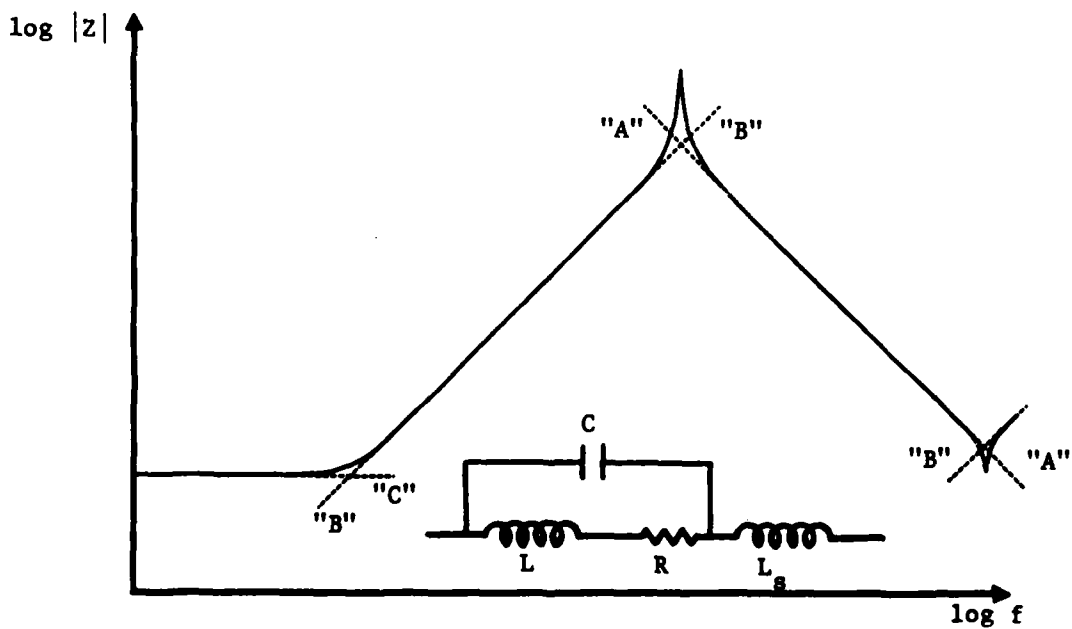


Figure 16. Generic Curve of the Magnitude of Impedance of the Measured Inductors and Configuration of the Resulting Model.

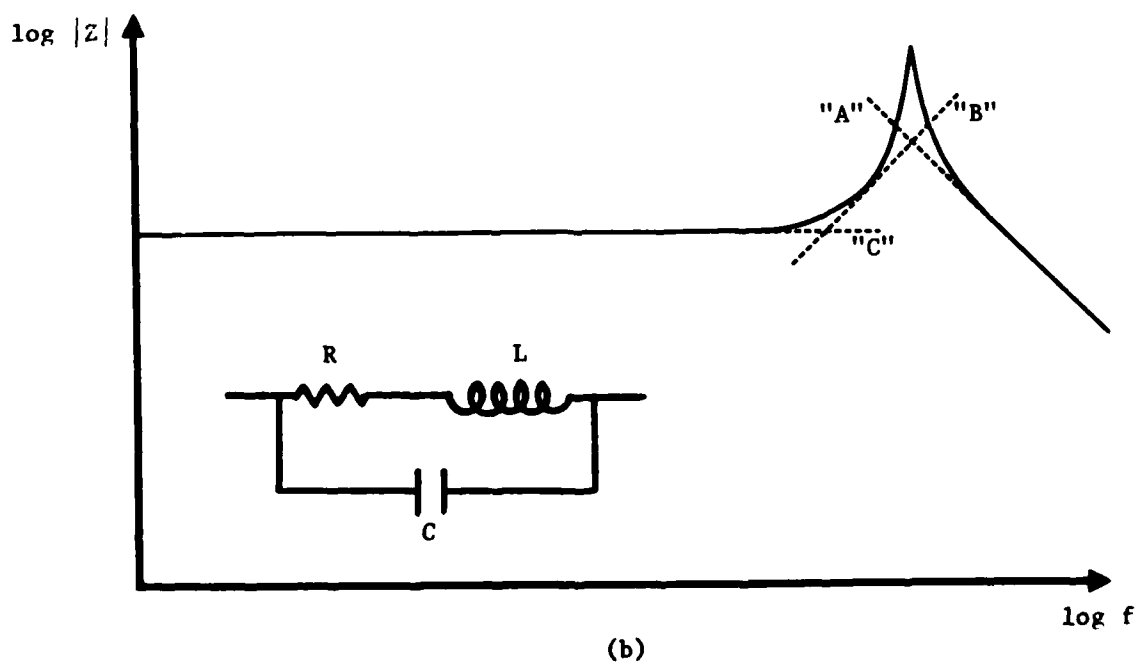
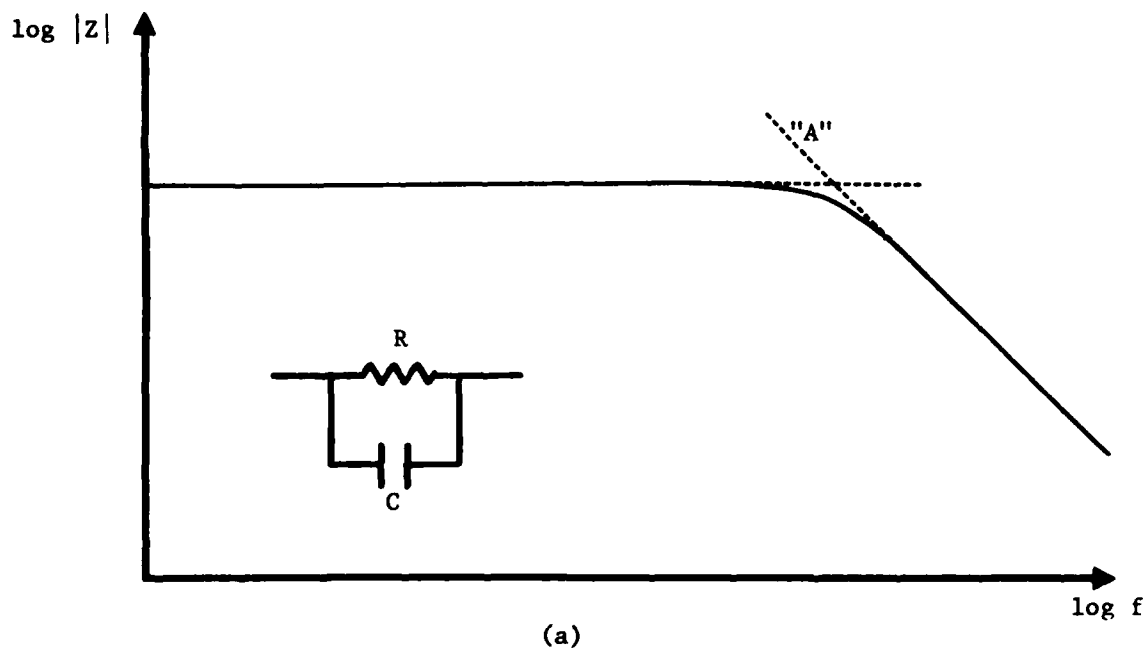


Figure 17. Generic Curves of the Magnitude of the Impedance of the Measured Resistors and Configurations of the Resulting Models.

in these generic curves do occur for different groups of components. Typically these variations involve the locations of the resonance frequencies and the sharpness of the curves at these resonances, e.g., see the dotted curves on Figure 15.

These impedance curves can be modeled using the engineering approximation approach. The resulting models consist of ideal capacitors (C), inductors (L), and resistors (R). The curves are, thus, approximated by asymptotes with slopes of -6 dB/octave representing ideal capacitors (lines "A" in Figures 15, 16, and 17), slopes of +6 dB/octave depicting ideal inductors (lines "B"), and slopes of zero (horizontal line) for ideal constant-valued resistors (lines "C"). These asymptotic approximations for the basic generic curves are illustrated in Figures 15, 16, and 17. The relative changes in the slopes of these asymptotes with increasing frequency determines the configuration in which the ideal components are interconnected. The criteria are listed in Table 5. It should be noted that when the change in slope is in a positive direction (i.e., to a more positive slope) the configuration is a series circuit while a slope change in the negative direction indicates a parallel configuration.

To accurately model the generic curves, the following guidelines are applied:

- o The asymptotes for an ideal capacitor and an ideal inductor intersect at the resonance frequency (f_R).

TABLE 5

MODEL CONFIGURATION SELECTION CRITERIA

Change in Slope with Increasing Frequency		Indicated Configuration of Model Components
From	To	
-6 dB/octave	zero	Series CR circuit
-6 dB/octave	+6 dB/octave	Series resonant LC circuit
zero	+6 dB/octave	Series RL circuit
+6 dB/octave	-6 dB/octave	Parallel resonant LC circuit
zero	-6 dB/octave	Parallel CR circuit

- o The asymptotes for an ideal resistor and an ideal inductor or capacitor intersect at the break-point frequency ($f_{3 \text{ dB}}$) where the difference between the asymptotes and the actual curve is 3 dB [5].
- o The 3 dB bandwidth of a peak or null determines the quality factor (Q) at that resonance and, hence, the associated resistance.
- o The value of the $|Z|$ curve at a series resonance (i.e., a minimum) is the value of the series resistance of the model at the resonance frequency.

Based on the above criteria, models for each of the generic curves were determined. The configurations of the resulting models are also presented in Figures 15, 16, and 17. The component values for these models are determined as follows:

- o The asymptotes representing ideal capacitors (with slopes of -6 dB/octave) are plots of $X_C = 1/\omega C$ versus f . Thus at any frequency, X_C can be determined from this straight line and the value of C can be calculated.
- o The asymptotes representing ideal inductors (with slopes of +6 dB/octave) are plots of $X_L = \omega L$ versus f . Thus, at any frequency, X_L can be determined from this straight line and the value of L can be calculated.
- o The asymptotes representing ideal constant-value resistors (zero slope) are plots of the constant R versus f . Therefore, R can be determined directly from this horizontal line.

Using the above guidelines, the representative components were modeled. The modeling techniques as well as the resulting models were analyzed in detail. The results of this modeling and analysis effort are presented in Figures D-1 through D-17. The (a) part of each figure in Appendix D is the $|Z|$ vs f curve with the ideal-component asymptotes used in the modeling techniques described above. The resulting model configuration and ideal-component values are also given on this part of the figure. In analyzing the modeling techniques and the resulting models, the $|Z|$ of the model was calculated as a function of frequency. The calculated data points are also plotted on the (a) part of each Appendix D figure. In general, the difference between these two curves is small except near resonances implying that the model

is accurate except in the vicinity of a resonance. As a measure of this difference, ϵ_Z , which is defined as

$$\epsilon_Z = \frac{|Z_{\text{calculated}}| - |Z_{\text{measured}}|}{|Z_{\text{measured}}|} \times 100\% \quad (18)$$

was calculated for each model. This curve is given as the (b) part of each figure in Appendix D for which a model was determined. If the measured data is defined as the correct value, then the ϵ_Z 's are indications of the errors resulting from use of the models, i.e., small ϵ_Z 's implies that the models are accurate. Review of these curves indicate that, in general, the difference between the $|Z|$ measured for the component and the $|Z|$ calculated from the resulting model are less than 20%, except in the vicinity of a resonance. In fact, the differences in many cases, with the above noted exception, were less than 10%. Therefore, it appears that this modeling technique (based on the criteria presented previously) results in a simple, accurate three-element model.

Using the above modeling technique, the remaining measured $|Z|$ curves were modeled to determine the range of the values of the elements in the models. Since the detailed analysis above indicates that this modeling technique results in simple, accurate models, the models resulting from all the measured data were not analyzed. The pertinent parameters* resulting from the modeling of the $|Z|$ vs f curves for 29 capacitors, 14 inductors, and 25 resistors are given in Tables 6, 7, and 8, respectively. (Characteristic models for each of these types of components are illustrated in Figures 15, 16, and 17, respectively.) Table 6 indicates that for the measured capacitors the series inductance (L) in the model range from 18 to 39 nH (the majority are between 25 and 30 nH) with a mean value of 27.2 nH. Similarly, the values of the series resistance (R) range from 0.13 to 6.8 Ω with over 80% between 0.5 and 1.3. The mean value of these R's is 1.05 Ω . Therefore, the data on the majority of the measured capacitors can be modeled fairly accurately as the cardinal capacitance in series with a 27 nH inductor and a 1 Ω resistor.

* It is to be noted that the effects of instrumentation parasitics are embedded in the derived parameters. See also discussion in Appendix E.

TABLE 6

RESULTING MODEL ELEMENTS AND DATA PARAMETERS FOR MEASURED CAPACITORS

Group #	Type of Capacitor	Cardinal Value	Manufacturer & Catalog #	C	f_R (MHz)	L (nH)	$R_s = Z_{min}$ (Ω)
1	Tantalum, Wet Sintered	10 μ F	Tansitor W10-50ClK	10.1 μ F	0.31	27	-
		15 μ F	Sprague 109D156C2075F2	13.3 μ F	0.25	26	-
		22 μ F	Sprague 109D226X0025C2	21.2 μ F	0.20	27	-
		820 μ F	Tansitor UW820-10C3M1	795.8 μ F	0.034	25	-
		10 μ F	Sprague 196D106X9035PC4	10.6 μ F	0.28	29	-
		15 μ F	Sprague 150D156X9035	15.2 μ F	0.23	29	-
2	Metalized Polyester Film	2 μ F	Sprague 431P-205	2.1 μ F	0.60	30	-
		0.47 μ F	Sprague 150D474X9035A2	0.50 μ F	1.2	30	1.3
		1.8 μ F	Sprague 196D185X9035JAI	1.77 μ F	0.8	21	1.0

(Continued)

TABLE 6 (continued)

RESULTING MODEL ELEMENTS AND DATA PARAMETERS FOR MEASURED CAPACITORS

Group #	Type of Capacitor	Cardinal Value	Manufacturer & Catalog #	C	f_R (MHz)	$\frac{L}{(nH)}$	$\frac{R_s = Z_{min}}{(\Omega)}$
3	Tantalum, Solid	0.033 μF	Sprague 150D333X0035	0.029 μF	6.3	22	6.8
	Aluminum Electrolytic	50 μF	Mallory TT25X50A	54.9 μF	0.12	30	1.0
4	Polyester	0.047 μF	CDE WMF-1S47	0.055 μF	3	27	0.9
		0.1 μF	Nytronics 197B104M	0.114 μF	3.7	25	0.54
5	Polystyrene Film	10,000 pF	Centralab CPR 10,000J	10,610.3 μF	8	37	0.77
	Ceramic	0.01 μF	Centralab DD 103	0.018 μF	6.8	30	0.78
6	Ceramic	1000 pF	Centralab DD 102	884.2 pF	32	29	1.15
	Mica	0.0047 μF	E1 Menco CM-30-E-472J	0.0047 μF	13	30	0.72
	Difilm	0.0025 μF	Sprague 6TM-D25	0.0031 μF	14	39	0.95
		0.005 μF	Sprague 6TM-D50	0.0055 μF	12.5	30	0.78

(Continued)

TABLE 6 (concluded)
 RESULTING MODEL ELEMENTS AND DATA PARAMETERS FOR MEASURED CAPACITORS

Group #	Type of Capacitor	Cardinal Value	Manufacturer & Catalog #	C	f_R (MHz)	L (nH)	$R_s = Z_{min}$ (Ω)
6	Polystyrene	3000 pF	Centralab CPR 3900J	4081 pF	13.5	35	0.66
7	Ceramic	10 pF	Centralab DD 100	11.1 pF	340	20	0.15
		20 pF	Sprague 10TCC-Q20	21.2 pF	270	18	0.13
		47 pF	Sprague 10TCC-047	53.1 pF	155	21	1.2
		200 pF	Sprague 1CFCC-T20	205.4 pF	68	27	1
	Mica, Silvered	20 pF	Arco DM-15-200J	22.7 pF	250	18	0.155
		200 pF	Arco DM-15-201J	212.2 pF	70	23	0.95
		470 pF	Arco DM-15-471J	468.1 pF	46	25	0.82
		510 pF	Sprague 424ME5100J501	530.5 pF	44	25	0.9
	Polyester	1000 pF	Nytronics 111B102K	982.4 pF	27	35	0.5

TABLE 7

RESULTING MODEL ELEMENTS AND DATA PARAMETERS FOR MEASURED INDUCTORS

Group #	Type of Inductor	Cardinal Value	Manufacturer & Catalog #	L (μ H)	R (Ω)	f R1 (MHz)	C (pF)	f R2 (MHz)	L (nH)
1	RF Choke	55 μ H	Miller 4629	51	0.79	15	2.2		
2	RF Choke	0.68 μ H	Miller 9230-16	0.68	0.47	165	1.5		
		1 μ H	Miller 4602	0.95	0.03	125	1.8		
	RF, Molded Shielded	0.1 μ H	Delevan 1641-101	0.12	0.17	400	1.3		
		0.47 μ H	Nytronics SWD-0.47	0.56	0.16	170	1.5		
		0.47 μ H	Nytronics WEE-0.47	0.4	0.1	200	1.5		
3	RF Choke	100 μ H	Miller 4632	95.5	2.5	10.5	2.3		
		100 μ H	Miller 9350-08	103.4	3.5	9	3		
	RF, Molded, Shielded	100 μ H	Nytronics WEE-100	97.5	1.6	10	2.5		
		1200 μ H	Nytronics SWD-1200	1194	15.6	3.1	2.3		

(Continued)

TABLE 7 (concluded)
 RESULTING MODEL ELEMENTS AND DATA PARAMETERS FOR MEASURED INDUCTORS

Group #	Type of Inductor	Cardinal Value	Manufacturer & Catalog #	L (μ H)	R (Ω)	f_{R1} (MHz)	C (pF)	f_{R2} (MHz)	L (nH)
3	RF, Molded	120 μ H	Nytronics DD-120	135.4	8.9	9	2.2		
4	RF Choke	3.9 mH	Miller 4668	3.7 mH	17.3	1.25	4.4	900	0.007
		100 mH	Miller 994	103.5 mH	382.5	0.17	7.6	330	0.03
	RF, Molded	10,000 μ H	Delevan 2500-76	9020	62.1	0.84	4	750	0.01

TABLE 8

RESULTING MODEL ELEMENTS AND DATA PARAMETERS FOR MEASURED RESISTORS

Group #	Type of Resistor	Cardinal Value (Ω)	Manufacturer & Catalog #	R (Ω)	f_3 dB (MHz)	L (μH)	f_R (MHz)	C (pF)
1	Metal Film	100	TRW/IRC MAR7	100	-	-	-	-
		100	Caddock MS151	100	-	-	-	-
2	Metal Film	47	Corning NA55-47R-1%	47	260* 500**	0.028* 0.015**	-	-
	Carbon Composition	56	Allen-Bradley CB5601	55	360* 590**	0.024* 0.015**	-	-
		390	Allen-Bradley CB3911	400	250	-	-	1.53
	Carbon Com- position Film	100	TRW/IRC RCR20G101KS	100	850	0.019	-	-
	Carbon Film	100	R-Ohm R-25J-100	100	970	0.018	-	-
3	Metal Film	28	Corning C4-28R-1	28	160	0.027	-	-
	Carbon Composition	2.7	Allen-Bradley CB27G1	3	16	0.3	-	-

(Continued)

TABLE 8 (continued)
 RESULTING MODEL ELEMENTS AND DATA PARAMETERS FOR MEASURED RESISTORS

Group #	Type of Resistor	Cardinal Value (Ω)	Manufacturer & Catalog #	R (Ω)	f_3 dB (MHz)	L (μ H)	f_R (MHz)	C (pF)
4	Metal Film	1.65 k	TRW/IRC MAR3	1.6 k	60	-	-	1.59
		12 k	Corning FP3-12k-10%	12 k	6.3	-	-	1.99
		50 k	Caddock MS310	49 k	1.45	-	-	2.07
		52.3 k	Corning MC65-52.3k-0.1%	52 k	1.95	-	-	1.52
		100 k	TRW/IRC AR40	99 k	0.98	-	-	1.61
	Carbon Composition	1.5 k	Allen-Bradley CBI521	1.4 k	73	-	-	1.53
	Carbon Composition Film	1 k	TRW/IRC RCR20G102KS	940	73	-	-	2.27
		10 k	TRW/IRC CR7	10 k	8.7	-	-	1.77
	Carbon Film	1 k	R-Ohm R-25J-1k	1 k	88	-	-	1.45

(Continued)

TABLE 8 (concluded)

RESULTING MODEL ELEMENTS AND DATA PARAMETERS FOR MEASURED RESISTORS

Group #	Type of Resistor	Cardinal Value (Ω)	Manufacturer & Catalog #	R (Ω)	f_3 dB (MHz)	L (μ H)	f_R (MHz)	C (pF)	
5	Wirewound	100	TRW/IRC	101	50	0.32	245	1.3	
			BW-20-100-5%						
			Sage/Nytronics	400	88	150	1.45		
		1 k	Memcor/E-Systems	990	10	15.9	28	1.83	
			VL-0010-4100						
			Ohmite	1 k	29	53	1.59		
6	Wirewound	10	Memcor/E-Systems	9.8	3.9	0.41	200	1.52	
			VL-0003-2100						
			Ohmite	10	4	205	1.52		
		25	Dale	24.7	6	0.66	175	1.22	
			RS-1B						

* Data measured with CR 1710 Network Analyzer.

** Data measured with Reflectometer System.

Table 7 shows that in general the parallel capacitance and the series resistance in the models of the measured inductors both increase with increasing cardinal inductance as follows:

<u>Cardinal Inductance</u>	<u>Parallel C (pF)</u>	<u>Series R (Ω)</u>
0.1 μ H	1.3	0.17
0.47 μ H	1.5	0.1
0.47 μ H	1.5	0.16
0.68 μ H	1.5	0.47
1 μ H	1.8	0.03
55 μ H	2.2	0.79
100 μ H	2.3	2.5
100 μ H	2.5	1.6
100 μ H	3	3.5
120 μ H	2.2	8.9
1.2 mH	2.3	15.6
3.9 mH	4.4	17.3
10 mH	4	62.1
100 mH	7.6	382.5

Thus, specific ranges of inductors can be modeled fairly accurately with values of C and values of R as follows:

<u>Range of Cardinal Values of Inductors</u>	<u>Parallel C (pF)</u>	<u>Series R (Ω)</u>
0.1 to 1 μ H	1.5	0.17
1 to 100 μ H	2.2	1.5
100 μ H to 1 mH	2.3	5
1 mH to 10 mH	4	*
10 mH to 100 mH	**	*

Except for the wirewound resistors, the data in Table 8 indicates that the series inductance in the models of the measured resistors was approximately 20 nH. The series inductance for the wirewound resistors varied considerably with the cardinal value and power rating. Similarly, the parallel capacitance of all the measured resistors varied from 1.22 to 2.27 pF with

* Representative value can not be determined.

** Insufficient data.

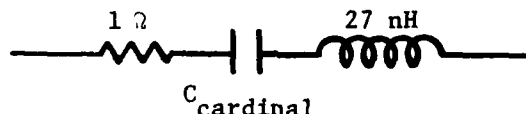
a mean value of 1.6 pF. Therefore, except for the wirewound resistors, a relatively accurate model of the measured resistors appears to be a 1.6 pF capacitor in parallel with a series combination of a 20 nH inductor and the cardinal resistance.

5.0 RECOMMENDED MODELING TECHNIQUES

The modeling and analyses based on data available from the manufacturers (Task 1) and data measured in the laboratory (Task 2) have identified the most appropriate techniques for modeling passive components. The identified modeling techniques depend on the type of data being used and the type of component being modeled. These recommended* modeling techniques are summarized as follows:

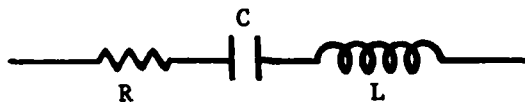
5.1. Capacitors

1. No Available Data - use the following model:



2. Available Data Does Not Include $|Z|$ vs f Curve - This category includes essentially all the capacitors with data available from manufacturers except for electrolytics. The only model that can be developed from this data is the cardinal value of capacitance in series with the resistance calculated from the dissipation factor. (Since it has been shown that this model is inaccurate at high frequencies (see Sec.3.2.1.2), it may be advisable to use the model in 1 above where only this type data is provided.)
3. Available Data Includes $|Z|$ vs f Curve - For the majority of the electrolytic capacitors, manufacturers provide a limited amount of data in this category. Also, if measurements are performed on capacitors, an impedance curve is the most appropriate data to measure. Capacitors with $|Z|$ vs f data available are modeled as follows:
 - o Draw low frequency and high frequency asymptotes to the curve with slopes of -6 dB/octave and +6 dB/octave, respectively.
 - o Use a configuration for the model of

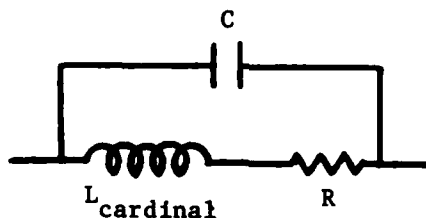
* The fixed component values (representing parasitic effects) in the models which are given for use when no (or insufficient) data is available include the effects of the parasitics inherent to the measurement systems used on this program. The existence of these instrumentation system effects should be considered when using these models. Upon determination of the magnitude of the parasitics for a particular measurement system, these fixed values should be adjusted (see Appendix E).



- o Determine the value of C from the low frequency asymptote. If this calculated C is within the tolerance of C_{cardinal} , use C_{cardinal} .
- o Determine the value of L from the high frequency asymptote or, as an alternative, determine the resonant frequency as the intersection of the two asymptotes, and then calculate L from the resonance frequency.
- o If the $|Z|$ vs f curve is symmetrical about Z_{min} on log-log graph paper, use the value of Z_{min} as R. If the $|Z|$ vs f curve is unsymmetrical then the method in Appendix F must be used to determine R as a function of frequency.

5.2. Inductors

1. No Available Data - Model the inductor as:



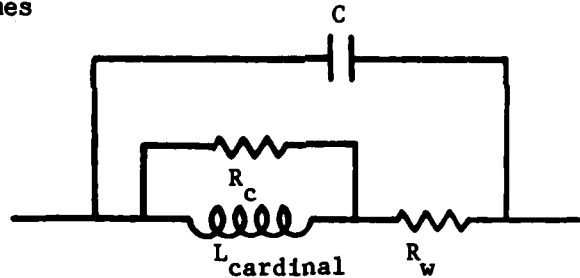
where the values of R and C depend on the value of L_{cardinal} as follows:

L_{cardinal} (μH)	C (pF)	R (Ω)
0.1 to 1.0	1.5	0.17
1.0 to 100	2.2	1.5
100 to 1000	4	5

Other values of inductors in this category can not be modeled without additional data.

2. Available Data Does Not Include $|Z|$ vs f Curve - This category includes all the inductors with data available from manufacturers. Other than the model in 1 above, the only model that can be determined from this category of data is as follows:

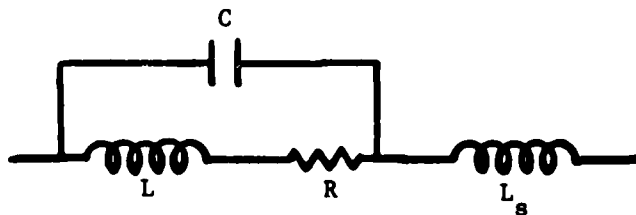
- o Assume the configuration of the model is the same as in 1 above.
- o Assume the inductance is L_{cardinal} .
- o Calculate C_{max} from the minimum resonance frequency ($f_{R \text{ min}}$) given by the manufacturer.
- o If no data related to the quality factor (Q) is given, assume that R is R_{dc} .
- o If Q_{min} @ f_i is given and a curve of Q vs f is not given, calculate R_{max} @ f_i from Q_{min} .
- o If a curve of Q vs f is given, use one of the following alternatives:
 - Calculate and plot R vs f from Q vs f using the equations in Step 4 of Sec. 3.4. Then approximate the R vs f curve as a parabola (as described in the paragraphs following Step 4 of Sec. 3.4). Note that R is a second-order function of frequency.
 - Add another resistor so that the configuration of the model becomes



where R_w (the winding loss) and R_c (the core loss) are calculated from the Q vs f curve as illustrated in Sec. 3.4.

3. Available Data Does Include |Z| vs f Curve - Inductors will have to be measured to place them in this category. They should be modeled as follows:

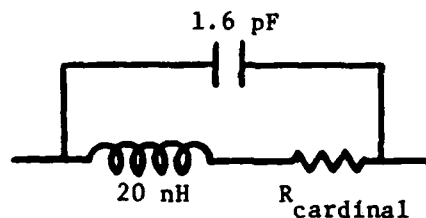
- o Draw asymptotes to curve as shown in Figure 16.
- o Use the following model:



- o Determine the value of L from the +6 dB/octave asymptote before the first resonance. If this calculated L is within the tolerance of L_{cardinal} , use L_{cardinal} .
- o Determine the value of C from the -6 dB/octave asymptote.
- o Determine the value of R from the value of the asymptote with zero slope at low frequencies. This R should be R_{dc} .
- o Determine L_s from the +6 dB/octave asymptote above the second resonance.

5.3. Resistors

1. No Available Data - Except for wirewound resistors, model as



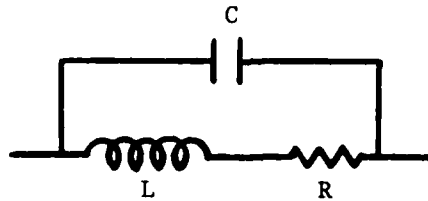
(Without additional data, wirewound resistors can not be completely modeled in this way because the value of the inductance is not known. The configuration of the models and the values of the R and C for wirewound resistors are the same as above; however, the value of the inductor in the model can not be determined for these resistors unless some additional data is obtained.)

2. Available Data Does Not Include $|Z|$ vs f^* Curve - This category includes approximately one-third of the surveyed resistors. Resistors in this category should be modeled as if no data exists.
3. Available Data Does Include $|Z|$ vs f Curve - Approximately two-thirds of the surveyed resistors had some form of data that gives the impedance as a function of frequency; however, the data does not appear to conform to the identified modeling approaches (see Sec. 3.5 for possible explanations). Therefore, this data from the manufacturers does not support the techniques described herein and, at present, the best approach appears to be either use 1 above or measure $|Z|$ vs f . Resistors for which $|Z|$ vs f has been measured are modeled as follows:

- o Draw asymptotes to the $|Z|$ vs f curve with slopes of 0, +6, and/or -6 dB/octave as illustrated in Figure 17.

* Here $|Z|$ vs f represents any form of impedance as a function of frequency as discussed in Appendix A.

- o Use a configuration for the model of



- o Determine the value of R from the horizontal (zero slope) asymptote of the $|Z|$ vs f curve. This is generally R_{dc} and is approximately $R_{cardinal}$.
- o Determine the value of L from the asymptote with a slope of +6 dB/octave. If such an asymptote does not exist, either remove L from the model or for a more accurate model assume $L = 20$ nH (see 1 above).
- o Determine the value of C from the asymptote with a slope of -6 dB/octave. If such an asymptote does not exist, either eliminate C from the model or for a more accurate model assume $C = 1.6$ pF.

(It should be noted that the majority of the components examined can be represented by simple three-element (or less) models at frequencies up to 1 GHz.)

6.0 CONCLUSIONS AND RECOMMENDATIONS

Modeling techniques for use with passive components (capacitors, inductors, and resistors) at frequencies up to 1 GHz have been developed and analyzed for accuracy and complexity. The modeling and analyses on Task 1 used data available from manufacturers whereas measured data was employed on the Task 2. As a part of the second task, measurement techniques were investigated and selected. Finally, the recommended modeling techniques for use with various types of components and data were summarized. The following general conclusions and recommendations have been formulated:

1. At frequencies up to 1 GHz, most passive components can be accurately modeled with simple 3-element models. In many cases, typical values for the parasitic elements can be assumed without measurement and usable results can be obtained.
2. The manufacturers' data appropriate for modeling components is available for only a limited number of component types and then for only a restricted frequency range. The manufacturers' data is generally labeled as "typical" and, in some cases, the curves are apparently intended to show the generic curve of the impedance for a large class of components and, thus, are not sufficiently accurate to model any single component. Many of the manufacturers' curves are physically small and do not provide sufficient resolution to permit extracting the data accurately enough to support modeling efforts.
3. The magnitude of the impedance of a passive component can be measured up to 1 GHz using currently available instrumentation.
4. The parasitics of the various measurement instrumentation systems do affect the data differently such that there are discrepancies at frequencies where the measurement systems overlap. Also, in some instances, preliminary measurements indicate that the instrumentation parasitics may be of the same order of magnitude as the parasitics of the component-under-test. Therefore, some of the variations in the measured data are due to these instrumentation parasitics. Initial investigations indicate that procedures for removing these effects (i.e., correcting the data) can be developed if sufficient measurements are performed to accurately define the instrumentation parasitics. Further studies should be performed and the resulting data correction procedures should be evaluated to ensure that the correction procedures do not impact the modeling techniques described herein.

5. Also, it is recommended that a sufficient number of additional components be measured to verify the developed data correction and modeling techniques for various cardinal values, manufacturing processes, and component types.

7. REFERENCES

1. J. J. Whalen and C. A. Paludi, Jr., "Computer-Aided Analysis of Electronic Circuits - The Need to Include Parasitic Elements," International Journal of Electronics, Vol. 43, November 1977, pp. 501-511.
2. J. J. Whalen, C. A. Paludi, Jr., and T. F. Fang, "Applications of the Nonlinear Circuit Analysis Program NCAP, "Proceedings of the 1977 IEEE International Symposium on Electromagnetic Compatibility, Seattle, WA, 2-4 August 1977, pp 467-474.
3. J. B. Valente, "The Nonlinear Circuit Analysis Program, "Proceedings of the 1977 IEEE International Symposium on Electromagnetic Compatibility, Seattle, WA, 2-4 August 1977, pp 461-466.
4. "Parasitic Effects in Discrete Passive Components," Statement of Work, PR No. N-8-5076, Contract No. F30602-78-C-0230, Rome Air Development Center, Griffiss AFB, New York, 7 December 1977.
5. M. E. Van Valkenburg, Introduction to Modern Network Synthesis, John Wiley & Sons, Inc., New York, NY, 1967.
6. W. R. Free and J. A. Woody, "Task 1 Test Plan, Parasitic Effects in Discrete Passive Components," Contract No. F30602-78-C-0230, Engineering Experiment Station, Georgia Institute of Technology, Atlanta, GA, December 1978.
7. V. G. Welsby, The Theory and Design of Inductance Coils, MacDonald & Co. (Publishers) Ltd., London, 1950.
8. The Theory and Application of Transformers and Inductors, BMP-2, Bourns, Inc., Romoland, CA.

APPENDIX A
DATA AVAILABLE FROM MANUFACTURERS

Several manufacturers have limited data that is appropriate for defining and modeling the parasitic behavior of passive components (i.e., resistors, capacitors, and inductors). The various component manufacturers were surveyed to determine the specific data available and to request samples for later measurements. In the survey, a total of 36 different manufacturers, including 74 manufacturing plants or divisions, were contacted. During each contact:

1. A catalog was requested as a minimum;
2. Any available data in addition to catalog data was requested;
3. Measurement facilities and techniques were discussed, and measurement information was requested; and
4. The possibility of obtaining sample components for later measurements was discussed.

The majority of the manufacturers' representatives contacted were very cooperative and indicated a willingness to help in any way possible. Some manufacturers have little or no data describing the parasitic behavior of their components while others have some data in addition to their published catalogs. Typical comments from manufacturers with very little data indicated that:

1. Not many customers request such data;
2. It requires too much effort to measure this data with its limited demand; and
3. The available data leaves a lot to be desired. (It is insufficient for designing on paper.)

Approximately 60 percent of the manufacturers' representatives contacted supplied current catalog information. Nearly 15 percent of them furnished data in addition to their catalogs. About 45 percent of the manufacturers forwarded sample components for use in measurements (a total of over 575 sample components were received).

The data obtained from the manufacturers, as well as some additional data available at Georgia Tech and data received from RADC, were classified and categorized according to component type.* Twenty-two tables describing the data available for 12 categories of capacitors, 6 categories of inductors, and 4 categories of resistors were presented in the Task 1 Test Plan.** These tables list several manufacturers that produce each specific category of component and the types and formats of the data they have available for that category of component. The information in these detailed tables is summarized in Tables A-4, A-5, and A-6 for capacitors, inductors, and resistors, respectively. It is apparent from these tables that data related to the parasitic behavior of a wide variety of passive components is available from the manufacturers. Most of this data is available in manufacturers' catalogs; however, the majority of it is labeled as "typical" for several (or all) values of a given type component. Furthermore, considerable variations exist in the type of data provided, in the test frequencies used, and in the frequency ranges over which the data are specified.

Typically, the maximum dc leakage and the maximum or typical dissipation factor (DF) at either 120 Hz, 1 kHz, or 1 MHz are given for all capacitors. For all nonelectrolytic capacitors except ceramics, this is the only type data available from the majority of manufacturers. For many ceramic capacitors, typical graphs of the change in capacitance (ΔC) and/or DF are also given as a function of frequency. Examples of these curves are given in Figure A-1. Instead of ΔC curves, many manufacturers of electrolytic capacitors furnish "typical" graphs of the magnitude of impedance ($|Z|$) versus frequency as illustrated in Figure A-2. (As this figure shows, some manufacturers give curves of the effective series resistance (ESR) instead of DF.) For capacitors where data is available as a function of frequency, it is usually for frequencies less than 10 MHz. Thus, the major drawbacks

* The manufacturers from which data was obtained are listed in Tables A-1, A-2, and A-3.

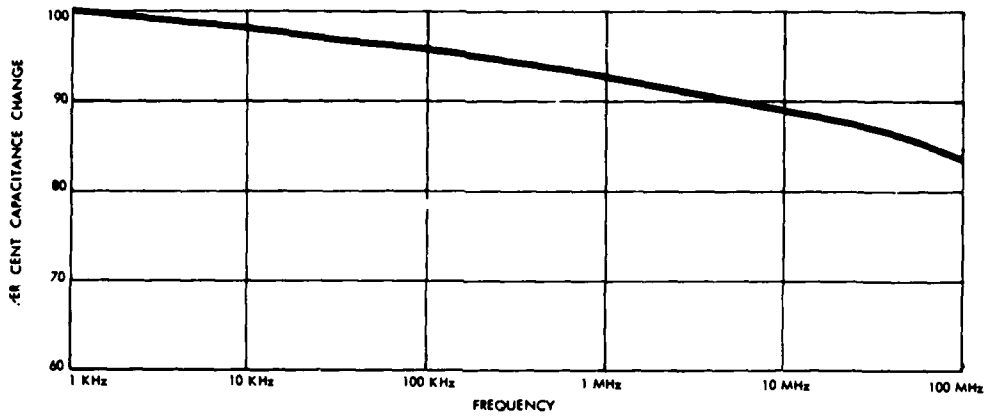
** W. R. Free and J. A. Woody, "Task 1 Test Plan, Parasitic Effects in Discrete Passive Components," Contract No. F30602-78-C-0230, Engineering Experiment Station, Georgia Institute of Technology, Atlanta, GA, December 1978.

of the data available on most capacitors are the lack of data as a function of frequency and the limited frequency range when such data is available.

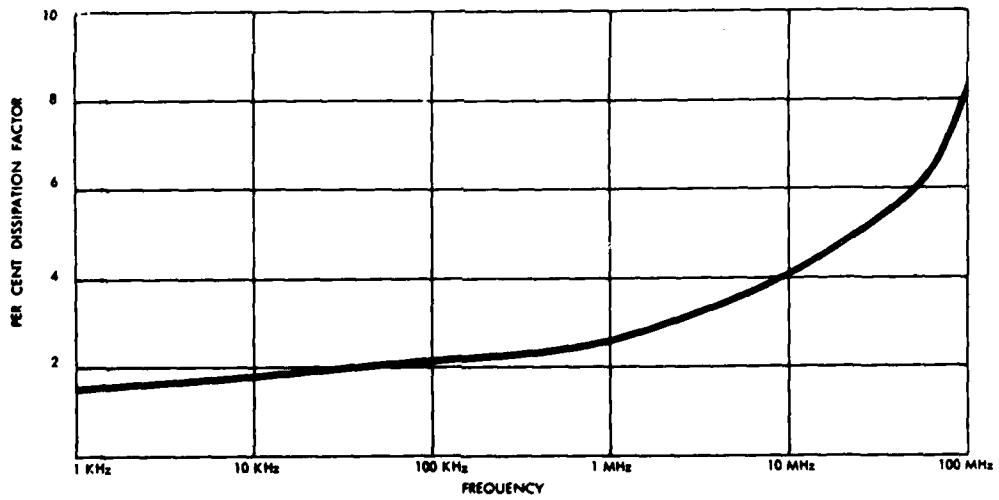
Table A-6 indicates that numerous resistor manufacturers provide "typical" graphs of impedance as some function of frequency. Examples of these graphs are given in Figure A-3. Again, the limited frequency range of most of this data is the most significant problem.

In contrast to the capacitor and resistor manufacturers, most of the inductor manufacturers provide no data as a function of frequency. The data that is available as a function of frequency consists of graphs of the quality factor (Q) as illustrated in Figure A-4. Therefore, the drawbacks of the available inductor data are also the sparse amount of data and the limited frequency range.

In summary, there is a lack of data available as a function of frequency for many passive components. When such data is available from the manufacturers, it is generally given for only a limited frequency range and does not directly describe a particular component.

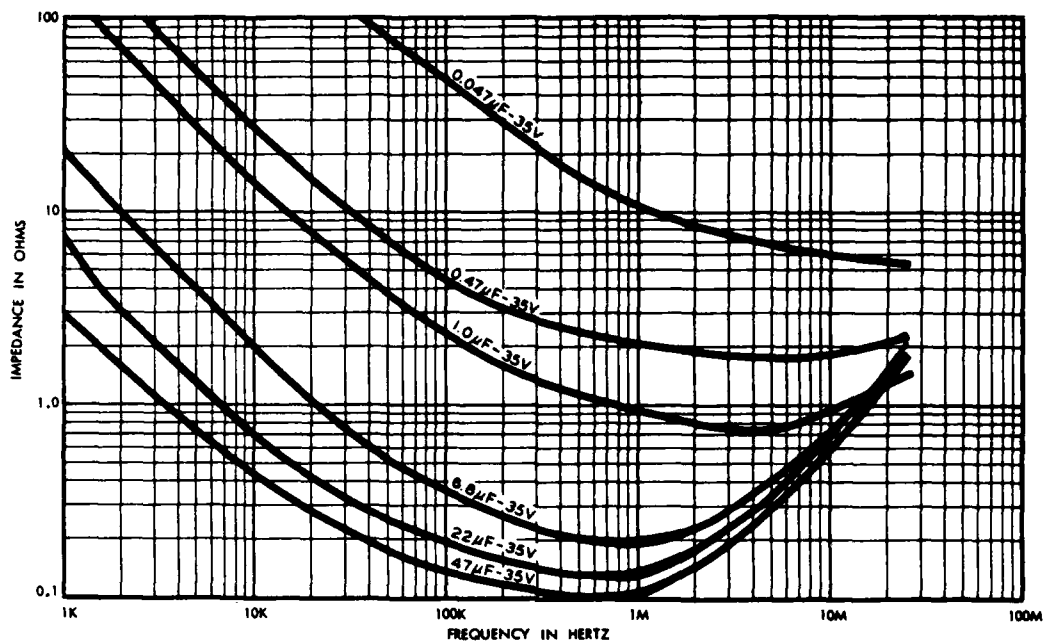


Reprinted courtesy of Sprague Products Co.

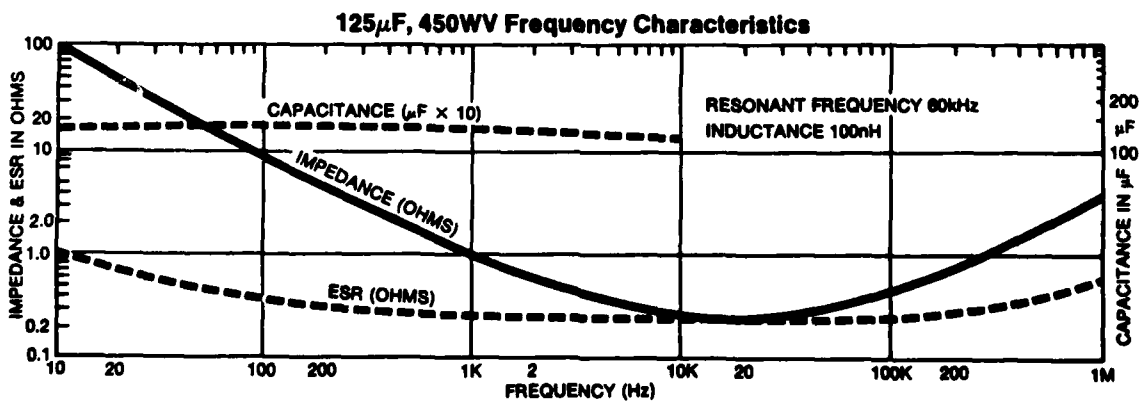


Reprinted courtesy of Sprague Products Co.

Figure A-1. Examples of Manufacturers' ΔC vs f and DF vs f Curves.

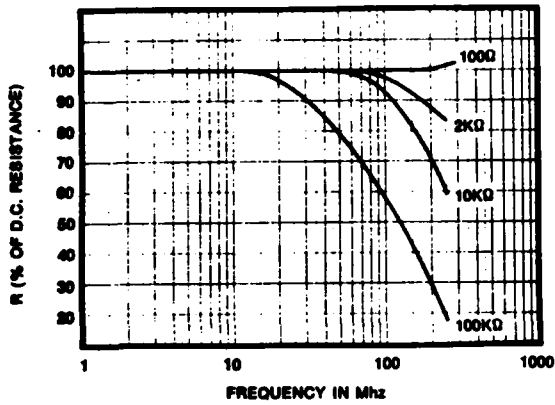


Reprinted courtesy of Sprague Products Co.

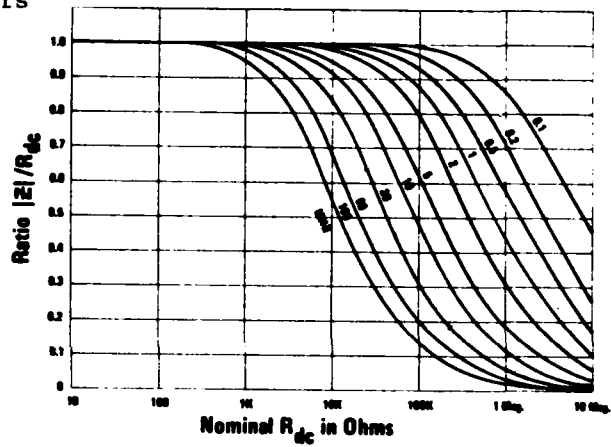


Reprinted courtesy of Mallory Capacitor Co.

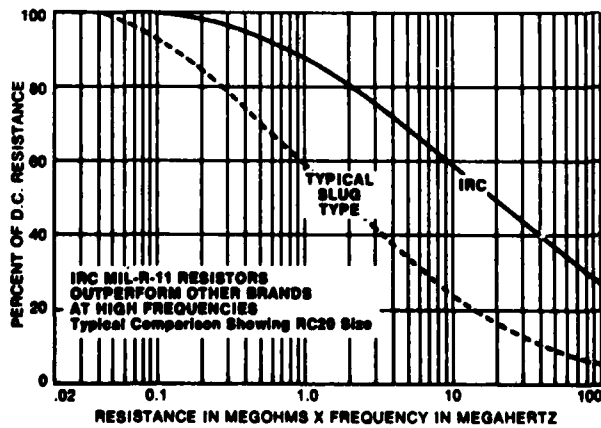
Figure A-2. Examples of Manufacturers' $|Z|$ vs f and ESR vs f Curves.



Reprinted courtesy of TRW/IRC Resistors

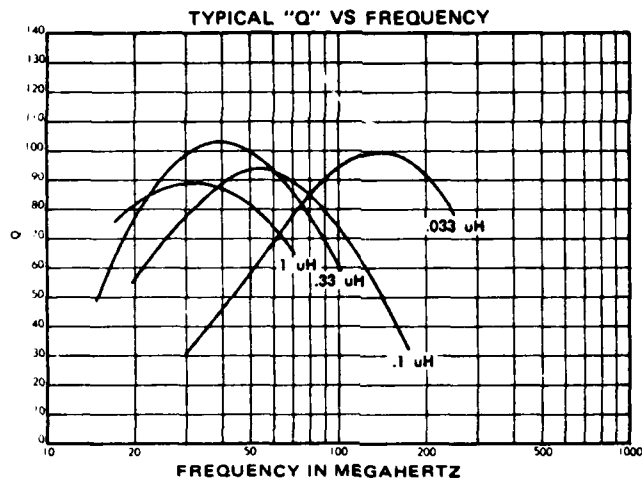


Reprinted courtesy of Allen-Bradley Co.



Reprinted courtesy of TRW/IRC Resistors

Figure A-3. Examples of Various Forms of Manufacturer Impedance vs Frequency Data.



Reprinted courtesy of Torotel, Inc.

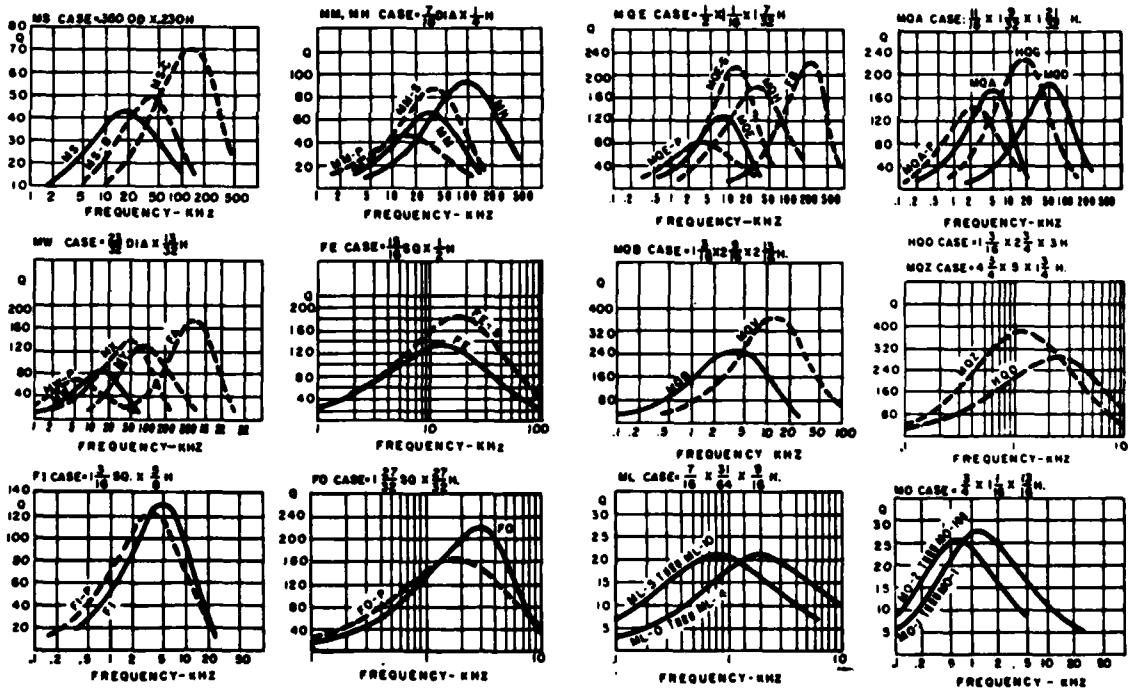


Figure A-4. Examples of Quality Factor Curves.

TABLE A-1
CAPACITOR MANUFACTURERS FROM WHICH DATA WAS OBTAINED

A-B	Allen-Bradley Co.
ATC	American Technical Ceramics
AVX	Aerovox Corp.
CAPAR	CAPAR Components Corp.
CDE	Cornell-Dubilier Electronics
Centralab	Centralab Electronics Division (Globe-Union Inc.)
CII	Components Importers International, LTD
Corning	Corning Glass Works
Dearborn	Dearborn Electronics, Inc. (Div. of Sprague)
Electrocube	Electrocube, Inc.
ELMAG	ELMAG Corp.
EL-MENCO	The Electro-Motive Mfg. Co.
IEC	International Electronics Corp.
Johanson	Johanson Mfg. Co.
KEMET	Union Carbide Corp.
Mallory	Mallory Capacitor Co.
Mepco	Mepco/Electra, Inc.
Mucon	Republic Electronics Corp.
Nytronics	Nytronics Components Group, Inc.
Sprague	Sprague Electric Co.
Tansitor	Tansitor Electronics

TABLE A-2
INDUCTOR MANUFACTURERS FROM WHICH DATA WAS OBTAINED

Airco-Speer	Airco Speer Electronics
Bourns	Bourns, Inc.
Caddell-Burns	Caddell-Burns Co.
Cramer	Cramer Coil Co.
Dale	Dale Electronics, Inc.
Delevan	Delevan Division (American Precision Industries)
Miller	J. W. Miller Division (Bell Industries)
Nytronics	Nytronics Components Group, Inc.
Torotel	Torotel, Inc.
TRW	TRW/UTC Transformers

TABLE A-3
RESISTOR MANUFACTURERS FROM WHICH DATA WAS OBTAINED

A-B	Allen-Bradley Co.
Airco-Speer	Airco-Speer Electronics
CAPAR	CAPAR Components Corp.
CII	Components Importers International, LTD
Corning	Corning Glass Works
Dale	Dale Electronics, Inc.
Ohmite	Ohmite Mfg. Co.
R-OHM	R-OHM Corp.
TRW/IRC	TRW/IRC Resistors

TABLE A-4
AVAILABLE DATA ON CAPACITORS

Type	Manufacturers	Z vs f	ΔC vs f	DF vs f	DF @ f	DCL	ESR vs f	ESR @ f	PF vs f	PF @ f*
<u>Solid Tantalum</u>										
Corning				X		X				
IEC				X		X				
KEMET				X		X				
CAPAR	X					X				
Corning	X				X	X				
Sprague	X			X		X				
KEMET	X			X	X	X				
Sprague	X				X	X		X		
Mallory	X		X		X	X			X	
Tansitor	X		X	X	X	X			X	X
<u>Tantalum Foil</u>										
CDE					X	X				
Sprague	X					X		X		
Tansitor			X			X		X	X	
<u>Wet Sintered Anode Tantalum</u>										
CDE						X		X		
Mallory						X		X		

(continued)

TABLE A-4 (continued)
AVAILABLE DATA ON CAPACITORS

Type	Manufacturers	Z vs f	ΔC vs f	DF vs f	DF @ f	DCL	ESR vs f	ESR @ f	PF vs f	PF @ f
<u>Wet Sintered Anode Tantalum (continued)</u>										
	KEMET				X	X				
	Sprague	X				X				
	Tansitor	X			X	X				
	Sprague	X				X		X		
	Mallory	X	X			X	X		X	
	Mallory		X			X	X			
<u>Aluminum Oxide</u>										
	Mallory				X					
	Sprague							X		
	CAPAR					X			X	
	IEC				X	X				
	Mepco					X		X		
	Sprague				X	X		X		
	Sprague	X				X		X		
	CII	X								
	CDE	X				X				
	Sprague	X				X				
	Mallory	X				X			X	

(continued)

TABLE A-4 (continued)

AVAILABLE DATA ON CAPACITORS

Type	Manufacturers	Z vs f	ΔC vs f	DF vs f	DF @ f	DCL	ESR vs f	ESR @ f	PF vs f	PF @ f
<u>Aluminum Oxide (continued)</u>										
	CDE	X			X	X		X		
	CDE	X				X		X		
	Mallory	X				X	X			
	Mepco	X		X		X				
	Sprague	X				X		X		
	Sprague	X				X	X			
	Sprague	X		X		X				
	Mepco			X		X				
<u>Ceramic</u>										
	AVX				X	X				
	Centralab				X	X				
	KEMET				X	X				
	Nytronics				X	X				
	Sprague				X	X				
	Mucon		X							X
	A-B		X		X	X				
	AVX		X	X	X	X				

(continued)

TABLE A-4 (continued)

AVAILABLE DATA ON CAPACITORS

Type	Manufacturers	Z vs f	ΔC vs f	DF vs f	DF @ f	DCL	ESR vs f	ESR @ f	PF vs f	PF @ f
<u>Ceramic (continued)</u>										
	AVX		X	X		X				
	Centralab		X	X	X	X				
	Sprague		X	X	X	X				
	Sprague				X	X				
	Mepco			X	X	X				
<u>Ceramic TC</u>										
	ATC				X	X				
	AVX				X	X				
	Corning				X	X				
	Mucon		X						X	X
	Sprague		X		X	X				
<u>Mica</u>										
	AVX				X	X				
	CDE				X	X				
	EI-Menco				X	X				
	Sprague				X	X				

(continued)

TABLE A-4 (continued)

AVAILABLE DATA ON CAPACITORS

Type	Manufacturers	Z vs f	ΔC vs f	DF vs f	DF @ f	DCL	ESR vs f	ESR @ f	PF vs f	PF @ f
Metalized Paper- Plastic Film Hermetically Sealed	AVX			X		X				
	Dearborn			X		X				
	Sprague			X		X				
	Sprague					X			X	
Metalized Paper- Plastic Film	CAP'R			X						
	AVX			X		X				
	CII			X		X				
	Electrocube			X		X				
	Nytronics			X		X				
	Sprague			X		X				
Mepro		X							X	

(continued)

TABLE A-4 (cont Inued)

AVAILABLE DATA ON CAPACITORS

Type	Manufacturers	Z vs f	ΔC vs f	DF vs f	DF @ f	DCL	ESR vs f	ESR @ f	PF vs f	PF @ f
	<u>Variable</u>									
	Johanson			X		X				
	Johanson			X		X				
	Johanson			X	X	X				
	Sprague			X	X	X				
	<u>Paper-Plastic Film</u>									
	CAPAR				X					
	ELMAG				X					
	AVX				X	X				
	CDE				X	X				
	CII				X	X				
	Nytronics				X	X				
	Sprague				X	X				
	Sprague				X	X				
	Sprague				X	X				
	IEC		X							
	Mepeco		X							

(continued)

TABLE A-4 (concluded)

AVAILABLE DATA ON CAPACITORS

Type	Manufacturers	$ Z $ vs f	ΔC vs f	DF vs f	DF @ f	DCL	ESR vs f	ESR @ f	PF vs f	PF @ f
Oil Paper										
Nytronics				X		X				
Sprague				X		X				

* $|Z|$ = Magnitude of impedance

f = Frequency

ΔC = Change in capacitance

DF = Maximum or "typical" dissipation factor

DCL = Maximum leakage current with constant dc power applied at rated voltage

ESR = Maximum or "typical" equivalent series resistance

PF = Maximum or "typical" power factor

TABLE A-5

AVAILABLE DATA ON INDUCTORS

Type	Q vs f	$Q @ f$	$\frac{f}{R}$	$\frac{C}{p}$	R_{dc}	$ Z $ vs f^*
<u>Manufacturers</u>						
<u>Molded Shielded RF</u>						
Airco-Speer	X	X	X		X	
Caddell-Burns	X	X	X		X	
Dale	X	X	X		X	
Delevan	X	X	X		X	
Nytronics	X	X	X		X	
Torotel	X	X	X		X	
<u>RF Chokes</u>						
Cramer	X					
Airco-Speer	X	X	X		X	
Caddell-Burns	X	X	X		X	X
Cramer	X	X	X		X	
Dale	X	X	X		X	
Delevan	X	X	X		X	
Miller	X	X	X		X	

(continued)

TABLE A-5 (continued)

AVAILABLE DATA ON INDUCTORS

Type	Manufacturers	Q vs f	Q @ f	f _R	C _p	R _{dc}	Z vs f
<u>Audio</u>	Bourns	X				X	
	TRW	X				X	
	Bourns		X			X	
	Torotel	X			X	X	
<u>Subminiature RF</u>	TRW	X				X	
	Delevan		X	X		X	
	Miller		X	X		X	
	Nytronics		X	X		X	
	Torotel	X	X	X		X	
<u>Chip</u>	Airco-Speer		X	X		X	
	Delevan		X	X		X	

(continued)

TABLE A-5 (concluded)

AVAILABLE DATA ON INDUCTORS

Type	Manufacturers	Q vs f	Q @ f	f _R	C _p	R _{dc}	Z vs f
Variable							
	TRW	X				X	
	Caddell-Burns		X	X		X	
	Cramer		X	X		X	
	Delevan		X	X		X	
	Miller		X	X		X	
	Nytronics		X	X		X	

* Q = Minimum or "typical" quality factor
 f = Frequency
 f_R = Minimum resonance frequency
 C_p = Equivalent parallel capacitance
 R_{dc} = Maximum or "typical" dc resistance
 |Z| = Magnitude of impedance

TABLE A-6

AVAILABLE DATA ON RESISTORS

Type	$ Z $ vs f	$Z @ f$	$(Z $ vs $R)$ $@ f's$	$ Z $ vs $(f \times R)$	$(X$ vs $R) @ f$	$X @ f$	$R, C, L, Q,$ $& Z\% @ f's$	L_s^* or C_p
<u>Carbon Composition</u>								
A-B			X					
Airco-Speer		X						
Ohmite		X						
TRW				X				
<u>Film</u>								
Ohmite								X
Dale							X	
A-B					X			
CAPAR	X							
CII				X				
Corning	X						X	
R-Ohm								
R-Ohm	X			X				
TRW	X							

(continued)

TABLE A-6 (concluded)
AVAILABLE DATA ON RESISTORS

Type	$ Z $ vs f	$Z @ f$	$(Z \text{ vs } R) @ f$'s	$ Z \text{ vs } (f \times R)$	$(X \text{ vs } R) @ f$	$X @ f$	$R, C, L, Q, \text{ or } Z\%$ @ f 's	L_s or C_p
<u>Film High Stability</u>								
A-B			X					
CAPAR	X							
CII	X							
Corning						X		
TRW	X							
<u>Wirewound</u>								
Dale								
TRW						X		
Ohmite	X							X
								X

* $|Z|$ = Magnitude of impedance (may be percent of R_{dc})

f = Frequency

R = Cardinal value of resistor (the value quoted by the manufacturer)

X = Equivalent reactance

C_p = Equivalent parallel capacitance

L_s = Equivalent series inductance

Q = Quality factor

Z% = Change in impedance

APPENDIX B
TASK 1 COMPONENTS AND APPLICABILITY
OF TWO MODELING APPROACHES

In developing and evaluating modeling techniques for use with data available from the manufacturers, a list of suggested components for consideration was mutually agreed upon and presented in the Task 1 Test Plan^{*}. The list was subsequently modified to include the cardinal (or catalog) values for which data was received from the manufacturers (see Appendix A). The revised list is given in Table B-1. (The "ID #" in this table is the identifier number assigned to each cardinal value for convenience in the modeling and analysis.)

The initial modeling effort on Task 1 was for the purpose of determining the ability to model components from manufacturers' data using the direct calculation and the engineering approximation approaches. To accomplish this purpose, each of the components in Table B-1 were modeled using these two approaches. (Only the models discussed in Section 3 of this report were analyzed in detail for accuracy.) The data available from the manufacturers was such that a given modeling approach (1) could be used to completely model the component; (2) could be used to partially model the component, or (3) could not be used at all. These three applicability conditions are identified in Table B-1 as completely, partially, and not, respectively. For example, if the only model that can be determined from the manufacturers' data is an ideal component of the type that is being modeled (e.g., a capacitor), the specific modeling approach under consideration is classified as not applicable. On the other hand, if a simple model such as an ideal component of the type being modeled and one other idealized component (e.g., a capacitor and a resistor) can be determined with one of the modeling approaches, this approach is classified as partially applicable. When a modeling approach can be used to develop a more extensive model (i.e., containing three or more elements) the approach is classified as completely applicable.

^{*} W. R. Free and J. A. Woody, "Task 1 Test Plan, Parasitic Effects in Discrete Passive Components," Contract No. F30602-78-C-0230, Engineering Experiment Station, Georgia Institute of Technology, Atlanta, GA, December 1978.

The applicability information given in Table B-1 indicates that the direct calculation modeling approach can be used with the manufacturers' data to completely model approximately one half and partially model one third of the selected components. In contrast, the engineering approximation approach can only be used with this data to completely model one of six and partially model one of four of the selected components. Thus, using data from the manufacturers, roughly 90 percent of the selected components could be modeled with the direct calculation approach and about 40% could be modeled with the engineering approximation approach.

TABLE B-1

SPECIFIC COMPONENTS SELECTED FOR MODELING IN TASK 1

Type of Component	Manufacturer & Type or Series	Cardinal Values	ID #	Applicability of Modeling Approaches	
				Direct Calc.	Engrg. Approx.
Tantalum Capacitor, Solid	Corning MD	0.1 μ F (35V)	A1	Completely	Completely
		10 μ F (15V)	A2	Completely	Completely
	Mallory TAC	0.1 μ F (50V)	B1	Partially	Partially
		3.3 μ F (50V)	B2	Partially	Partially
		56 μ F (6V)	B3	Partially	Partially
	Tansitor DT	4.7 μ F (20V)	C1	Completely	Completely
47 μ F (6.3V)		C2	Completely	Completely	
Tantalum Foil, Capacitor	Tansitor TES	6 μ F (50V)	D1	Partially	Not
		20 μ F (100V)	D2	Completely	Not
Tantalum Capacitor, Wet Sintered Anode	Mallory XT	4 μ F (360V)	E1	Completely	Completely
		700 μ F (60V)	E2	Completely	Completely
Aluminum Oxide Capacitor	Mepco 121	2.2 μ F (40V)	F1	Completely	Completely
		4.7 μ F (40V)	F2	Completely	Completely
Ceramic Capacitor	Aerovox Sky Cap	10 pF (50V)	G1	Partially	Not
		4.7 μ F (50V)	G2	Partially	Not
	Sprague EB-6251	1200 pF (50V)	H1	Completely	Not
		0.01 μ F (50V)	H2	Completely	Not

(Continued)

TABLE B-1 (Continued)
 SPECIFIC COMPONENTS SELECTED FOR MODELING IN TASK 1

Type of Component	Manufacturer & Type or Series	Cardinal Values	ID #	Applicability of Modeling Approaches	
				Direct Calc.	Engrg. Approx.
Mica Capacitor	Sprague EB-1220	5000 pF (100V)	I1	Partially	Not
		0.033 μ F (100V)	I2	Partially	Not
	E1-Menco TDM 43	100 pF (1500V)	J1	Partially	Not
		0.01 μ F (750V)	J2	Partially	Not
Metalized Paper-Plastic Film Capacitor	Mepco C280	0.1 μ F (100V)	K1	Partially	Not
		4.7 pF (100V)	K2	Partially	Not
Variable Capacitor	Johanson 5200	0.8-10 pF (250V)	L1	Completely	Not
		1-16 pF (250V)	L2	Completely	Not
Plastic Film Capacitor	Mepco 424	1100 pF (63V)	M1	Partially	Not
		6800 pF (63V)	M2	Partially	Not
RF Inductor, Molded Shielded	Nytronics MS	0.47 μ H	N1	Completely	Not
		1200 μ H	N2	Completely	Not
RF Choke	Caddell-Burns 660	0.1 μ H	O1	Completely	Not
		100 μ H	O2	Completely	Not

(Continued)

TABLE B-1 (Continued)
 SPECIFIC COMPONENTS SELECTED FOR MODELING IN TASK 1

Type of Component	Manufacturer & Type or Series	Cardinal Values	ID #	Applicability of Modeling Approaches	
				Direct Calc.	Engrg. Approx.
Audio Inductor	Bourns 4222	0.7 H 6 H	P1	Partially	Not
			P2	Partially	Not
	Torotel 84	50 mH 360 mH	Q1	Completely	Not
			Q2	Completely	Not
RF Coil, Subminiature	Delevan 155	0.1 μ H 100 μ H	R1	Completely	Not
			R2	Completely	Not
	Torotel TA & TB	0.1 μ H 100 μ H	S1	Completely	Not
			S2	Completely	Not
Variable Inductor, Shielded	Miller 9100	0.099-0.134 μ H 64.57-163 μ H	T1	Completely	Not
			T2	Completely	Not
Carbon Composition Resistor	Allen-Bradley CB	100 Ω 100 k Ω	U1	Not	Partially
			U2	Not	Partially
Carbon Composition Film Resistor	TRW/TRC RCR	100 Ω 100 k Ω	V1	Partially	Partially
			V2	Partially	Partially
Carbon Film Resistor	CII Y	100 Ω 100 k Ω	W1	Not	Partially
			W2	Not	Partially

(Continued)

TABLE B-1 (Concluded)
 SPECIFIC COMPONENTS SELECTED FOR MODELING IN TASK 1

Type of Component	Manufacturer & Type or Series	Cardinal Values	ID #	Applicability of Modeling Approaches	
				Direct Calc.	Engrg. Approx.
Metal Film Resistor	Dale MF	100 Ω 10 k Ω	X1	Completely	Not
			X2	Completely	Not
Metal Film Resistor, High Stability	TRW/IRC RN & RL	100 Ω 100 k Ω	Y1	Not	Partially
			Y2	Not	Partially
Wirewound Resistor	Ohmite	100 Ω 10 k Ω (12W)	Z1	Partially	Partially
			Z2	Partially	Partially

APPENDIX C
MEASUREMENT TECHNIQUES

Based on observations made while using manufacturers' data during Task 1 and on investigations of the types of measurement equipments available, it was concluded that the most appropriate data for use in modeling passive components is their complex impedance as a function of frequency. For this reason, techniques for measuring the impedance of components over the frequency range of 5 Hz^{*} to 1 GHz were selected for use on Task 2.

During this selection process, various impedance measurement techniques were investigated. The operational procedures, the measurable quantities, the applicable frequency ranges, and the associated difficulties and limitations of each potential measurement technique were considered. The measurement equipment and systems listed in Table C-1 were chosen for use over the indicated frequency ranges.

The two vector impedance meters (HP 9800A and HP 4815A) complement each other in their applicable frequency ranges and together were used at discrete frequencies between 5 Hz and 108 MHz to directly measure complex impedances (magnitude and phase) with magnitudes from approximately 1 Ω to at least 100 k Ω (up to 550 kHz, the HP 4800A will measure magnitudes of impedance up to 10 M Ω). Photographs of these two instruments with the respective component mounts are shown in Figures C-1 and C-2. The HP 4800A, the top instrument in Figure C-1, has banana jacks for mounting components, while the HP 4815A has a probe terminated in a component mount as shown in Figure C-3.

The Network Analyzer System (GR 1710) with its Immittance Probe (GR 1710-P5) was used to make swept frequency measurements from 500 kHz to 500 MHz. It measures the magnitude and phase of the complex impedance for components between 0.5 Ω and 1 M Ω . This measurement system is shown in Figures C-2 and C-4. The impedance and frequency outputs of the Network Analyzer were connected to a Houston Instrument Series 2000 Omnigraphic X-Y Recorder. The GR 1710-P5 Immittance Probe is terminated in the specially fabricated

^{*}The 5 Hz low frequency was determined by the limitations of the available equipment; however, it should be possible to evaluate the data at lower frequencies by extrapolating from the measured data.

component mount shown in the photographs in Figure C-5. This component mount was made from a 1/2-inch (13-mm) thick aluminum plate with a center hole, threaded to screw on the Immittance Probe. A 1/4-inch (6-mm) long teflon rod was also threaded such that it would screw into the center hole in the aluminum plate. The purpose of this rod was to hold a No. 6 screw which made contact with the center conductor of the probe and to insulate this center-conductor screw from the aluminum plate. The component-under-test was then mounted between the center-conductor screw and the aluminum plate. * (Figure C-5b shows the component mount with a short.)

A block diagram of the insertion loss measurement system is given in Figure C-6a. This swept frequency system was used for a quick, uncalibrated determination of the general characteristics of the component-under-test from 500 kHz to 1 GHz. The resulting plot of the relative insertion loss as a function of frequency was used to determine which frequency ranges should be measured in detail with the other equipments or systems. The Insertion Unit in Figure C-6a is a coaxial component mount. If the component was expected to have a relatively high impedance (parallel resonance) at its first resonance (e.g., inductors), it was mounted in series in the Insertion Unit as shown in Figure C-6b. In contrast, components (such as most capacitors) with anticipated low values at their first resonance were mounted in shunt in the Insertion Unit as shown in Figure C-6c. Components (such as resistors) for which the relative magnitude of their impedance at the first resonance could not be anticipated were measured in both series and shunt configurations.

The final measurement system used on this program was a reflectometer system as shown in Figure C-7. This system was used at discrete frequencies from 100 MHz to 1 GHz to measure the complex reflection coefficient resulting when the component-under-test is used to terminate a 50 Ω coaxial line. The complex impedance was then calculated from the measured reflection coefficient. ** The component was mounted on the component mount described previously and shown in Figure C-5. The component mount was then connected to the direc-

* The nominal lead length was 1 cm for each end of the component.

** "Measurement of Complex Impedance," Application Note 77-3, Hewlett Packard, Palo Alto, CA, April 1967.

tional coupler through appropriate 50Ω coaxial adapters as shown in Figure C-7(a). (The digital voltmeter shown on top of the vector voltmeter in this photo was used for convenience in reading the incident and reflected voltages measured with the vector voltmeter.)

For each component-under-test (see Appendix D), the insertion loss measurement system was first used to determine the generic shape of the impedance characteristics of the component, i.e., the frequencies at which resonances occur. Then the other measurement techniques were employed to obtain more detailed impedance data. Measurements were made with the vector impedance meters and the reflectometer system at discrete frequencies of 10-20-50-100-200-500-1000-etc. (This sequence was chosen because these frequencies are approximately the same linear distances apart on logarithmic paper.) Near resonances the number of measurement frequencies were increased to ensure that the characteristics of the impedance were well defined around resonance. The measurements made with the network analyzer were swept frequency in nature and, thus, completely described the characteristics at all frequencies.

For each component, impedance data were obtained using the five selected measurement techniques. The measured data were combined into graphs each covering the frequency range from 1 Hz to 1 GHz. The graph for each measured component is presented in Appendix D.

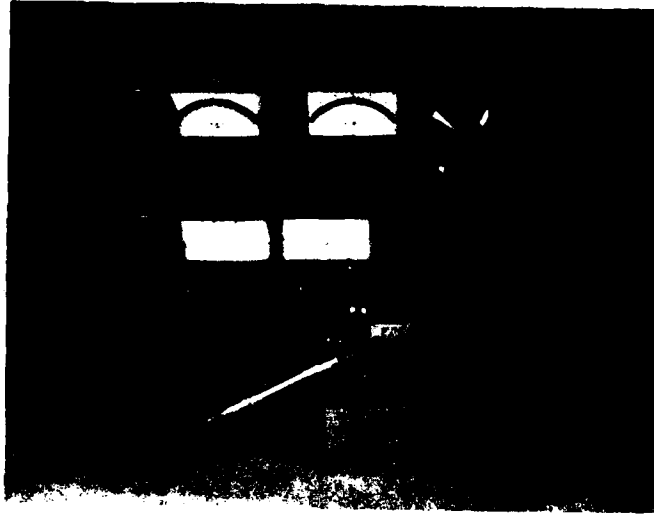


Figure C-1. Vector Impedance Meters--HP 4800A
on the top and HP 4815A on the bottom.

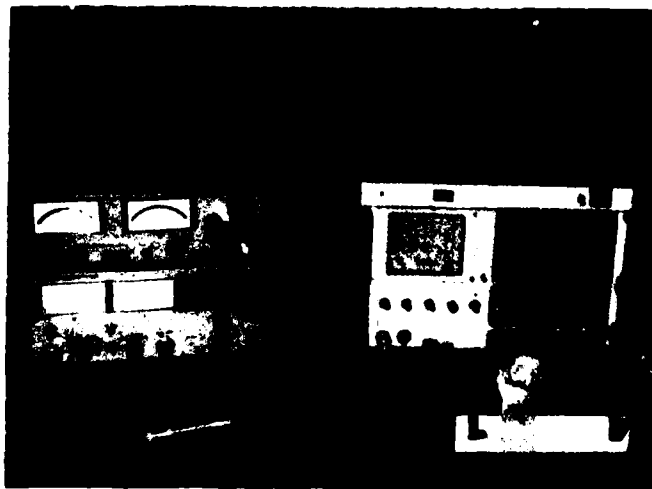


Figure C-2. Vector Impedance Meters and Network Analyzer System--
GR 1710 Network Analyzer System on the Right.

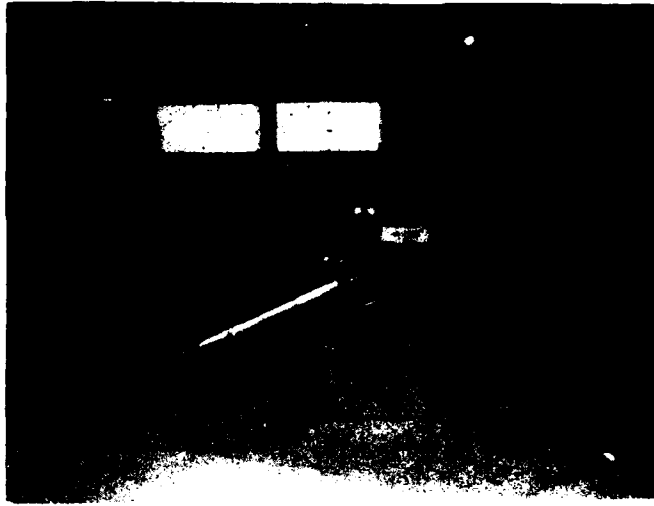
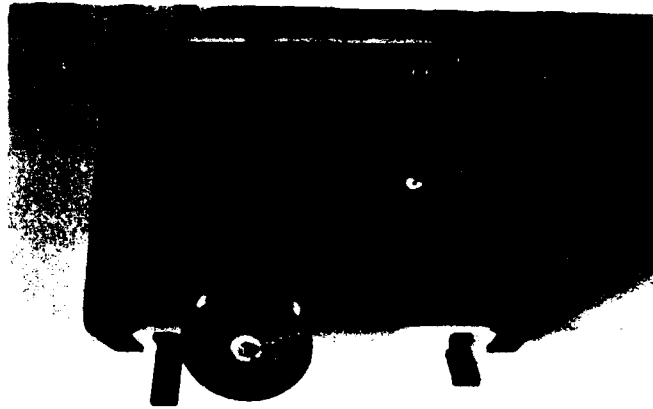


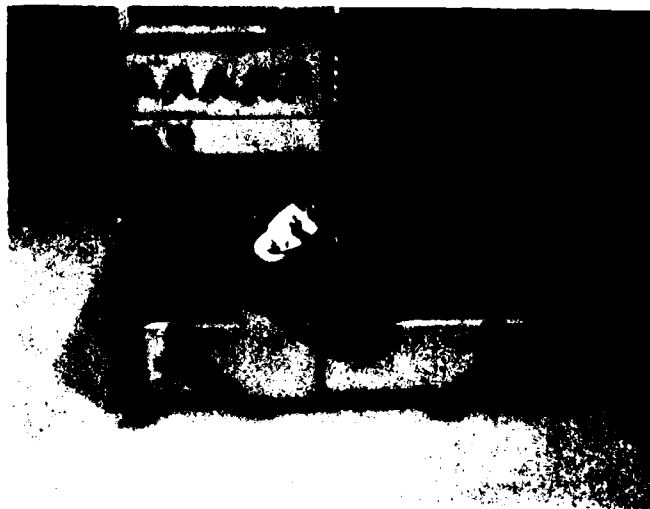
Figure C-3. Component Mount/Probe for HP 4815A Vector Impedance Meter.



Figure C-4. GR 1710 Network Analyzer System.

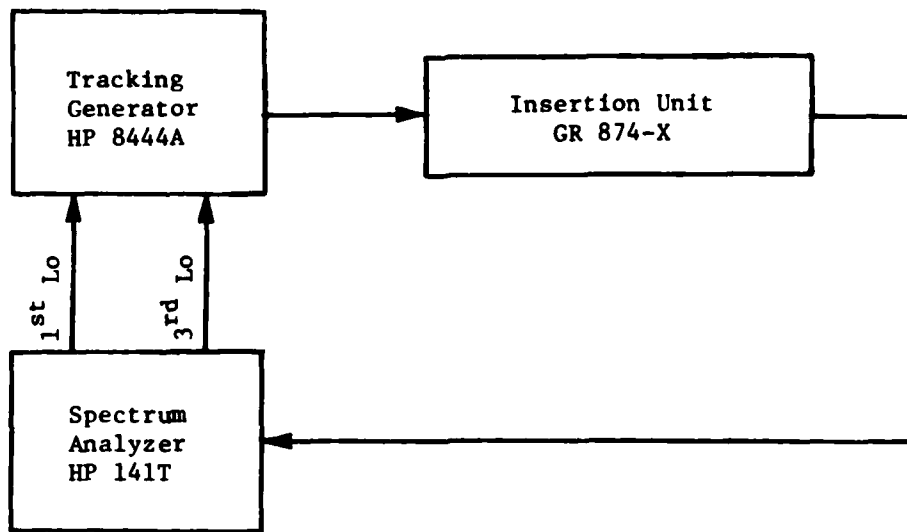


(a) Component Mount with a Resistor.



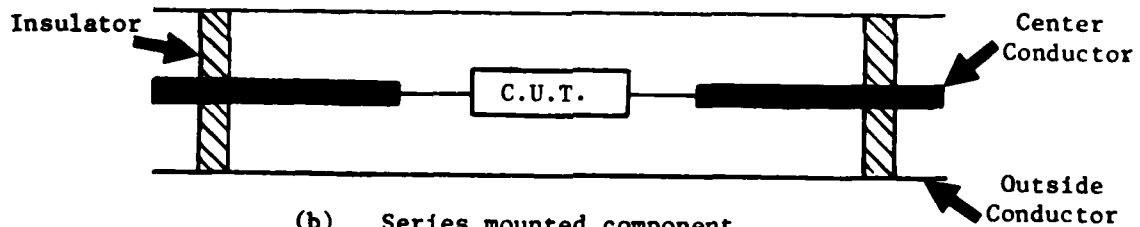
(b) Component Mount with a Short.

Figure C-5. Component Mount for GR 1710 Network Analyzer System.



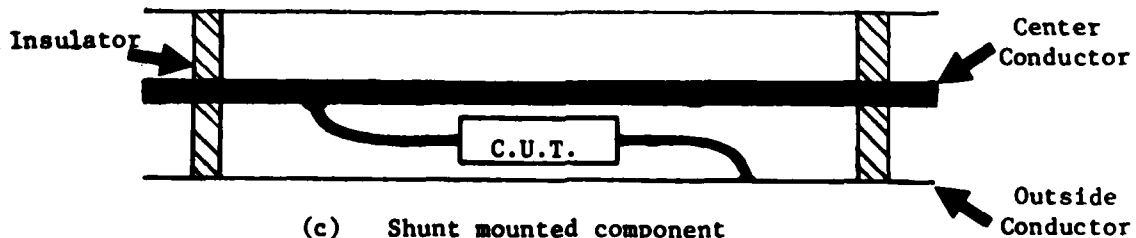
(a) Insertion Loss System.

C.U.T. = Component Under Test



(b) Series mounted component in coaxial insertion unit.

C.U.T. = Component Under Test

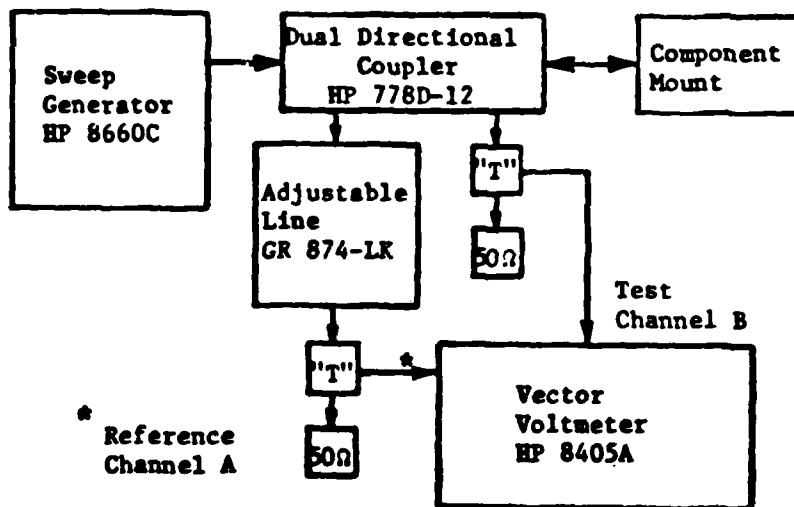


(c) Shunt mounted component in coaxial insertion unit.

Figure C-6. Insertion Loss Measurement System in Component Mounts.



(a) Measurement System with component *mount* removed.



(b) Block Diagram.

Figure C-7. Reflectometer Measurement System.

TABLE C-1

TASK 2 MEASUREMENT EQUIPMENT AND SYSTEMS

Type	Manufacturer	Model #	Applicable Frequency Range	Quantities Measured	* Measurement Range
Vector Impedance Meter	Hewlett Packard	4800A	5 Hz to 550 kHz	$ Z $ θ_Z	$\rightarrow 1 \Omega$ to $10 M\Omega$ $\rightarrow -90^\circ$ to $+90^\circ$
RF Vector Impedance Meter	Hewlett Packard	4815A	500 kHz to 108 MHz	$ Z $ θ_Z	$\rightarrow 0.6 \Omega$ to $100 k\Omega$ $\rightarrow -180^\circ$ to $+180^\circ$
RF Network Analyzer System: Main Frame	General Radio	1710 System	500 kHz to 500 MHz	$ Z $ θ_Z	$\rightarrow 0.5 \Omega$ to $1 M\Omega$ $\rightarrow -180^\circ$ to $+180^\circ$
Immittance Probe	General Radio	1710-P5			
Insertion Loss System:					
Spectrum Analyzer	Hewlett Packard	141T System			IL _{series} $\rightarrow 0$ to 60 dB
Tracking Generator	Hewlett Packard	8444A	500 kHz to 1 GHz		IL _{shunt} $\rightarrow 0$ to 60 dB
Insertion Unit	General Radio	847-X			
Reflectometer System:					
Sweep Generator	Hewlett Packard	8660C		$ \rho $	$\rightarrow 0$ to 1
Vector Voltmeter	Hewlett Packard	8405A	100 MHz to 1 GHz	θ_p	$\rightarrow -180^\circ$ to $+180^\circ$
Dual Directional Coupler	Hewlett Packard	778D-12			

(continued)

TABLE C-1 (concluded)

TASK 2 MEASUREMENT EQUIPMENT AND SYSTEMS

-
- * $|Z|$ = magnitude of the complex impedance
 θ_Z = phase angle of the complex impedance
 IL_{series} = insertion loss measured when component is mounted in series with the measurement circuit. Refer to Figure C-6b
 IL_{shunt} = insertion loss measured when component is mounted in shunt across the measurement circuit. Refer to Figure C-6c
 $|\rho|$ = magnitude of the reflection coefficient
 θ_ρ = phase angle of the reflection coefficient
-

APPENDIX D
TYPICAL MEASURED DATA

Using the measurement techniques described in Appendix C, the impedance of various components as a function of frequency were measured on Task 2 of this program. A total of 68 components including 29 capacitors, 14 inductors, and 25 resistors were selected for measurement. These components were selected primarily from the sample components received from manufacturers (see Appendix A). Where necessary, these samples were supplemented by purchases from local distributors. The types of components were chosen from those identified in the Task 1 Test Plan. Descriptions of the selected capacitors, inductors, and resistors are given in Tables D-1, D-2, and D-3, respectively. The type of component, manufacturer, catalog number, cardinal value, and other pertinent data are included in these tables.

The complex impedances (magnitude and phase) of all the components identified in these tables were measured from 5 Hz to 1 GHz (see Appendix C). For each component two graphs were plotted: (1) the magnitude of Z ($|Z|$) versus frequency (f) and (2) the phase of Z (θ_Z) versus f . Thus, a total of 136 graphs of measured data, each covering an eight and one-half decade frequency range, was obtained. To reduce this amount of data to a more manageable level, the $|Z|$ vs f curves for each of the three categories of components (capacitors, inductors, and resistors), were divided into groups according to the general shape of the curves. One curve from each group was then selected as being representative of that group.

The groups are defined according to their characteristics in Tables D-4, D-5, and D-6 for the capacitor, inductors, and resistors, respectively. In these tables the "Y" (for Yes) indicates that a given characteristic of the curve applies to a specific group while "N" (for No) indicates that it does not apply. (It is noted that the definition of the characteristics of each group is somewhat arbitrary and was based on a subjective visual examination of each curve.) Based on these definitions, the measured capacitors, inductors, and resistors are grouped in Tables D-7, D-8, and D-9, respectively. These tables also identify the specific components whose $|Z|$ vs f curves were chosen as representative of each group. The $|Z|$ vs f curves selected

as representative are given in the "a" parts of Figures D-1 through D-17. The modeling and analysis of the measured data as described in Sec. 4.0 are also shown on this part of each figure. The "b" parts show the resulting per cent difference between the measured data and the data calculated from the model.* The curves are arranged in these 17 figures in the same order as the components are listed in Tables D-7, D-8, and D-9.

In summary, the complex impedances of 68 components were measured over the 5 Hz to 1 GHz frequency range. The resulting 136 $|Z|$ vs f graphs were reduced to a more practical number of 17. This reduction was accomplished by grouping the $|Z|$ vs f curves according to the characteristics of their shapes and then selecting a representative curve from each group. These representative curves are given in Figures D-1 through D-17.

* It should be noted that the "b" curves are plotted on a linear scale and thus tend to exaggerate the differences between the measured data and the model data. Thus relatively good correlation on the "a" curves between the calculated and measured behavior can in many cases result in seemingly wide variations on the "b" curves. These same comments apply to corresponding curves in Appendix F.

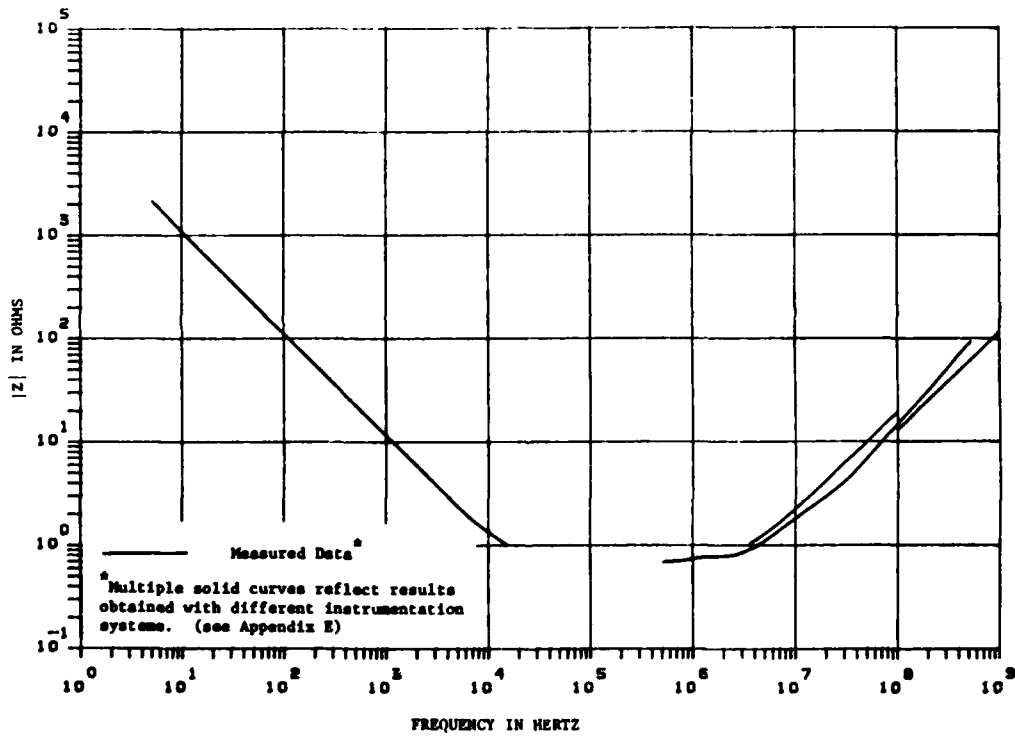


Figure D-1. Data for the Capacitor Representing Group #1 in Table D-7.

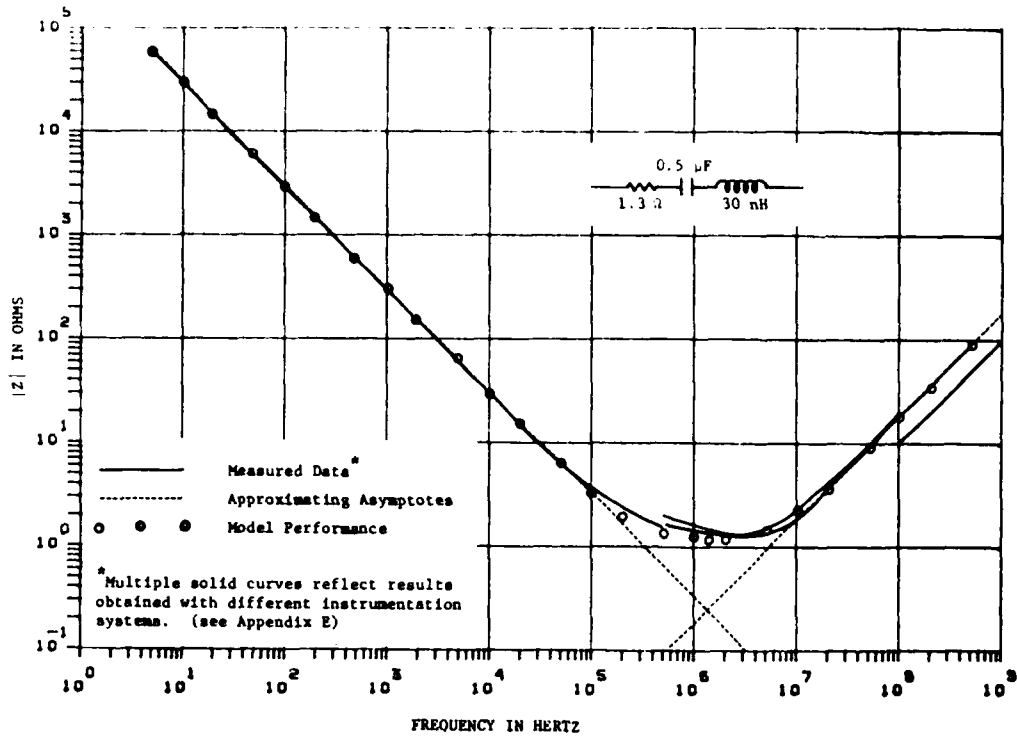


Figure D-2(a). Data for the Capacitor Representing Group #2 in Table D-7.

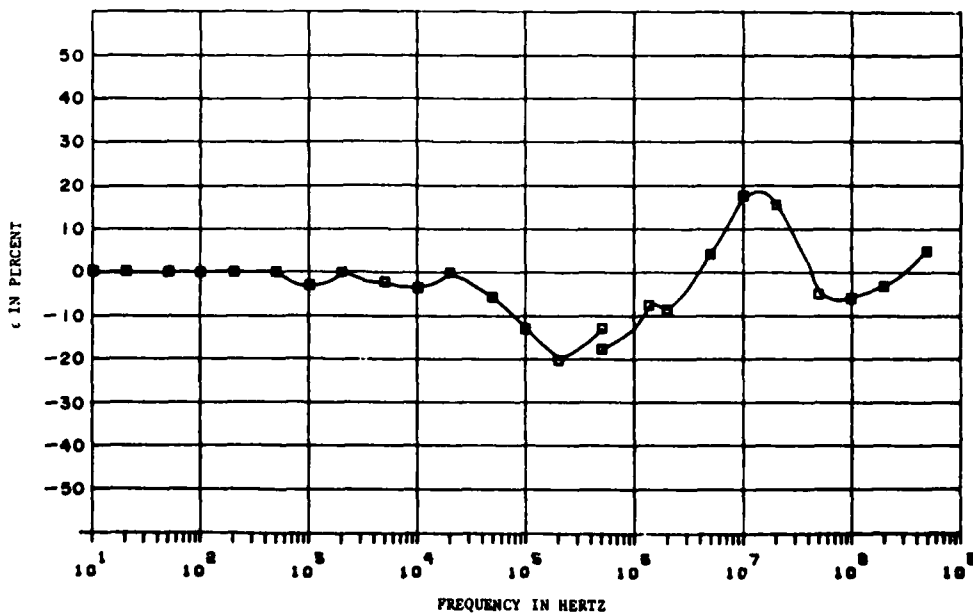


Figure D-2(b). Difference Between Calculated and Measured $|Z|$ in (a).

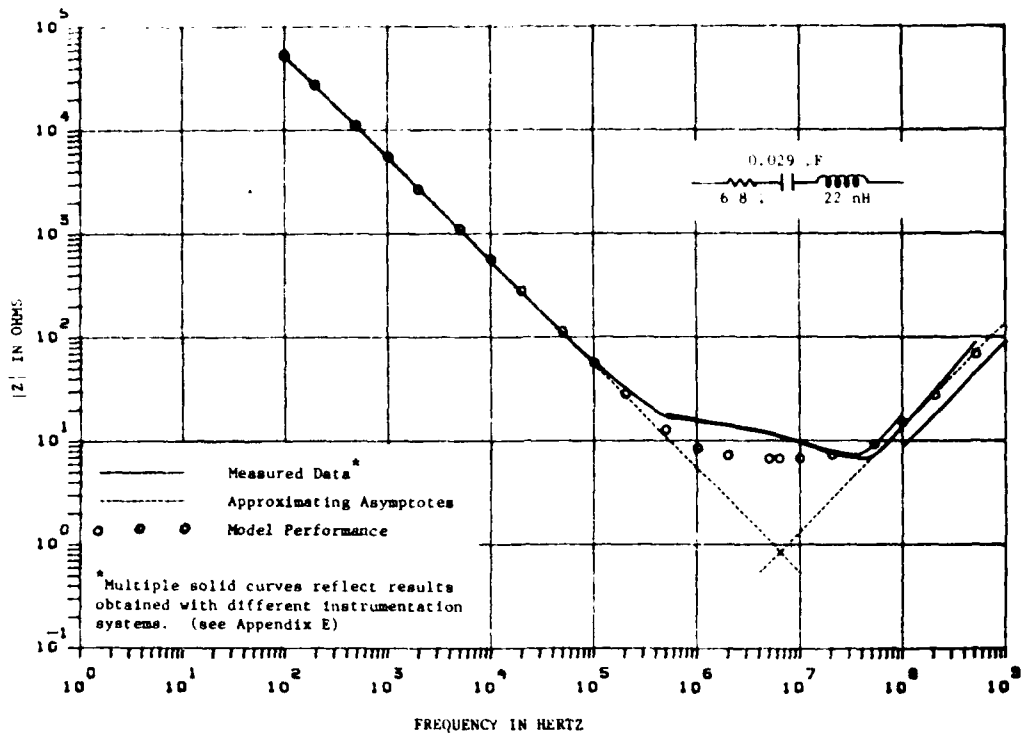


Figure D-3(a). Data for the Capacitor Representing Group #3 in Table D-7.

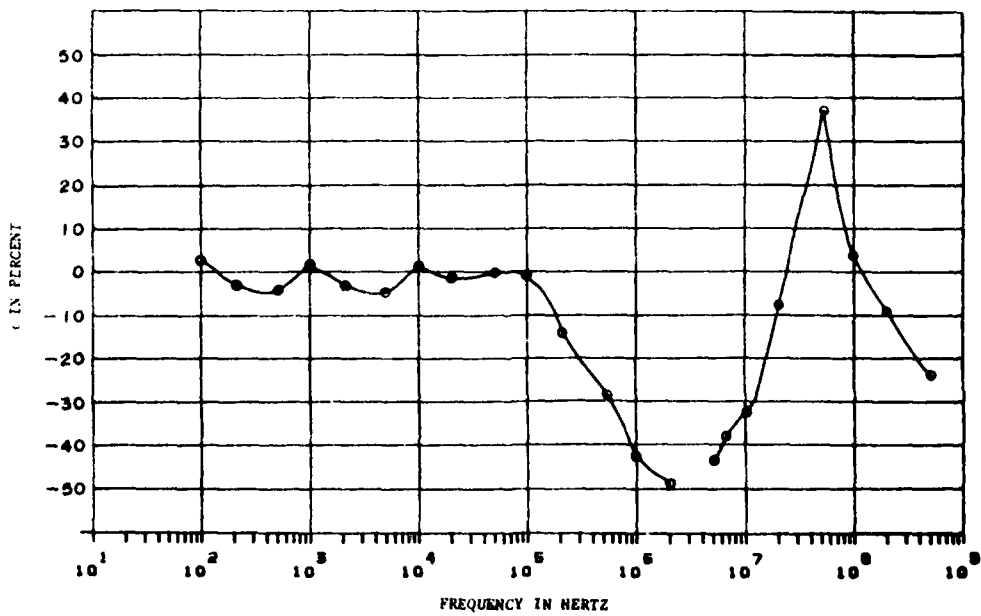


Figure D-3(b). Difference Between Calculated and Measured $|Z|$ in (a).

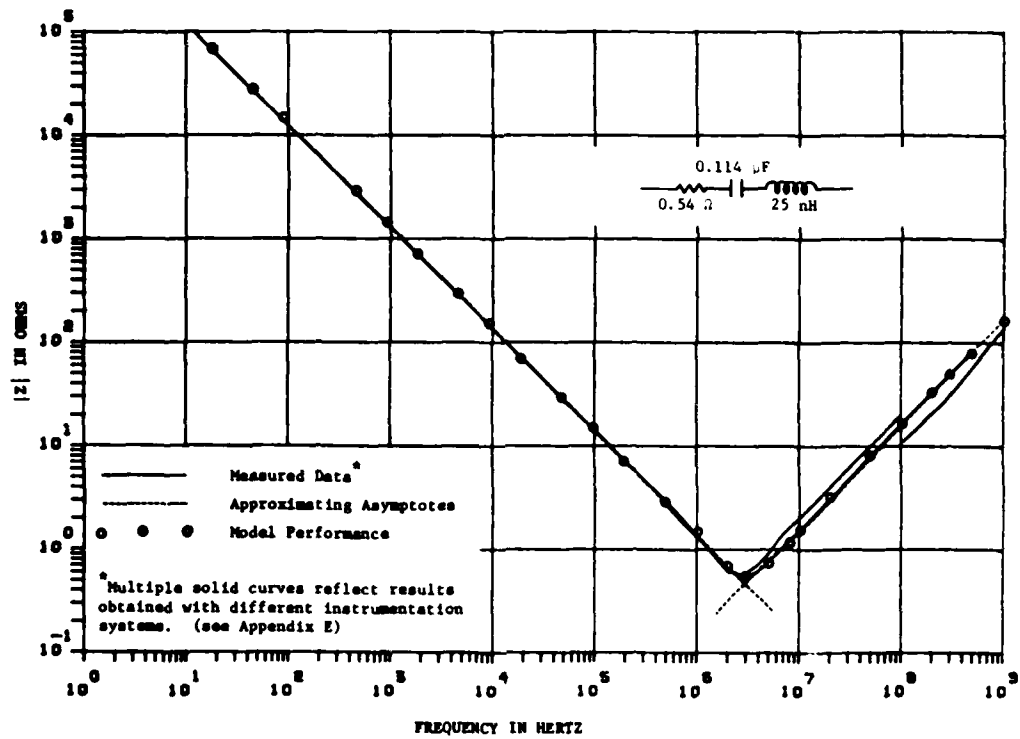


Figure D-4(a). Data for the Capacitor Representing Group #4 in Table D-7.

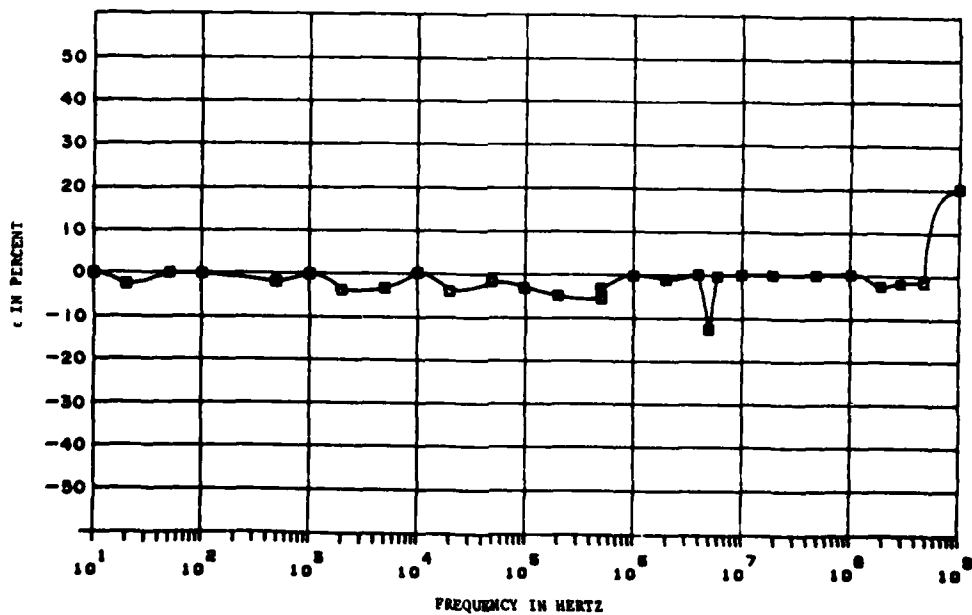


Figure D-4(b). Difference Between Calculated and Measured |Z| in (a).

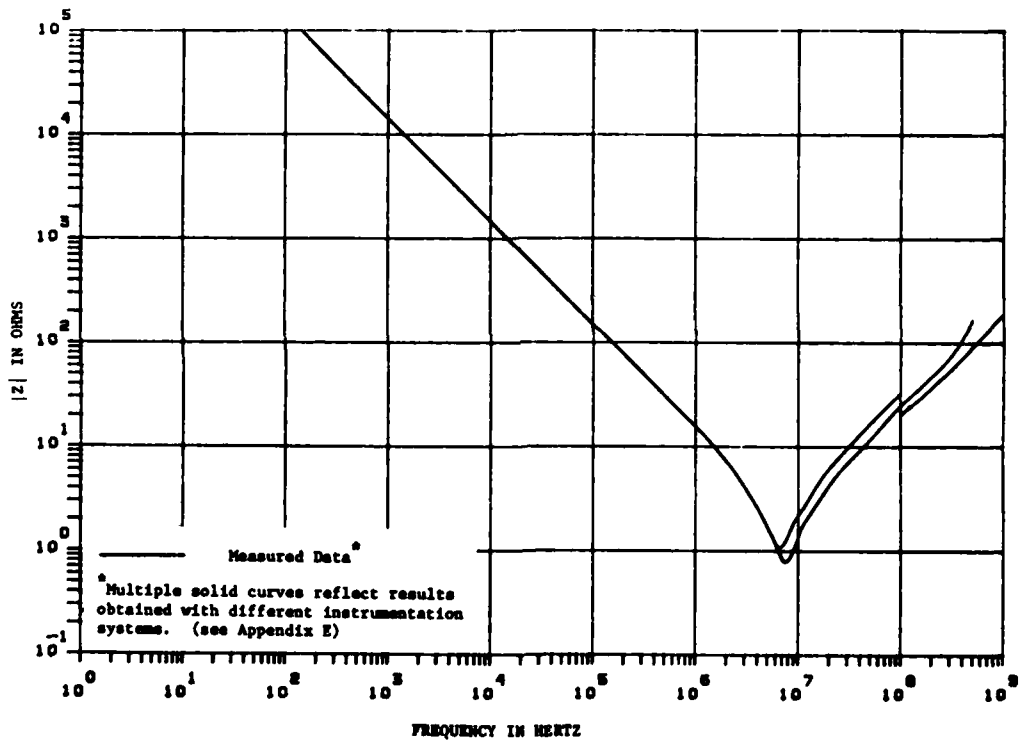


Figure D-5. Data for the Capacitor Representing Group #5 in Table D-7.

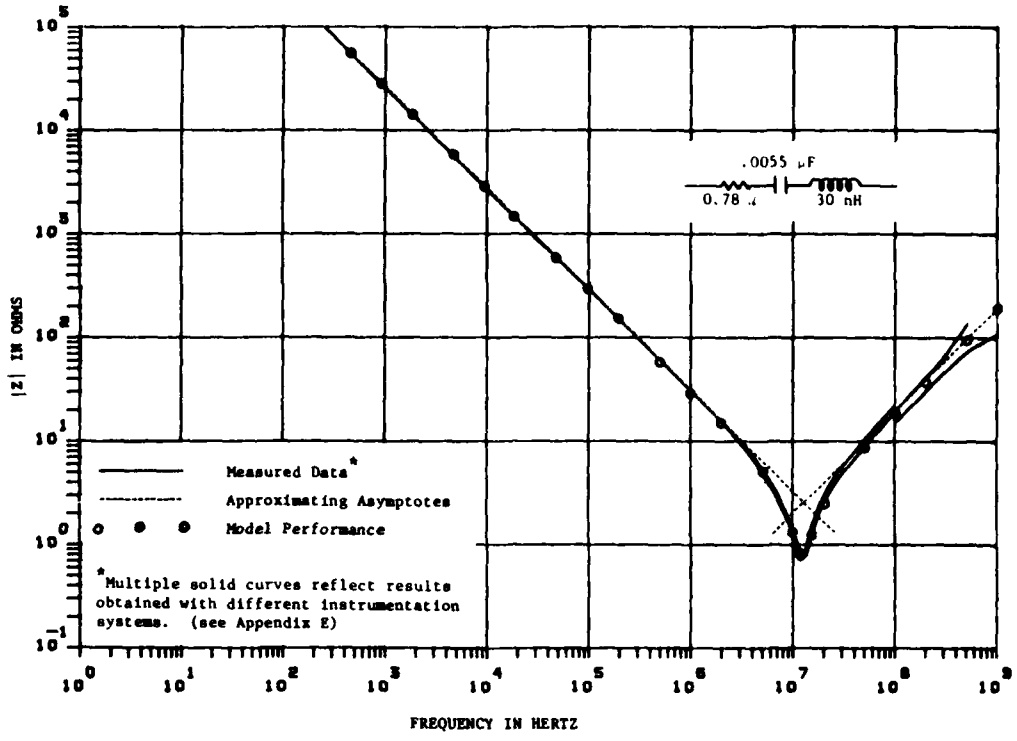


Figure D-6(a). Data for the Capacitor Representing Group #6 in Table D-7.

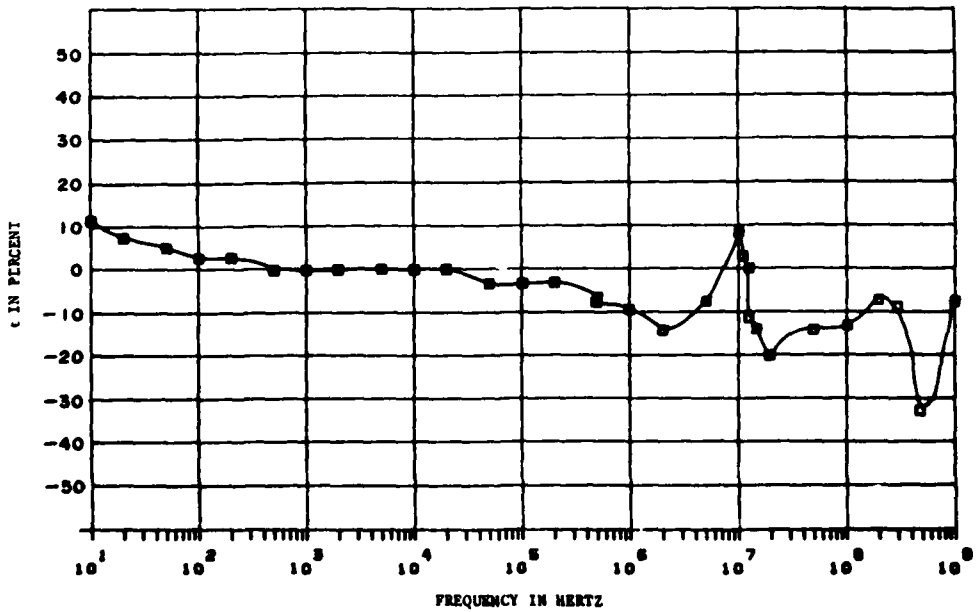


Figure D-6(b). Difference Between Calculated and Measured $|Z|$ in (a).

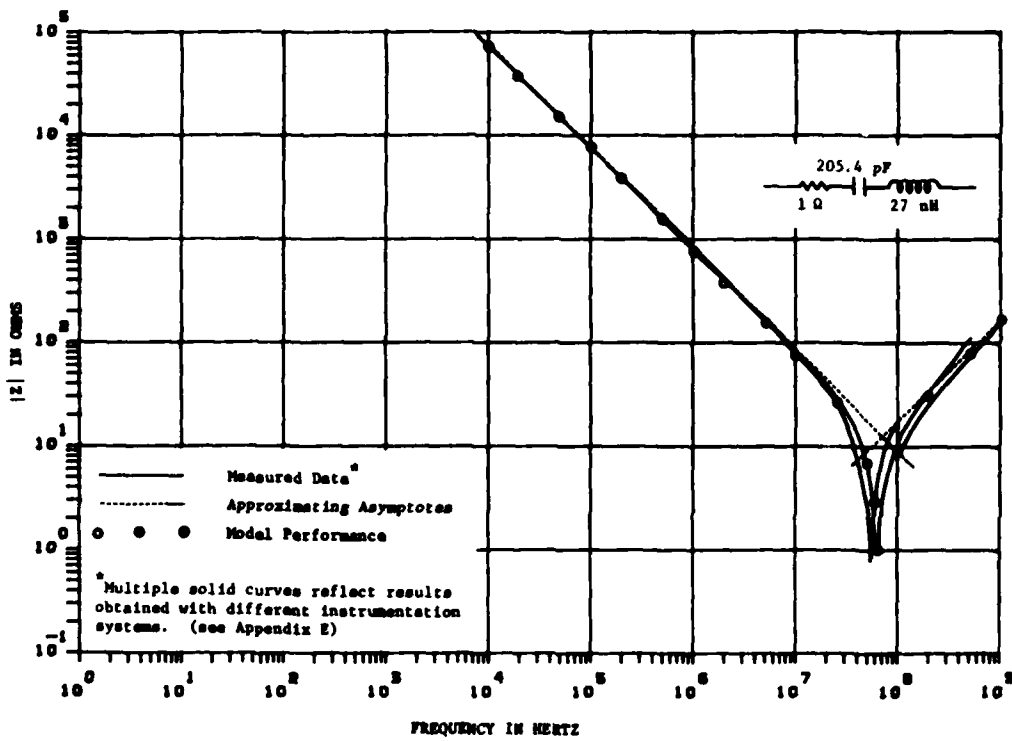


Figure D-7(a). Data for the Capacitor Representing Group #7 in Table D-7.

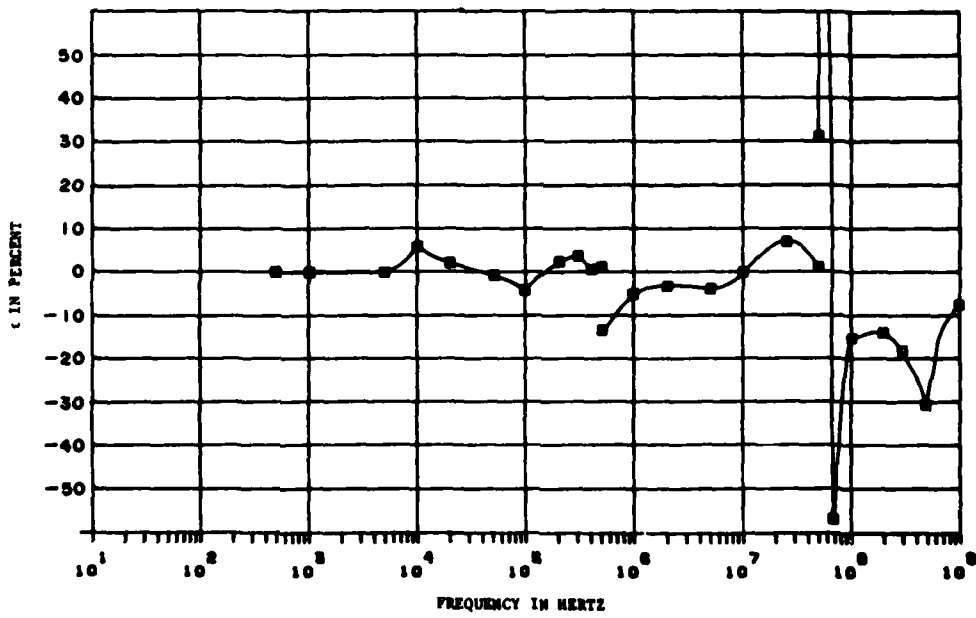


Figure D-7(b). Difference Between Calculated and Measured $|Z|$ in (a).

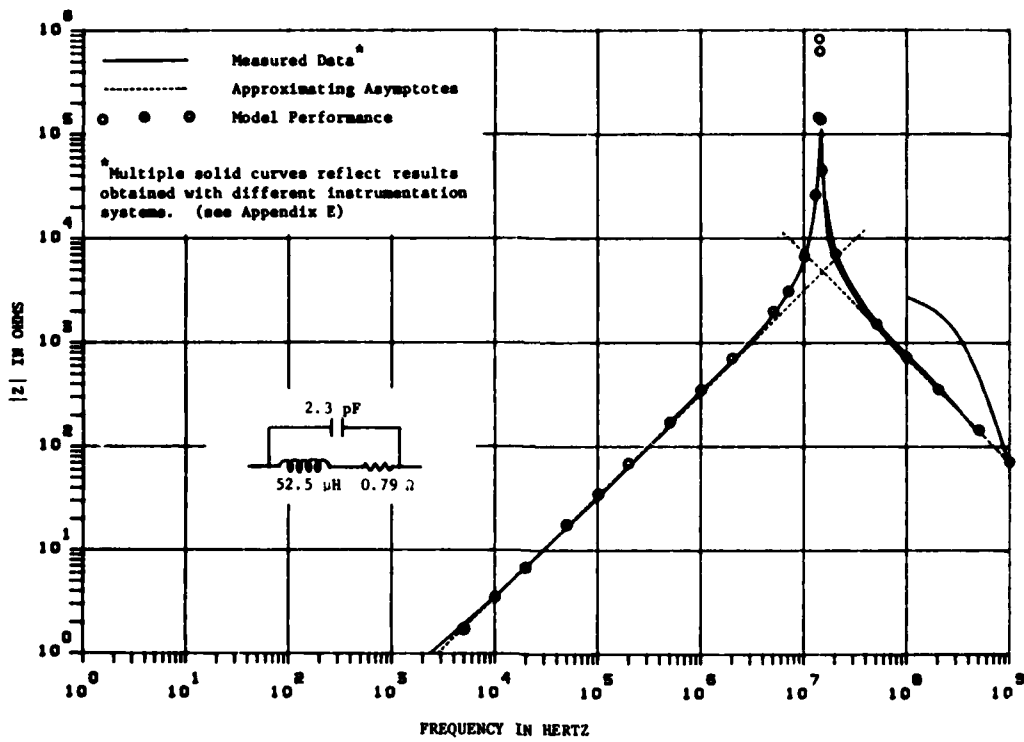


Figure D-8(a). Data for the Inductor Representing Group #1 in Table D-8.

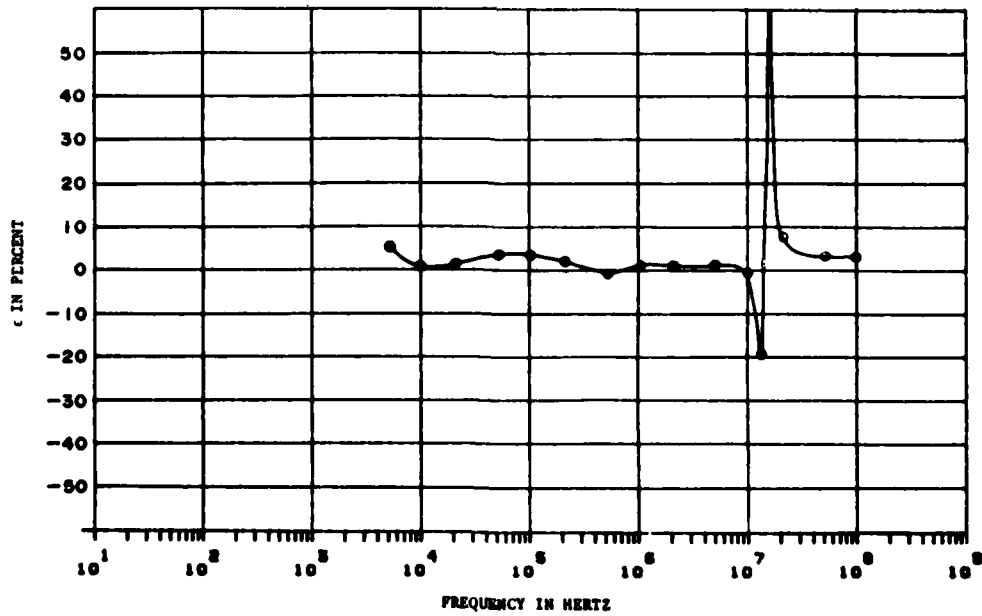


Figure D-8(b). Difference Between Calculated and Measured $|Z|$ in (a).

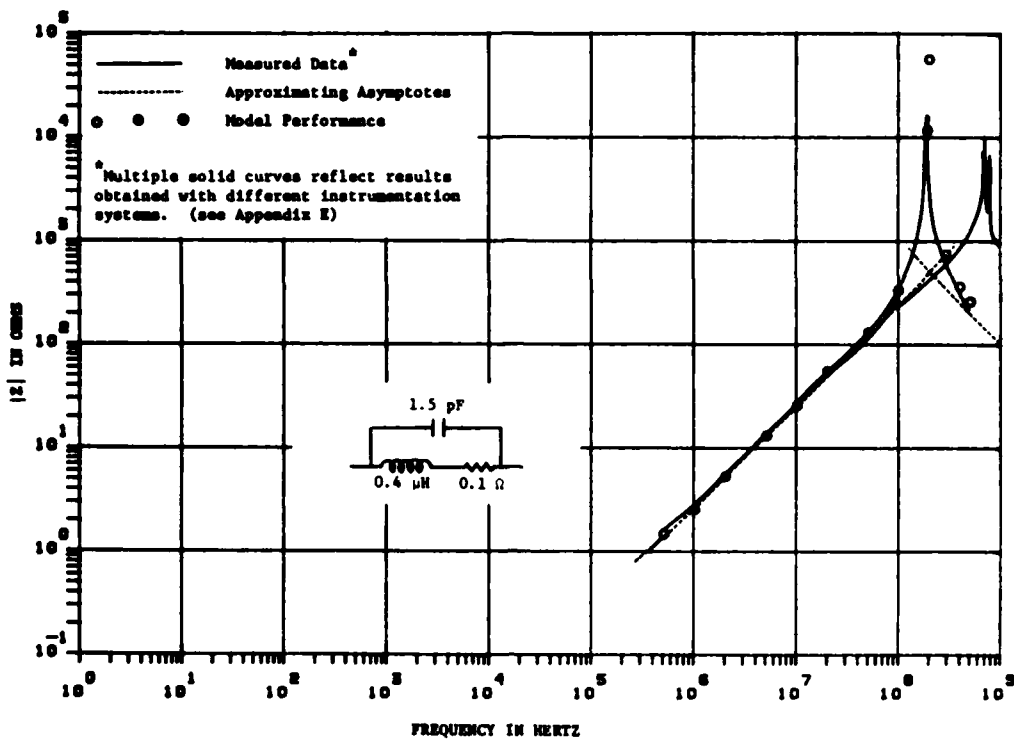


Figure D-9(a). Data for the Inductor Representing Group #2 in Table D-8.

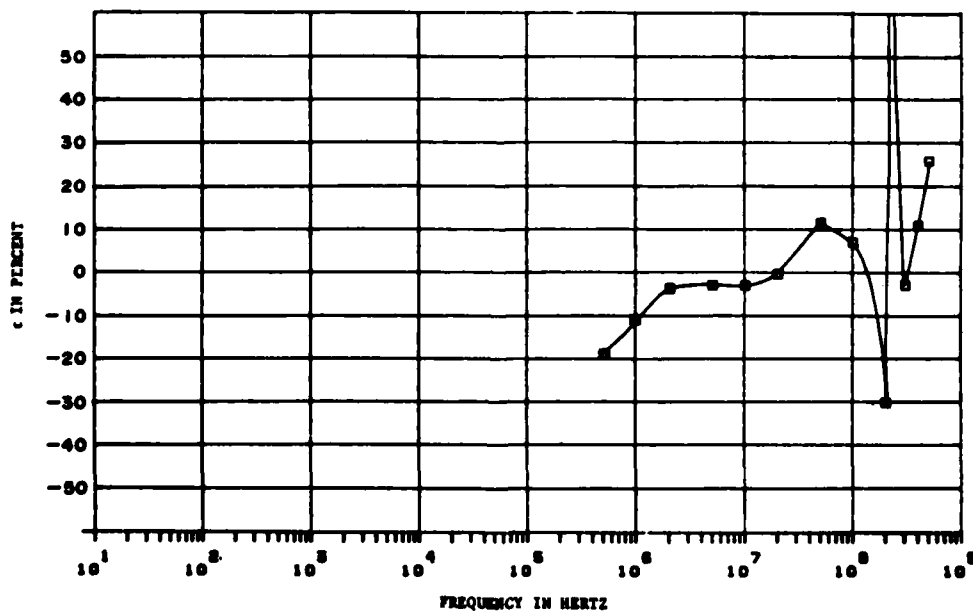


Figure D-9(b). Difference Between Calculated and Measured $|Z|$ in (a).

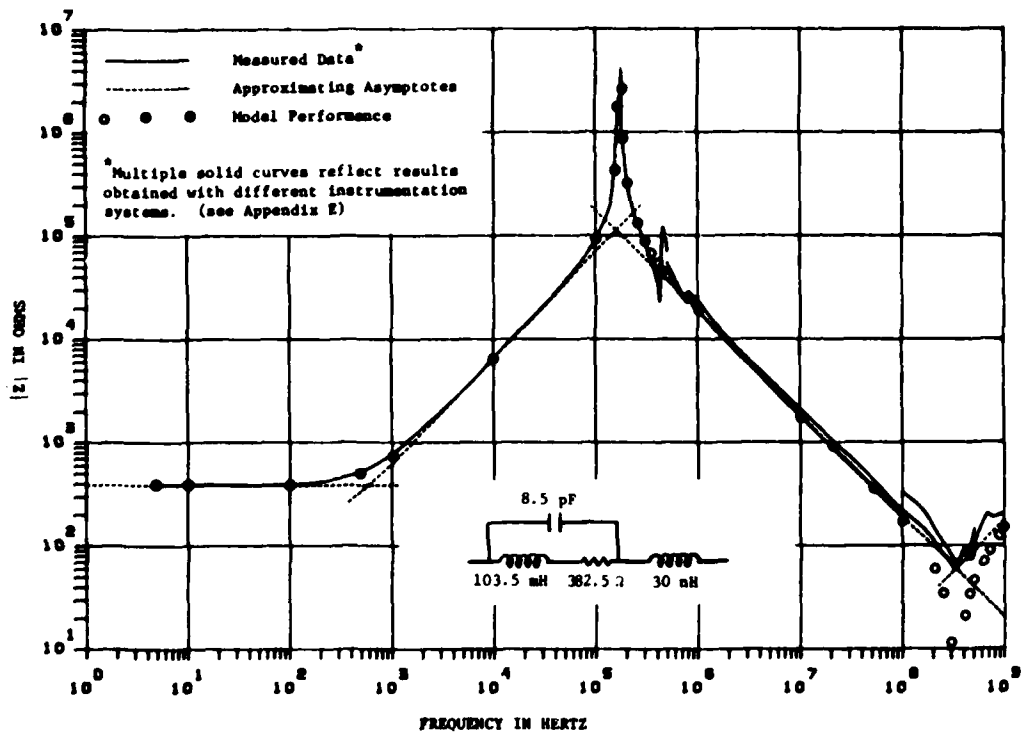


Figure D-11(a). Data for the Inductor Representing Group #4 in Table D-8.

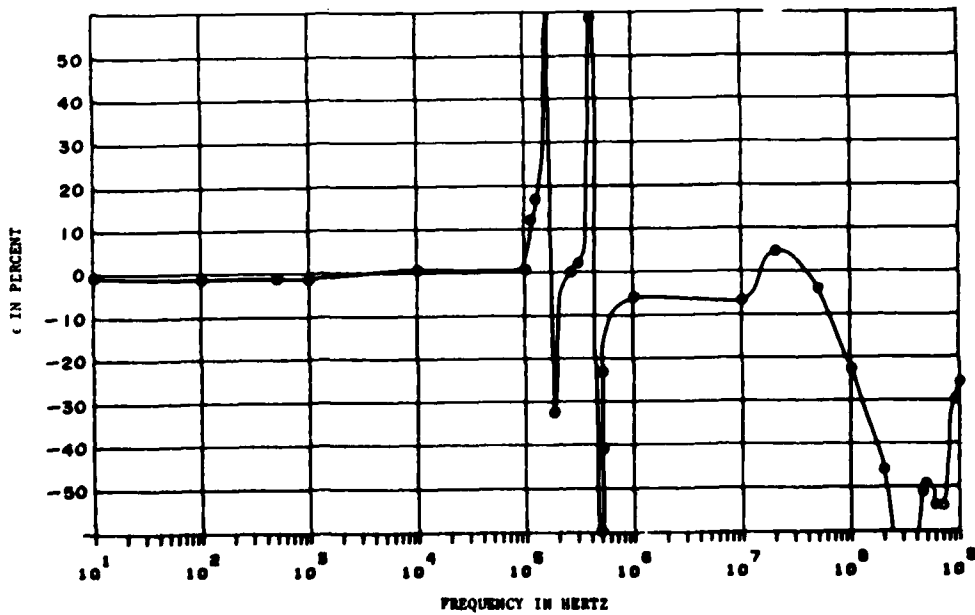


Figure D-11(b). Difference Between Calculated and Measured $|Z|$ in (a).

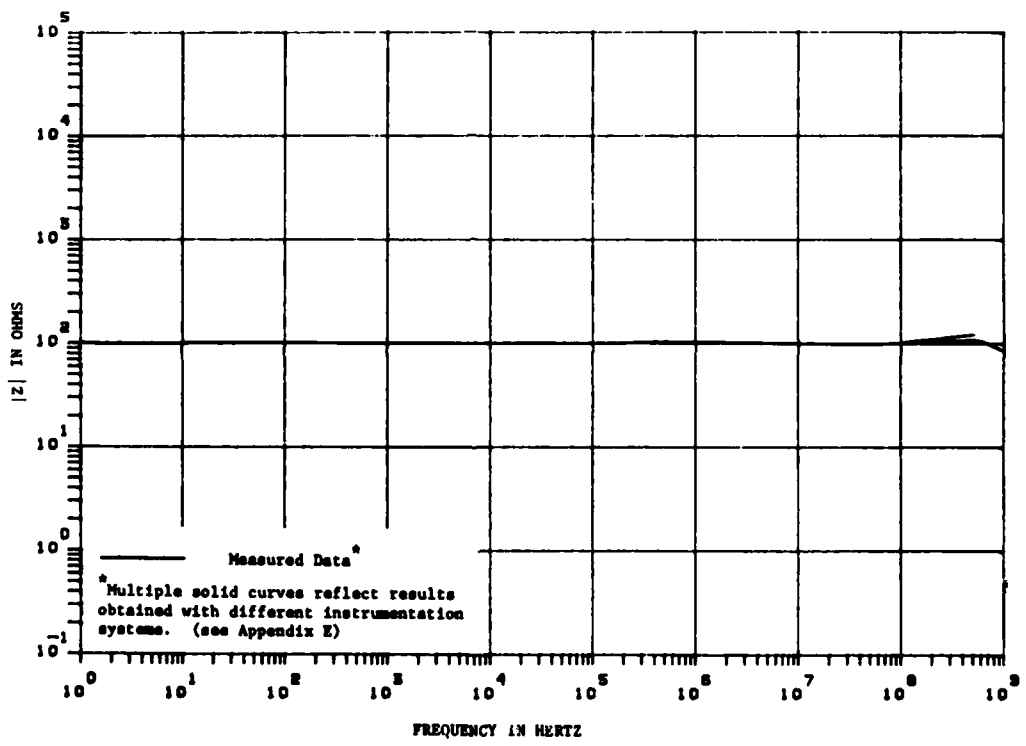


Figure D-12. Data for the Resistor Representing Group #1 in Table D-9.

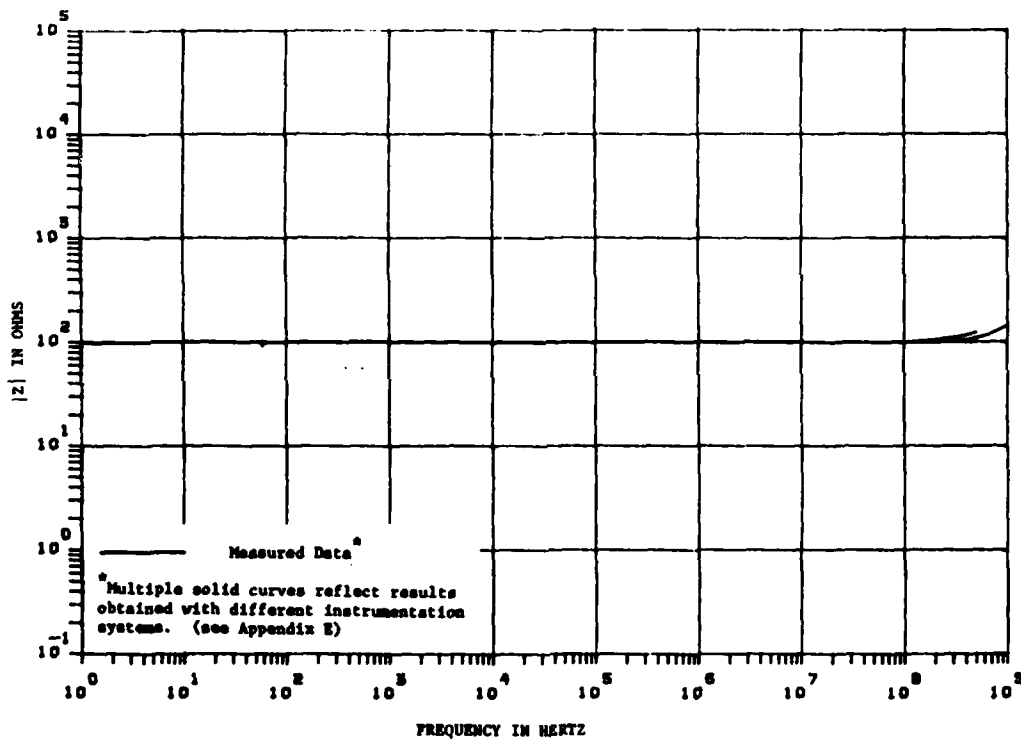


Figure D-13. Data for the Resistor Representing Group #2 in Table D-9.

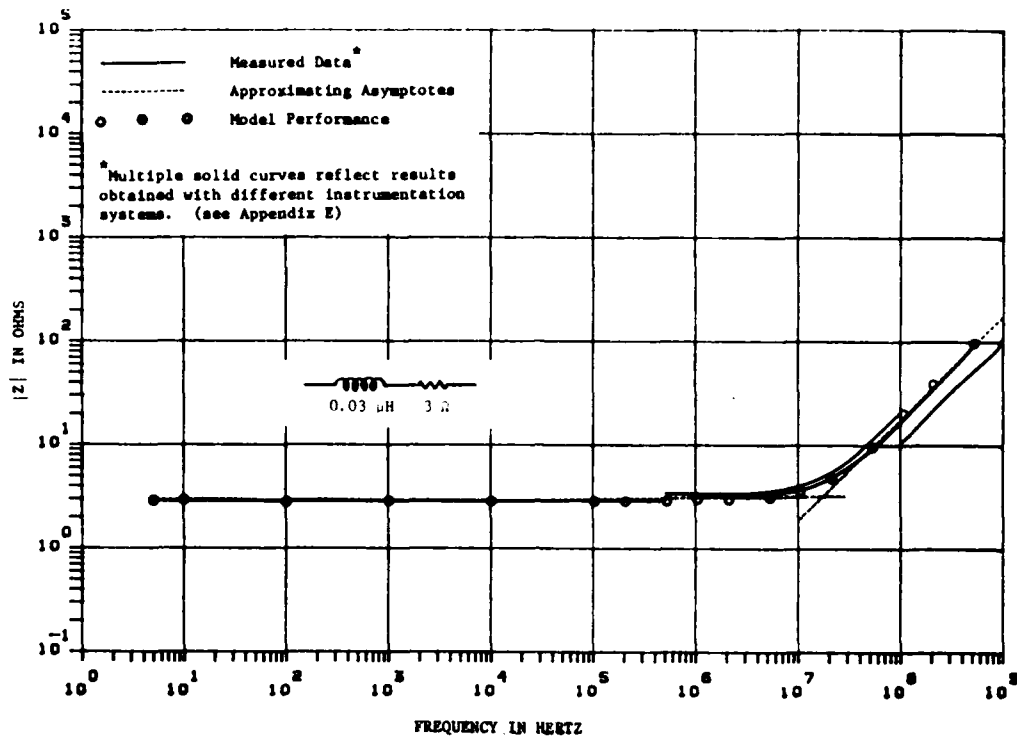


Figure D-14(a). Data for the Resistor Representing Group #3 in Table D-9.

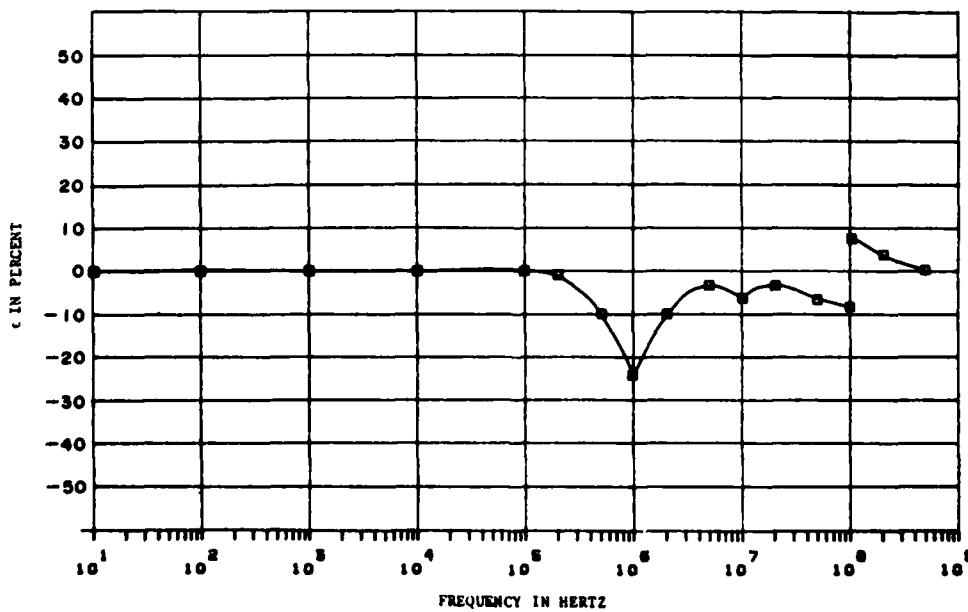


Figure D-14(b). Difference Between Calculated and Measured $|Z|$ in (a).

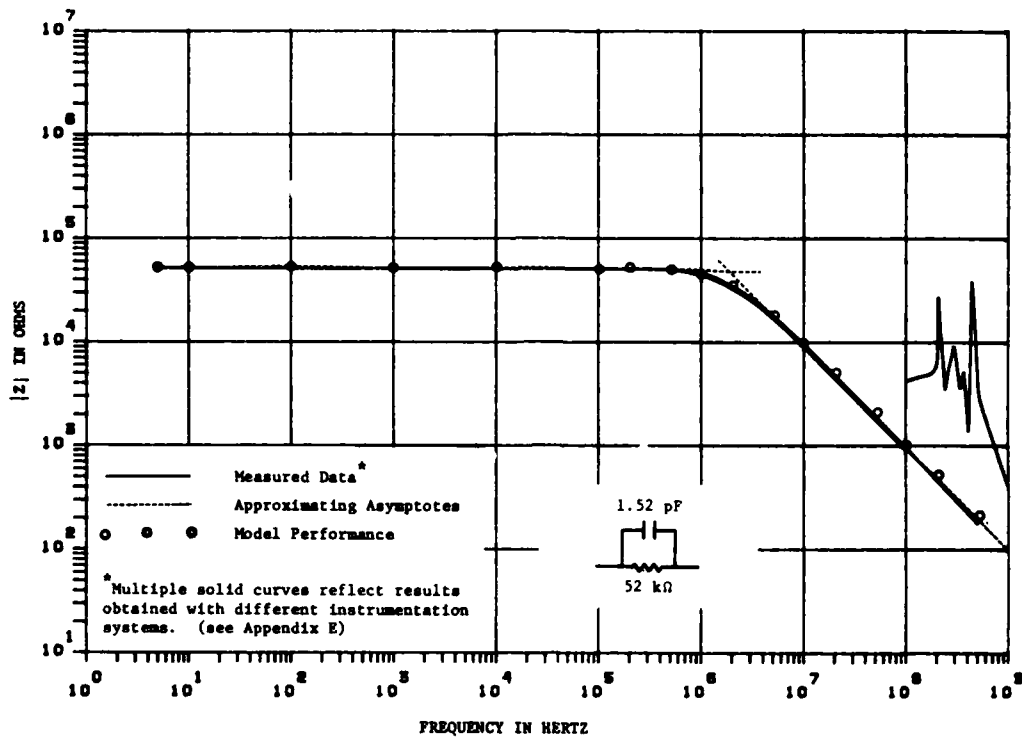


Figure D-15(a). Data for the Resistor Representing Group #4 in Table D-9.

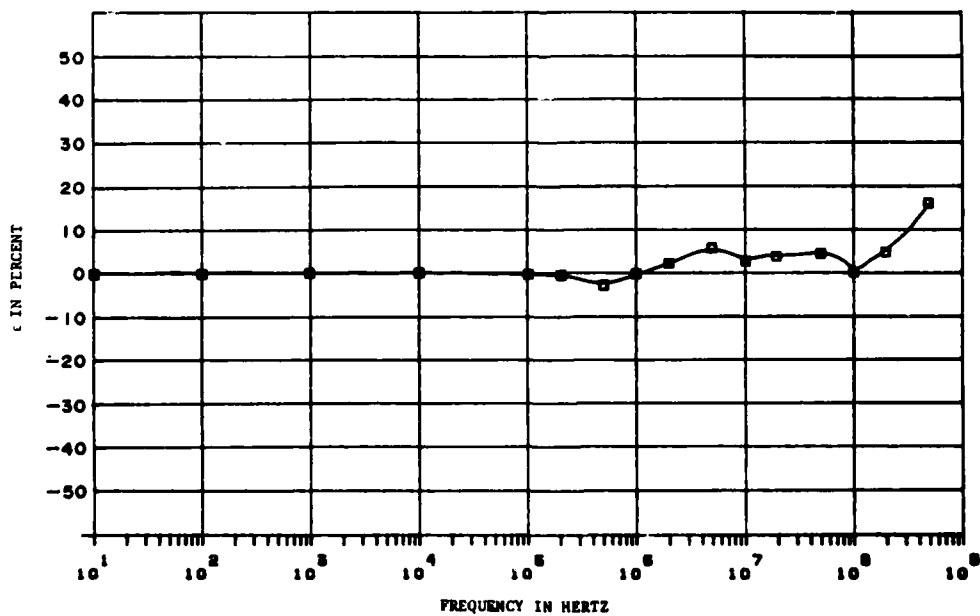


Figure D-15(b). Difference Between Calculated and Measured $|Z|$ in (a).

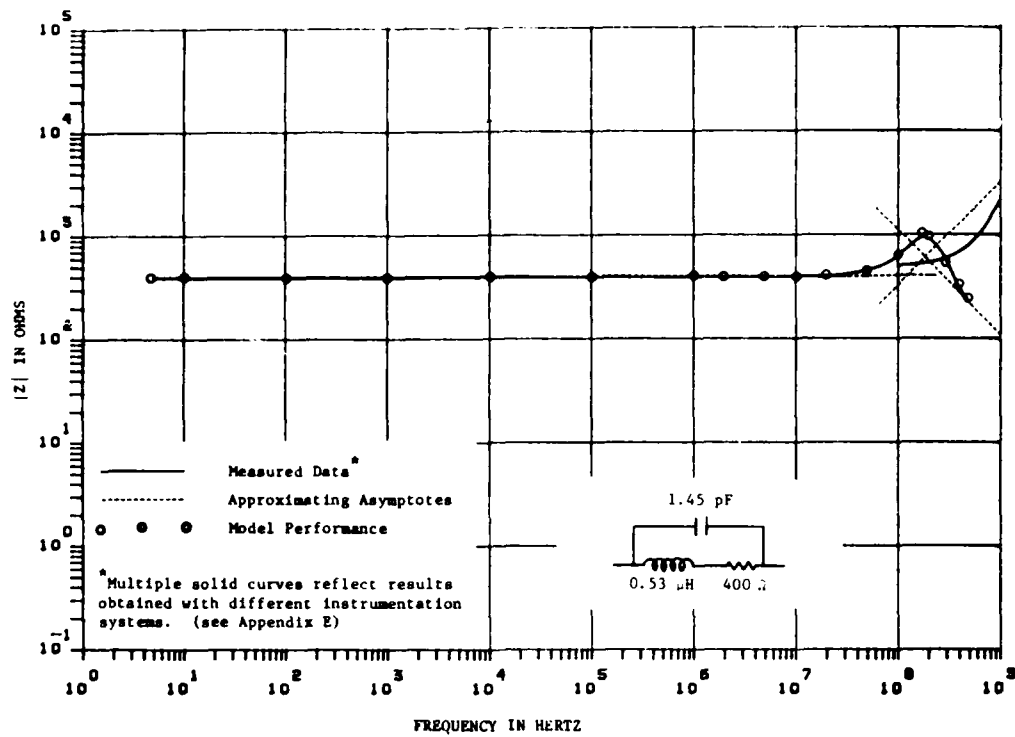


Figure D-16(a). Data for the Resistor Representing Group #5 in Table D-9.

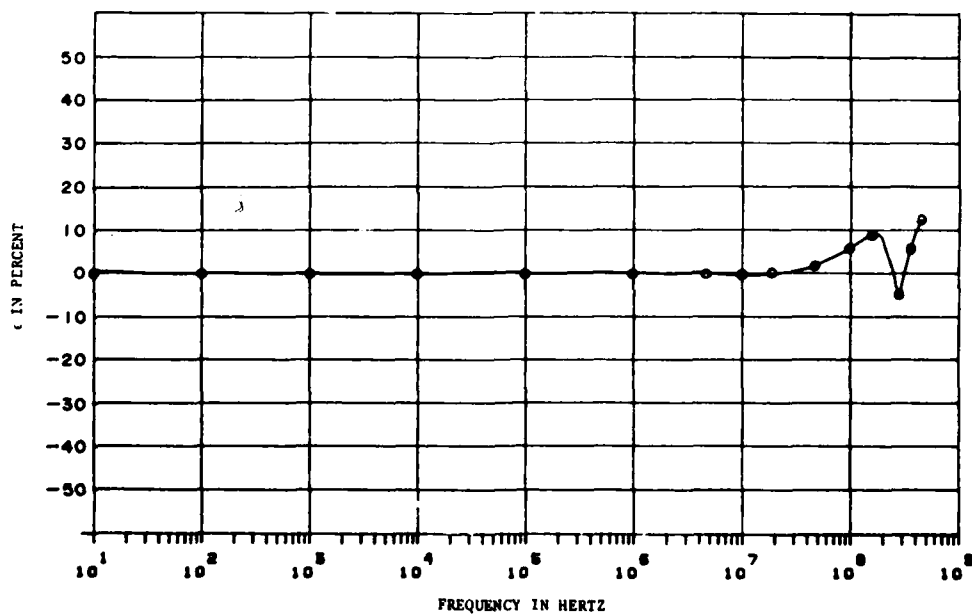


Figure D-16(b). Difference Between Calculated and Measured $|Z|$ in (a).

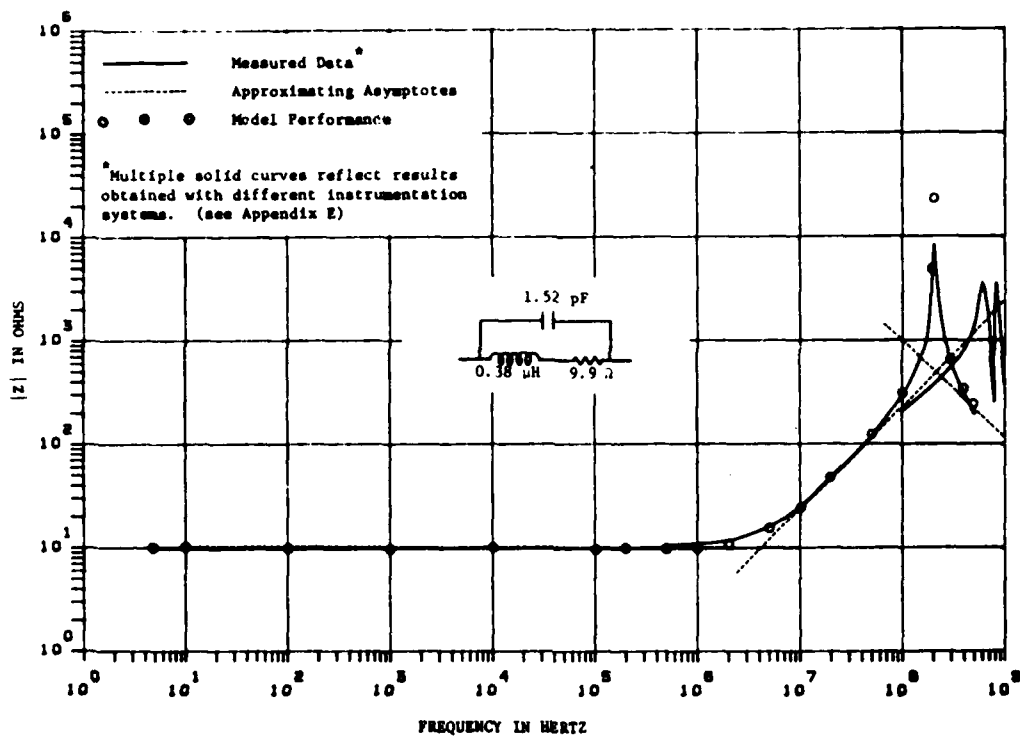


Figure D-17(a). Data for the Resistor Representing Group #6 in Table D-9.

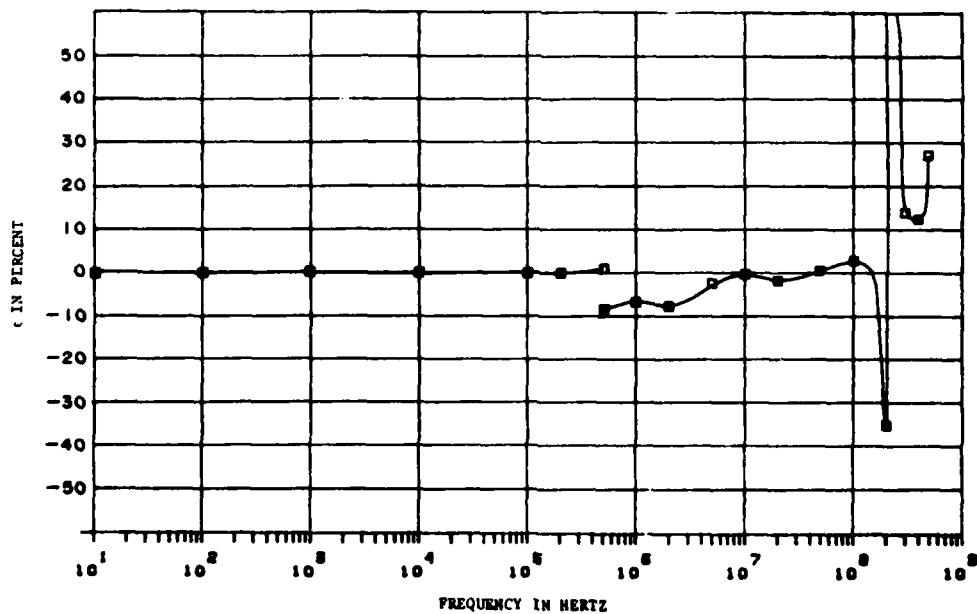


Figure D-17(b). Difference Between Calculated and Measured $|Z|$ in (a).

TABLE D-1
CAPACITORS SELECTED FOR MEASUREMENT

Type of Component	Manufacturer	Catalog #	Cardinal Value	Tolerance (%)	Working Voltage (VDC)	Comments
Tantalum, Wet Sintered	Tansitor	W10-50CIK	10 μ F	± 10	50	
	Tansitor	UW820-10C3M1	820 μ F	± 20	10	Ultra high C
	Sprague	109D156C2075F2	15 μ F		75	Gelled Electrolyte
	Sprague	109D2226X0025C2	22 μ F	± 20	25	Gelled Electrolyte
	Sprague	150D156X9035	15 μ F	± 10	35	Hermetically sealed; axial leads
Tantalum, Solid	Sprague	150D333X0035	0.033 μ F	± 20	35	Hermetically sealed; axial leads
	Sprague	150D474X9035A2	0.47 μ F	± 10	35	Hermetically sealed; axial leads
	Sprague	196D106X9035PC4	10 μ F	± 10	35	Hermetically sealed; axial leads
	Sprague	196D185X9035JA1	1.8 μ F	± 10	35	Resin dipped; radial leads
	Sprague	196D185X9035JA1	1.8 μ F	± 10	35	Resin dipped; radial leads
Aluminum Electrolytic	Mallory	TT25X50A	50 μ F	-10 +75	25	

(continued)

TABLE D-1 (continued)
CAPACITORS SELECTED FOR MEASUREMENT

Type of Component	Manufacturer	Catalog #	Cardinal Value	Tolerance (%)	Working Voltage (VDC)	Comments
Polyester	Nytronics	111B102K	0.001 μ F	± 10	100	Mylar
	Nytronics	107B104M	0.1 μ F	± 20	100	
	CDE	WMF-1S47	0.047 μ F	± 10	100	
Difilm	Sprague	160P 6TM-D25	0.0025 μ F	± 10	600	Dual polyester - paper dielectric
	Sprague	160P 6TM-D50	0.005 μ F	± 10	600	Dual polyester - paper dielectric
Metalized Polyester Film	Sprague	431P-205	2 μ F	± 10	50	
	Centralab	CPR 3900J	3900 pF	± 5	500	
Polystyrene Film	Centralab	CPR 10,000J	0.01 μ F	± 5		
	EL Menco	CM-30-E-472J	0.0047 μ F	± 5	500	Layers of mica & metal foil
Mica	Sprague	424ME5100J501	510 pF	± 5	500	Silvered

(continued)

TABLE D-1 (concluded)
CAPACITORS SELECTED FOR MEASUREMENT

Type of Component	Manufacturer	Catalog #	Cardinal Value	Tolerance (%)	Working Voltage (VDC)	Comments
Mica	Arco	DM-15-200J	20 pF	±5	500	Silvered
	Arco	DM-15-201J	200 pF	±5	500	Silvered
	Arco	DM-15-471J	470 pF	±5	500	Silvered
Ceramic	Centralab	DD 100	10 pF	±10	1k	
	Centralab	DD 102	1000 pF	±10	1k	
	Centralab	DD 103	0.01 μF	±10	1k	
	Sprague	10TCC-Q20	20 pF	±5	1k	NPO, Temperature Compensating
	Sprague	10TCC-Q47	47 pF	±5	1k	NPO, Temperature Compensating
	Sprague	10TCC-T20	200 pF	±5	1k	NPO, Temperature Compensating

TABLE D-2
INDUCTORS SELECTED FOR MEASUREMENT

Type of Component	Manufacturer	Catalog #	Cardinal Value	Tolerance (%)	Comments
RF, Shielded Molded Miniature (epoxy)	Nytronics	Wee-0.47	0.47 μ H	± 10	Phenolic core
	Nytronics	Wee-100	100 μ H	± 5	Ferrite core
	Nytronics	SWD-0.47	0.47 μ H	± 10	Phenolic core; MIL-STD Type
	Nytronics	SWD-1200	1200 μ H	± 10	Ferrite core; MIL-STD Type
RF, Molded	Delevan	1641-101	0.1 μ H	± 10	Phenolic core; iron sleeve
	Delevan	2500-76	10,000 μ H	± 5	Iron (LT = 10k) core
	Nytronics	DD-120	120 μ H	± 10	Ferrite core; subminiature
RF Choke	Miller	4602	1 μ H	± 20	Phenolic core; single layer
	Miller	4629	55 μ H	± 5	Iron core; single layer
	Miller	4632	100 μ H	± 5	Iron core; single layer
	Miller	4668	3.9 mH	± 5	Iron core; 3 section
	Miller	9230-16	0.68 μ H	± 10	Micro-miniature molded phenolic core
	Miller	9350-08	100 μ H	± 10	Molded iron core
	Miller	994	100 mH	± 5	Air core PC RF choke

TABLE D-3
RESISTORS SELECTED FOR MEASUREMENT

Type of Component	Manufacturer	Catalog #	Cardinal Value (Ω)	Tolerance (%)	Wattage (Watts)	Comments
Carbon Composition	Allen-Bradley	CB27G1	2.7	± 10	1/4	RCR07G2R7K Type
	Allen-Bradley	CB5601	56	± 10	1/4	RCR07G560K Type
	Allen-Bradley	CB3911	390	± 10	1/4	RCR07G391K Type
	Allen-Bradley	CB1521	1.5k	± 10	1/4	RCR07G152K Type
Carbon Composition Film	TRW/IRC	RCR20G101KS	100	± 10	1/2	Non-Spiral
	TRW/IRC	RCR20G102KS	1k	± 10	1/2	Non-Spiral
	TRW/IRC	CR7	10k	± 5	1	Thick Film Spiral
Carbon Film	R-Ohm	R-25J-100	100	± 5	1/4	Spiral
	R-Ohm	R-25J-1 k	1k	± 5	1/4	Spiral
Metal Film	Caddock	MS 151	100	± 1	1/2	Metal Oxide; spiral; power; thick film
	Caddock	MS 310	50k	± 1	10	Metal Oxide; spiral; power; thick film

(continued)

TABLE D-3 (continued)
RESISTORS SELECTED FOR MEASUREMENT

Type of Component	Manufacturer	Catalog #	Cardinal Value (Ω)	Tolerance (%)	Wattage (Watts)	Comments
Metal Film	Corning	C4-28R-1	28	± 1	1/4	RL075 Type, Tin Oxide; Thick Film
	Corning	FP3-12K-10%	12 k	± 10	3	Tin Oxide; Thick Film
	Corning	NA55-47R-1%	47	± 1	1/8	RN55D Type; Tin Oxide; Thick Film
	Corning	MC65-52.3K-0.1%	52.3 k	± 0.1	1/4	RN65C Type; Nichrome; Thick Film
	TRW/IRC	AR40	100 k	± 0.05	0.3	Radial Leads; Thin Film
	TRW/IRC	MAR 3	1.65 k	± 1	1/20	Thin Film
	TRW/IRC	MAR 7	100	± 0.5	1/4	Thin Film
Wirewound	TRW/IRC	BW-20-100-5%	100	± 5	1	Alloy resistance wire on fiberglass core
	Dale	RS-1B	25	± 1	1.1	Copper-nickel or nickel-chrome alloy on ceramic core
	Sage/Nytronics	250SB-4000F-1	400	± 1	1	Beryllia core
	Memcor/E-systems	VL-0003-2100	10		3	
	Memcor/E-systems	VL-0010-4100	1 k		10	Leads = 2 cm

(continued)

TABLE D-3 (concluded)
RESISTORS SELECTED FOR MEASUREMENT

<u>Type of Component</u>	<u>Manufacturer</u>	<u>Catalog #</u>	<u>Cardinal Value</u> (Ω)	<u>Tolerance</u> (%)	<u>Wattage</u> (Watts)	<u>Comments</u>
Wirewound	Ohmite	995-5B(4561)	10	± 5	5	Vitreous Enamel Coating on Steatite Ceramic Core
	Ohmite	995-1A(4123)	1 k	± 5	1-1/2	

TABLE D-4
CHARACTERISTICS OF EACH GROUP OF
MEASURED CAPACITOR DATA

Characteristics of $ Z $ vs f Curves	Group Number						
	<u>1</u>	<u>2</u>	<u>3</u>	<u>4</u>	<u>5</u>	<u>6</u>	<u>7</u>
Q* undefined because of insufficient data	Y	N	N	N	N	N	N
Q << 1	N	Y	Y	N	N	N	N
Q ≈ 1	N	N	N	Y	N	N	N
Q ≈ 2	N	N	N	N	Y	N	N
3 < Q < 5	N	N	N	N	N	Y	N
Q ≥ 7	N	N	N	N	N	N	Y
Slope of curve suddenly decreased approximately 2 decades below the resonance frequency	N	N	Y	N	N	N	N

* Q is defined as the ratio of the resonance frequency and the 3 dB bandwidth where this bandwidth is the difference in the frequencies at which the $|Z|$ is 3 dB greater than $|Z|_{\min}$ (i.e., 1.414 times $|Z|_{\min}$)

TABLE D-5
CHARACTERISTICS OF EACH GROUP OF
MEASURED INDUCTOR DATA

Characteristics of $ Z $ vs f Curves	Group Number			
	<u>1</u>	<u>2</u>	<u>3</u>	<u>4</u>
Number of resonance frequencies	1	1	1	2
Curve has constant low frequency value	N	N	Y	Y
Curve extends at least a frequency decade above the first resonance	Y	N	Y	Y

TABLE D-6
 CHARACTERISTICS OF EACH GROUP OF
 MEASURED RESISTOR DATA

Characteristics of $ Z $ vs f Curves	Group Number					
	<u>1</u>	<u>2</u>	<u>3</u>	<u>4</u>	<u>5</u>	<u>6</u>
Curve stops at a frequency lower than f_3^* dB	Y	N	N	N	N	N
Curve stops at a frequency only slightly greater than f_3 dB	N	Y	N	N	N	N
Curve has only positive slope above f_3 dB	N	N	Y	N	N	N
Curve has only negative slope above f_3 dB	N	N	N	Y	N	N
Curve has a resonance and $Q < 5$	N	N	N	N	Y	N
Curve has a resonance and $Q > 10$	N	N	N	N	N	Y

* f_3 dB is the frequency at which the $|Z|$ curve and its asymptote differ by 3 dB.

TABLE D-7

MEASURED CAPACITORS--LISTED ACCORDING TO THE
GROUPS DEFINED IN TABLE D-4

Group #	Type of Capacitor	Cardinal Value	Manufacturer & Catalog #	Components Whose Curves Were Chosen as Representative of Each Group
1	Tantalum, Wet Sintered	10 μ F	Tansitor W10-50CLK	X (See Figure D-1)
		15 μ F	Sprague 109D156C2075F2	
		22 μ F	Sprague 109D226X0025C2	
		820 μ F	Tansitor UW820-10C3M1	
		10 μ F	Sprague 196D106X9035PC4	
2	Metalized Polyester Film	15 μ F	Sprague 150D156X9035	X
		2 μ F	Sprague 431P-205	
		0.47 μ F	Sprague 150D474X9035A2	
2	Tantalum, Solid	1.8 μ F	Sprague 196D185X9035JAI	X

(continued)

TABLE D-7 (Continued)
 MEASURED CAPACITORS--LISTED ACCORDING TO THE
 GROUPS DEFINED IN TABLE D-4

Group #	Type of Capacitor	Cardinal Value	Manufacturer & Catalog #	Components Whose Curves Were Chosen as Representative of Each Group
3	Tantalum, Solid	0.033 μ F	Sprague 150D333X0035	X
	Aluminum Electrolytic	50 μ F	Mallory TT25X50A	
4	Polyester	0.047 μ F	CDE WMF-1S47	X
		0.1 μ F	Nytronics 170B104M	
5	Polystyrene Film	10,000 pF	Centralab CPR 10, 000J	X
	Ceramic	0.01 μ F	Centralab DD 103	X
6	Ceramic	1000 pF	Centralab DD 102	
	Mica	0.0047 μ F	EI Menco CM-30-E-472J	

(continued)

TABLE D-7 (Continued)

MEASURED CAPACITORS--LISTED ACCORDING TO THE
GROUPS DEFINED IN TABLE D-4

Group #	Type of Capacitor	Cardinal Value	Manufacturer & Catalog #	Components Whose Curves Were Chosen as Representative of Each Group
6	Difilm	0.0025 μ F	Sprague 6TM-D25	X
			Sprague 6TM-D50	
7	Polystyrene	3900 pF	Centralab CPR 3900J	X
			Centralab DD 100	
			Sprague 10TCC-Q20	
7	Ceramic	10 pF	Sprague 10TCC-Q47	X
			Sprague 10TCC-T20	
			Arco DM-15-200J	
			Mica, Silvered	

(continued)

TABLE D-7 (Concluded)
 MEASURED CAPACITORS--LISTED ACCORDING TO THE
 GROUPS DEFINED IN TABLE D-4

Group #	Type of Capacitor	Cardinal Value	Manufacturer & Catalog #	Components Whose $ Z $ vs f Curves Were Chosen as Representative of Each Group
7	Mica, Silvered	200 pF	Arco DM-15-201J	
		470 pF	Arco DM-15-471J	
		510 pF	Sprague 424ME5100J501	
	Polyester	1000 pF	Nytronics 111B102K	

TABLE D-8

MEASURED INDUCTORS--LISTED ACCORDING TO THE
GROUPS DEFINED IN TABLE D-5

Group #	Type of Inductor	Cardinal Value	Manufacturer & Catalog #	Components Whose $ Z $ vs f Curves Were Chosen as Representative of Each Group
1	RF Choke	55 μ H	Miller 4629	X
2	RF Choke	0.68 μ H	Miller 9230-16	
		1 μ H	Miller 4602	
	RF, Molded Shielded	0.1 μ H	Delevan 1641-101	
3		0.47 μ H	Nytronics SWD-0.47	X
		0.47 μ H	Nytronics Wee-0.47	
	RF Choke	100 μ H	Miller 4632	X
	RF, Molded Shielded	100 μ H	Miller 9350-08	
4		100 μ H	Nytronics Wee-100	
		1200 μ H	Nytronics SWD-1200	
	RF, Molded	120 μ H	Nytronics DD-120	
	RF Choke	3.9 mH	Miller 4668	
4		100 mH	Miller 994	X
	RF, Molded	10,000 μ H	Delevan 2500-76	

TABLE D-9

MEASURED RESISTORS--LISTED ACCORDING TO THE
GROUPS DEFINED IN TABLE D-6

Group #	Type of Resistor	Cardinal Value (Ω)	Manufacturer & Catalog #	Components Whose Curves Were Chosen as Representative of Each Group
1	Metal Film	100	TRW/IRC MAR7	X
			Caddock MS151	
2	Metal Film	47	Corning NA55-47R-1%	
			Allen-Bradley CB5601	
	Carbon Composition	56	Allen-Bradley CB3911	
			TRW/IRC RCR20C101KS	
3	Metal Film	28	R-Ohm R-25J-100	X
			Corning C4-28R-1%	
	Carbon Composition	2.7	Allen-Bradley CB27G1	X

(Continued)

TABLE D-9 (Continued)

MEASURED RESISTORS--LISTED ACCORDING TO THE GROUPS DEFINED IN TABLE D-6

Group #	Type of Resistor	Cardinal Value (Ω)	Manufacturer & Catalog #	Components Whose Curves Were Chosen as Representative of Each Group
4	Metal Film	1.65 k	TRW/IRC MAR3	X
			Corning FP3-12k-10%	
		12 k	Caddock MS310	
			Corning MC65-52.3k-0.1%	
	Carbon Composition	50 k	TRW/IRC AR40	
			Allen-Bradley CB1521	
	Carbon Composition Film	52.3 k	TRW/IRC CR7	
			R-Ohm R-25J-1K	
	Carbon Film	100 k		
Carbon Film	1.5 k			
Carbon Film	1 k			
Carbon Film	10 k			
Carbon Film	1 k			

(continued)

TABLE D-9 (Concluded)
 MEASURED RESISTORS--LISTED ACCORDING TO THE
 GROUPS DEFINED IN TABLE D-6

Group #	Type of Resistor	Cardinal Value (Ω)	Manufacturer & Catalog #	Components Whose $ Z $ vs f Curves Were Chosen as Representative of Each Group
5	Wirewound	100	TRW/IRC	X
			BW-20-100-5%	
		400	Sage/Nytronics	X
			250SB-4000F-1	
6	Wirewound	1 k	Memcor/E-Systems	X
			VL-0010-4100	
		1 k	Ohmite	X
			995-1A	
10	Wirewound	10	Memcor/E-Systems	X
			VL-0003-2100	
			Ohmite 995-5B	
25	Wirewound	25	Dale	X
			RS-1B	

APPENDIX E
PRELIMINARY ANALYSIS OF INSTRUMENTATION PARASITICS

The applicable frequency ranges of several of the measurement techniques overlapped (see Table D-1). At the common frequencies, measurements were made using each of the different measurement techniques. (The data obtained from each technique is plotted on the graphs in Appendix D.) It should be noted that, at these common measurement frequencies, different values of the complex impedance were obtained for the same component. Furthermore, these differences obtained with the various measurement techniques appear to be greater at the higher measurement frequencies.

As a preliminary investigation of these differences, several components were measured at a common frequency of 100 MHz using the HP 4815A RF Vector Impedance Meter, the GR 1710 RF Network Analyzer, and the reflectometer system. The magnitudes of the impedances obtained from these measurements are given in Table E-1. This data shows that the differences vary with the measurement techniques, the types of components, and the cardinal values of the components. Therefore, nine different cardinal values of the same type component (1/4 watt, carbon composition resistor by Allen-Bradley) were measured at 100 MHz using the same three measurement techniques as above. The results of these measurements and the dc resistances are given in Table E-2. Figure E-1 shows how the magnitude of the impedance of the resistors as measured with the GR 1710 Network Analyzer varies as a function of frequency.

These initial investigations indicate that the differences are probably due to the parasitics of the different instrumentation systems, cables, and component mounts. Such differences and their variations appear to be a result of the relationship between the magnitudes of the impedance of the component under test, of the component's parasitics, and of the instrumentation parasitics. If the magnitude of the impedance-to-be-determined is high, then the distributed parallel capacitance of the measurement system is likely to be of the same order-of-magnitude and, thus, cause the measured impedance to be too low. On the other hand, if the magnitude of the impedance-to-be-determined is low, the parasitic series inductance of the measurement system may be of the same order-of-magnitude and, thus, cause the measured impedance to be too high.

There are some exceptions to these two rules-of-thumb. For example, preliminary measurements indicate that the "open-circuit" impedance of the reflectometer system is inductive with a magnitude of approximately 1 k Ω . (equivalent to a 0.16 μ H inductor at 1 GHz). Therefore, obviously if the component being measured is an inductor with an impedance on the order of 1 k Ω , the measured value will be approximately 500 Ω . Conversely, if the component being measured is capacitive, it can form a parallel resonant circuit with the parasitic inductance of the measurement system and the impedance can become very large at the resonance frequency.

In order to determine the feasibility of removing the effects of the instrumentation parasitics from the measured data, a brief analysis of the GR 1710 Network Analyzer data given in Table E-2 was performed. In Figure E-1, the measured impedance curves for the short-circuit and "open-circuit" (no component on the mount) conditions are given. The "open-circuit" impedance curve decreases at a rate of approximately 6 dB/octave (20 dB/decade) and, thus, implies that the combination of the component mount, probe, cabling, etc. are capacitive under "open-circuit" conditions. The $|Z| = 1.3$ k Ω at 100 MHz represents a capacitance of 1.2 pF. Similarly, the fact that the short-circuit curve increases at a rate of approximately 20 dB/decade implies that the instrumentation is inductive under short-circuit conditions. On the straight line approximation (dotted line) to this curve, the $|Z| = 2.9$ k Ω at 100 MHz indicates an inductance of 4.6 nH. Therefore, assume that the equivalent circuit of the instrumentation parasitics is as shown in Figure E-2.

Using the impedances given in Table E-2 for the GR 1710 Network Analyzer as the measured Z (Z_m) and the circuit in Figure E-2, the corrected impedance of the component (Z_u) was calculated. The calculated Z_u 's given in Table E-3 are obviously not equal to the R_{dc} 's and are not even pure resistances. Therefore, a circuit model was synthesized for the Z_u 's. If the phase of Z_u was positive, the model was assumed to be an R representing R_{dc} in series with an inductor (L). Thus, $Z_u = R + j\omega L$. Alternatively, if the phase of Z_u was negative, the model was assumed to be the R in parallel with a capacitor (C) and, thus, $Z_u = R(1/j\omega C)/(R + 1/j\omega C)$. The calculated R's, L's, and C's for the models for each of the nine cardinal values are given in Table E-4.

Also, a measure of the difference (ϵ) between the calculated R and the dc R is given in percent (ϵ would be the percent error if R_{dc} was the correct value of R at 100 MHz). From this data, the following observations were made:

- o Except for very small and very large cardinal values, the differences between R and R_{dc} are small (typically <20%).
- o The majority of the L's are approximately 14nH.
- o The majority of the C's are approximately 0.5pF.

Based on the above and related preliminary analyses (of the impedance of one type of component at one measurement frequency), the following conclusions have been developed related to instrumentation parasitics:

- o If the parasitics of the instrumentation system are characterized, the measured data can be corrected by removing their effects.
- o Such data is needed for each measurement technique.
- o Such data is needed as a function of frequency or at least at each measurement frequency.

Thus, a correction technique for removing the instrumentation parasitics from measured impedance data is indicated. However, before this technique is employed on all measured data, its appropriateness for all the measurement techniques, for each type of component, and for each measurement frequency must be ascertained. Therefore, it is recommended that further investigations be directed toward defining each measurement system's inherent parasitics, defining the effects of the parasitics on the measured impedance, investigating the variation of these effects with the magnitude of the impedance being measured and with the type of component under test, identifying the most appropriate techniques for removing the effects from the measured data, and analyzing the validity of each technique and accuracy of the resulting data.

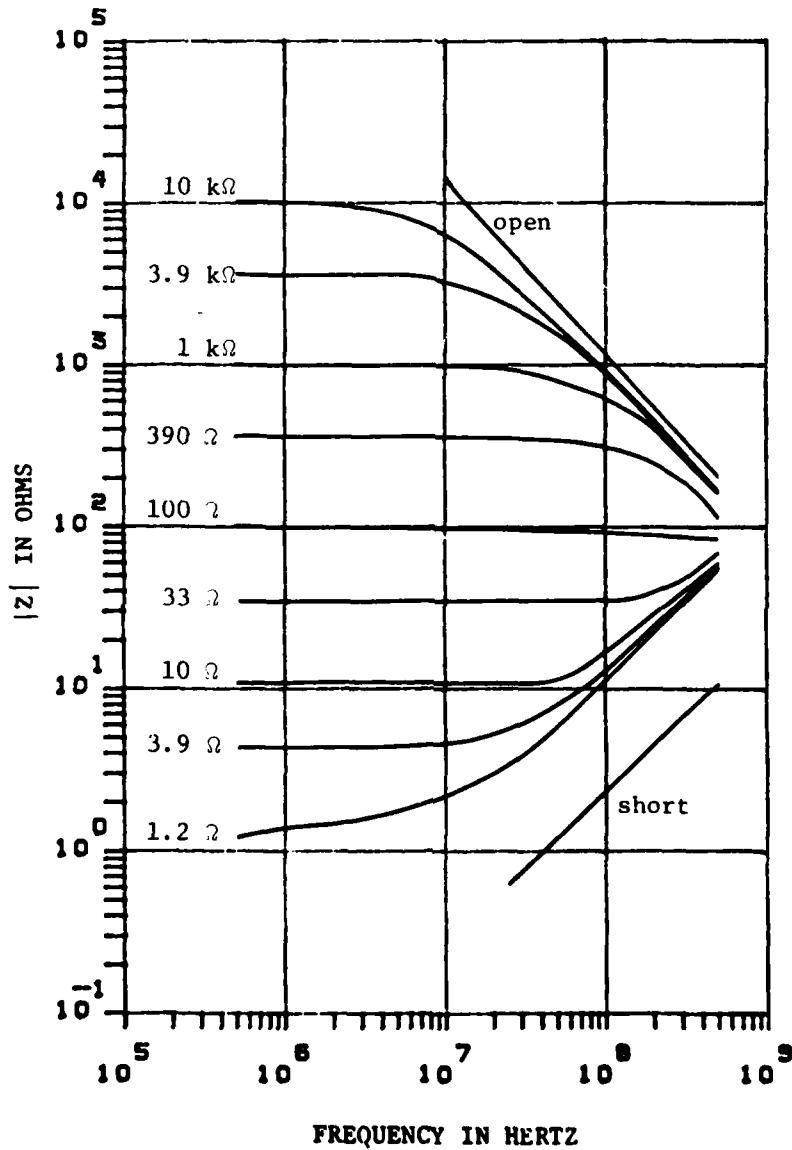


Figure E-1. Measured Impedance of Various Cardinal Values of 1/4-watt Carbon Composition Allen-Bradley Resistors.

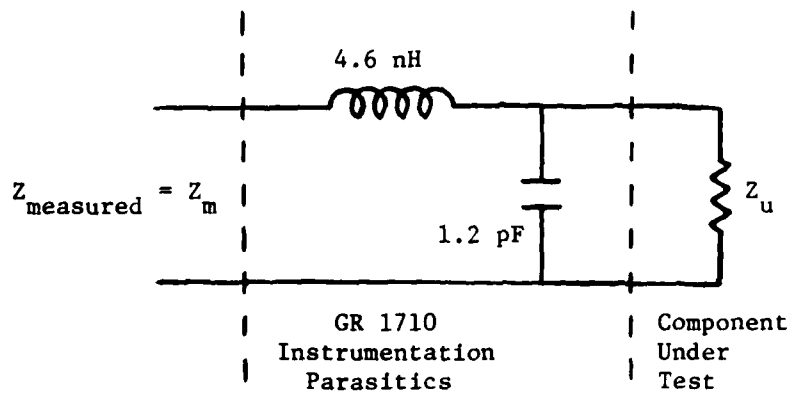


Figure E-2. Circuit Showing Possible Instrumentation Parasitics Relative to the Measured Z and the Component-under-Test.

TABLE E-1

MAGNITUDE OF THE IMPEDANCE MEASURED FOR SELECTED
COMPONENTS AT 100 MHZ USING DIFFERENT MEASUREMENT TECHNIQUES

Component Under Test	Impedance Magnitude		
	HP 4815A Vector Impedance Meter	GR 1710 Network Analyzer	Reflectometer System
C = 2200 pF	13.7 Ω	8 Ω	6.6 Ω
C = 10 μ F	25.5 Ω	20 Ω	14.7 Ω
L = 0.1 μ H	43 Ω	38 Ω	37 Ω
L = 100 μ H	0.58 k Ω	0.55 k Ω	1.79 k Ω
R = 1 k Ω	0.57 k Ω	0.6 k Ω	1.3 k Ω

TABLE E-2

MEASURED COMPLEX IMPEDANCE FOR VARIOUS CARDINAL VALUES
OF 1/4-WATT, CARBON COMPOSITION RESISTORS

Cardinal Resistance (Ω)	DC Resistance (Ω)	Impedance (ohms/degrees)		
		HP 4815A Vector Impedance Meter	GR 1710 Network Analyzer	Reflectometer System
1.2	1.3	1.93/89	10.3/80	10.4/82
3.9	4.2	6/80	13/67	10.4/69
10	10.8	23/64	16/48.5	15.5/47
33	36.4	42/28	36/17.5	37.8/16
100	108.1	109/5	92/-1	111.4/8
390	371.6	325/-21	310/-20.5	389.8/4
1 k	1057	660/-49	680/-46	1141/17
3.9 k	3739	780/-75	850/-72.5	6360/88
10 k	10.5 k	830/-84	940/-81	4079/121*

* Invalid data point due to instrument limitations.

TABLE E-3

UNKNOWN COMPONENT IMPEDANCE CALCULATED FROM
MEASURED IMPEDANCE ASSUMING INSTRUMENTATION
PARASITICS GIVEN IN FIGURE E-2.

R_{cardinal} (Ω)	R_{dc} (Ω)	Z_m ($\Omega/\text{degrees}$)	Z_u ($\Omega/\text{degrees}$)
1.2	1.3	10.3/80	7.4/76.2
3.9	4.2	13/67	10.3/61
10	10.8	16/48.5	13.9/41.1
33	36.4	36/17.5	35.0/14.5
100	108.1	92/-1	92.2/1.2
390	371.6	310/-20.5	330.3/-7.6
1 k	1057	680/-46	943.6/-16.6
3.9 k	3739	850/-72.5	1974.1/-46.1
10 k	10.5 k	940/-81	2967.1/-60.6

TABLE E-4

SYNTHESIZED CIRCUIT MODELS FOR CORRECTED
IMPEDANCE DATA GIVEN IN TABLE C-4

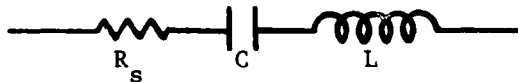
R_{cardinal} (Ω)	R_{dc} (Ω)	Z_u ($^\circ/\text{degrees}$)	Synthesized Model	$\frac{R - R_{\text{dc}}}{R_{\text{dc}}} \times 100$ (%)
1.2	1.3	7.4/76.2	$R = 1.8 \Omega$ & $L = 11.4 \text{ nH}$	38.5
3.9	4.2	10.3/61	$R = 5.0 \Omega$ & $L = 14.3 \text{ nH}$	19
10	10.8	13.9/41.1	$R = 10.5 \Omega$ & $L = 14.5 \text{ nH}$	-2.8
33	36.4	35/14.5	$F = 33.9 \Omega$ & $L = 13.9 \text{ nH}$	-6.9
100	108.1	92.2/1.2	$R = 92.2 \Omega$ & $L = 3.1 \text{ nH}$	-14.7
390	371.6	330.3/-7.6	$R = 333.2 \Omega$ & $C = 0.64 \text{ pF}$	-10.3
1k	1057	943.6/-16.6	$R = 984.6 \Omega$ & $C = 0.48 \text{ pF}$	-6.8
3.9k	3739	1974.1/-46.1	$R = 2847 \Omega$ & $C = 0.58 \text{ pF}$	-23.9
10k	10.5k	2967.1/-60.6	$R = 6044 \Omega$ & $C = 0.47 \text{ pF}$	-42.4

APPENDIX F

MODELING AND ANALYSIS OF EXCEPTIONS TO GENERIC CURVES

With the exception of three curves, the impedance curves for all the measured data match one of four generic curves (see Figures 15, 16, and 17). Therefore, these generic curves were used in Sec. 4.0 to illustrate the modeling techniques used with the measured data. The modeling and analysis for the three components whose impedance curves were exceptions to the generic curves are summarized in this appendix.

The first curve which is given in Figure F-1 is for the 15 μ F tantalum capacitor (Sprague 109D156C2075F2) which represents Group #1 in Table D-7. This curve is similar to the generic curve given in Figure 15; however, the minimum value of this curve is below the measurement capabilities of the instrumentation (i.e., $<1\Omega$). Thus, the series resistance (R_s) in the following model can not be accurately determined:

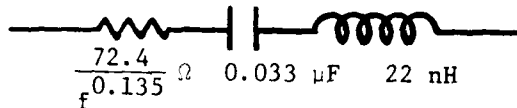


This resistance can be approximated in most cases by visually estimating the minimum value of the impedance ($|Z|$) on the curve. For example, in Figure F-1 the minimum value is estimated to be 0.65Ω . Thus, R_s is assumed to be $650\text{ m}\Omega$ and C and L are determined from the asymptotes on Figure F-1 as described in Sec. 3.0. The resulting element values are

$$\begin{aligned}R_s &= 650\text{ m}\Omega, \\C &= 13.3\text{ }\mu\text{F}, \text{ and} \\L &= 26\text{ nH}.\end{aligned}$$

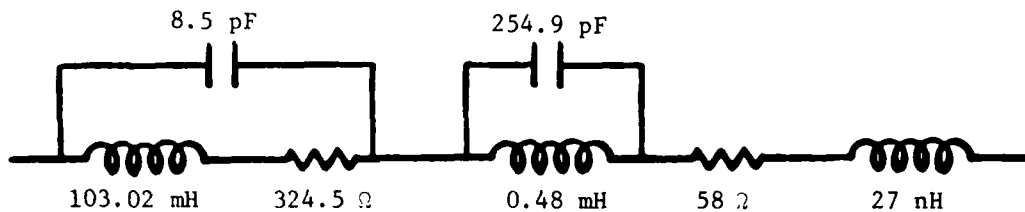
The impedances calculated from this model are also shown in Figure F-1.

The second exception to the generic curves is given in Figure F-2. This impedance curve is for the 0.033 μ F tantalum capacitor (Sprague 150D333X0035) which represents Group #3 in Table D-7. Again, this curve is similar to the generic curve given in Figure 15. In fact, it was modeled using the techniques given in Sec. 4.0 and the results were presented in Figure D-3. However, the model is very inaccurate approximately one frequency decade below $|Z|_{\min}$. This inaccuracy appears to be due to assuming that the series resistance is a constant. Therefore, the $|Z|$ curve was remodeled using the technique which assumes that the series resistance is a function of frequency as described in Step 4 in Sec. 3.2.2.1. The resulting model is



The impedances calculated from this model are shown in Figure F-2. This technique results in a more accurate model for this group of capacitors as can be seen in Figure F-3. This figure give the differences between the measured $|Z|$ and the calculated $|Z|$ in per cent for both modeling techniques (i.e., assuming R is a constant and assuming R is a function of frequency). Figure F-3 shows that the percentage difference is reduced considerably (i.e., the model accuracy is improved) by assuming that R is frequency dependent.

The final exception to the generic curves is given in Figure F-4 for the 100 mH RF choke (Miller 994) which represents Group #4 in Table D-8. This impedance curve is similar to the generic curve given in Figure 16 and it was modeled in Sec. 4.0 (see Figure D-11) as if it matched the generic curve. However, this curve has additional resonances above the first resonant frequency of 170 kHz. In order to account for these other resonances and, thus, refine the model, successive applications of the guidelines and rules-of-thumb presented in Sec. 4.0 were employed to obtain a considerably more complex model. The resulting model is



The impedances calculated from this model are also shown on Figure F-4. This figure indicates that the model accurately predicts all the characteristics of the inductor except for the value of $|Z|$ at some of the resonance frequencies. The value of the model $|Z|$ could be improved at the resonances by continued refinement through the application of the guidelines in Sec. 4.0; however, the model obviously would become more complex.

In summary, three exceptions to the generic impedance curves in Sec. 4.0 have been presented. Techniques for modeling these curves have been described based upon application of the guidelines and rules-of-thumb presented in Sec. 4.0. It is concluded that as the impedance curve is modeled in more detail, the complexity of the resulting model increases either in element count or through frequency dependency of some of the elements.

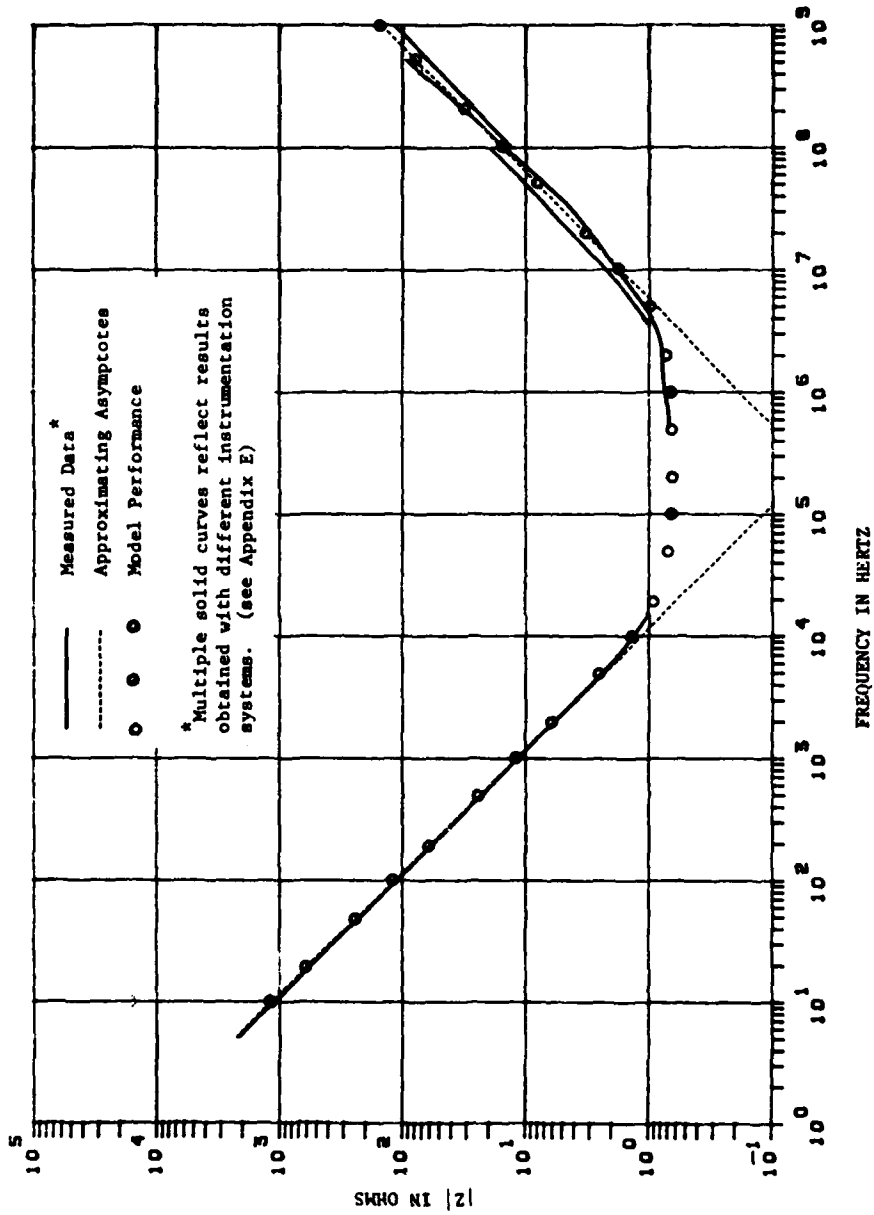


Figure F-1. Data for the Capacitor Representing Group #1 in Table D-7.

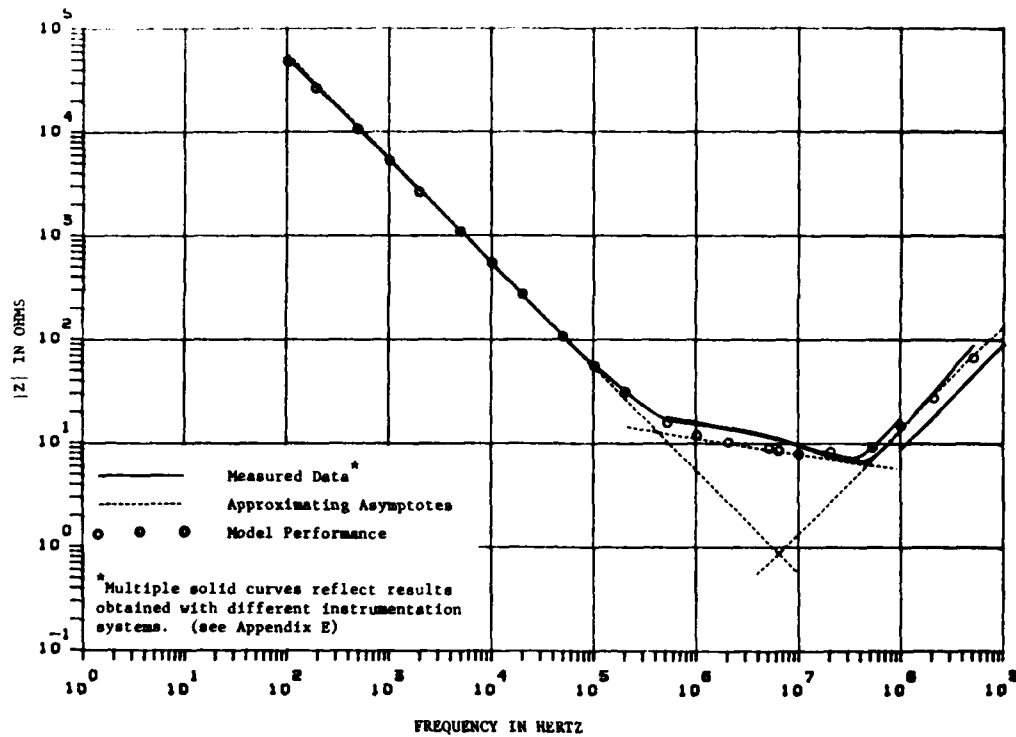


Figure F-2. Data for the Capacitor Representing Group #3 in Table D-7.

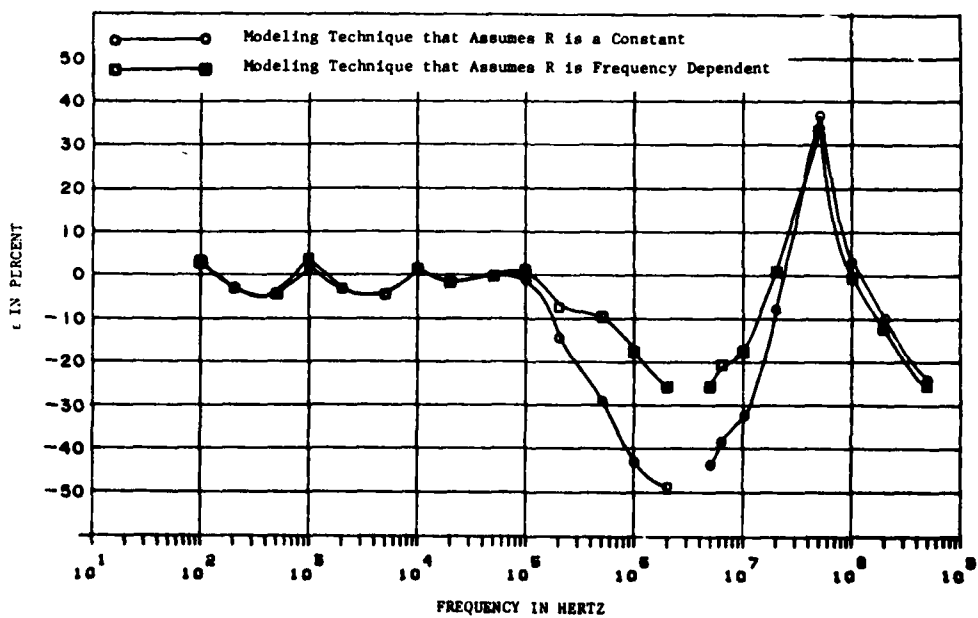


Figure F-3. Difference in Model and Measured Impedances in F-2.

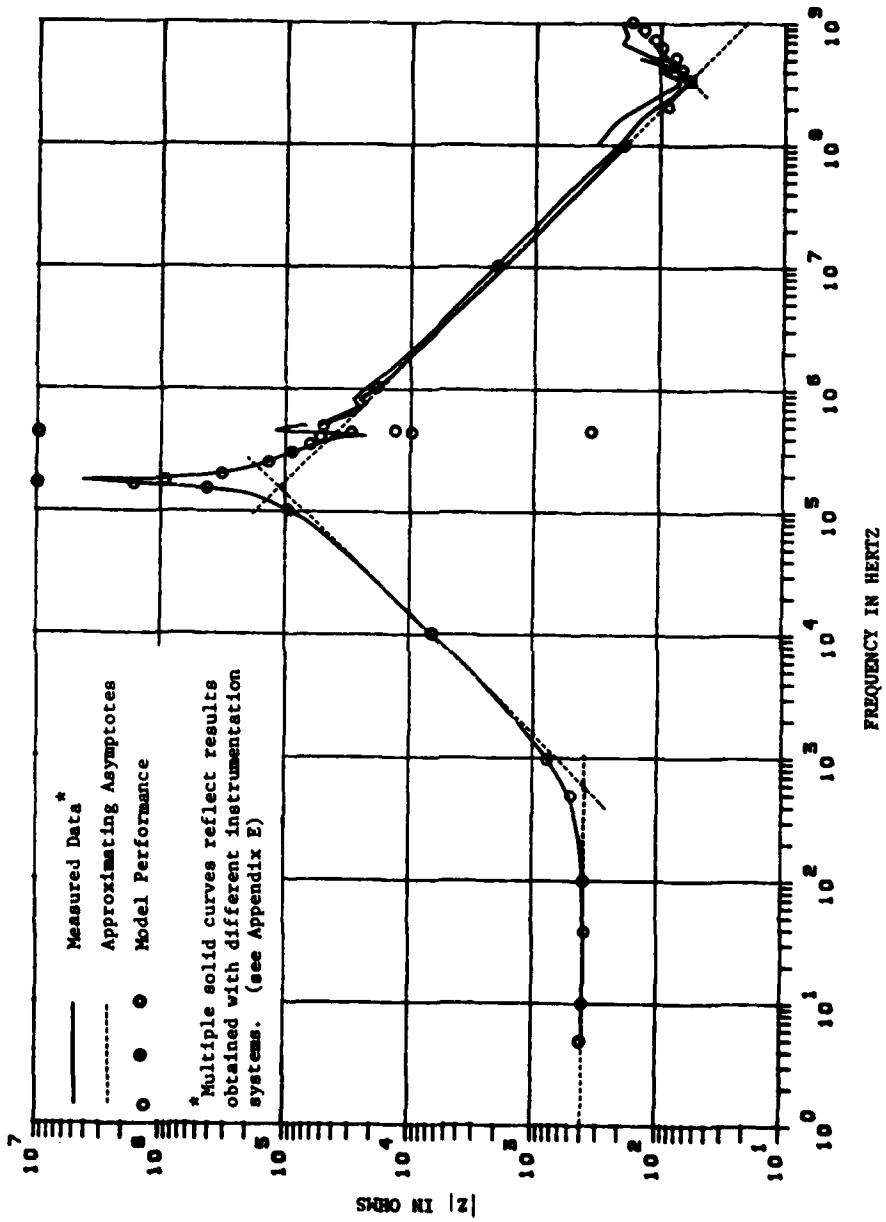


Figure F-4. Data for the Inductor Representing Group #4 in Table D-8.



MISSION
of
Rome Air Development Center

RADC plans and executes research, development, test and selected acquisition programs in support of Command, Control Communications and Intelligence (C³I) activities. Technical and engineering support within areas of technical competence is provided to ESD Program Offices (POs) and other ESD elements. The principal technical mission areas are communications, electromagnetic guidance and control, surveillance of ground and aerospace objects, intelligence data collection and handling, information system technology, ionospheric propagation, solid state sciences, microwave physics and electronic reliability, maintainability and compatibility.